

January 2014

# Manipulating the Tumor Microenvironment for Therapeutic Benefit

Kate M. Bailey

*University of South Florida*, [katebailey10@gmail.com](mailto:katebailey10@gmail.com)

Follow this and additional works at: <http://scholarcommons.usf.edu/etd>

 Part of the [Biology Commons](#), [Cell Biology Commons](#), and the [Medicine and Health Sciences Commons](#)

---

## Scholar Commons Citation

Bailey, Kate M., "Manipulating the Tumor Microenvironment for Therapeutic Benefit" (2014). *Graduate Theses and Dissertations*.  
<http://scholarcommons.usf.edu/etd/5175>

This Dissertation is brought to you for free and open access by the Graduate School at Scholar Commons. It has been accepted for inclusion in Graduate Theses and Dissertations by an authorized administrator of Scholar Commons. For more information, please contact [scholarcommons@usf.edu](mailto:scholarcommons@usf.edu).

Manipulating the Tumor Microenvironment for Therapeutic Benefit.

by

Kate M. Bailey

A dissertation submitted in partial fulfillment  
of the requirements for the degree of  
Doctor of Philosophy  
Department of Cell Biology, Microbiology, and Molecular Biology  
College of Arts and Sciences  
University of South Florida

Major Professor: Robert J. Gillies, Ph.D.  
Robert A. Gatenby, M.D.  
Keiran S. Smalley, Ph.D.  
Jeffrey S. Weber, M.D., Ph.D.  
Kenneth L. Wright, Ph.D.

Date of Approval:  
June 26, 2014

Keywords: hypoxia, acidosis, buffer therapy, TH-302, Steal phenomenon

Copyright © 2014, Kate M. Bailey

## DEDICATION

I dedicate this dissertation to...

...my husband, Mike, who has supported me through the mine field of grad school. You were there with me for every celebration, and more importantly, every failure. You always knew when I needed tough love, a sympathetic ear, or when only sushi dinner would cheer me up. You probably know more than you ever wanted to know about pipettes, westerns, and tumor metabolism; and while you still think that all I do is “move small amounts of liquid from one tube to another” all day, you are the first to brag to people about my accomplishments. I could not have made it through grad school without your support, and I cannot wait to take this next adventure with you, wherever it takes us.

...my parents, Jim and Lori, who have given everything for me to succeed in life. I know you have made countless sacrifices through the years, probably many I will never know about, and for that I am eternally grateful. You taught me the importance of hard work, encouraged my curiosity, and were always there to pick me up when I stumbled. I have always been proud to call you my parents, and am fortunate to now call you my friends. I could not have done any of this without your love and support.

...my brother, Jared, who always reminds me to be appreciative of everything in life, especially fire trucks with their lights on, Disney movies on repeat, and John Deere tractors. The world would be a better place if more people shared your positive outlook on life.

## ACKNOWLEDGMENTS

I would like to thank my mentor, Dr. Robert J. Gillies, for your guidance and support. I know you took a chance on hiring me, and I hope that I have made you proud. When we first met, you told me your goal was to get me to remember why I loved science to begin with. It was not always easy, and sometimes I was mad at you and at science; but I can truly say that joining your lab was the best decision I could have ever made. You have encouraged me to think outside of the box, and reminded me how exciting science could be. I can't thank you enough for your mentorship over the last three years.

I would also like to thank the other Bob, Dr. Robert A. Gatenby. Stopping by your office was always an enjoyable part of my day. Whether you were talking about cancer evolution, theoretical physics, or New Jersey hit men, I was always guaranteed a laugh and a new perspective. Besides, without your life lessons I would still be boarding planes with two bags of luggage and a full cup of coffee.

To the members of my committee: Dr. Kenneth L. Wright, Dr. Keiran S. Smalley and Dr. Jeffery S. Weber, thank you for your continuous guidance. Your thoughtful insight has helped to shape this dissertation. I would also like to thank Dr. Zaver Bhujwala for agreeing to serve as my outside chair.

My labmates, past and present, have made my time in the Gillies lab so enjoyable. I have never been surrounded by such kind, intelligent and thoughtful people. Arig and Jonathan, I could not have done any of this without you two. I can't thank you enough for taking me under your wing when I joined the lab three years ago, Arig. You taught me so many techniques,

helped me learn a new field in no time at all, and helped me gain my confidence back when I needed it most. You are one of the most genuine people I know and I will miss our early morning chats. Jonathan, I probably suckered you into being my mentor, but I don't regret it for a second. You are one of the smartest people I know, while being so kind and patient at the same time. I have learned so much from you as a scientist, but will forever be grateful to consider you and Maggie my lifelong friends. And getting to watch that little nugget, Chace, grow up hasn't been terrible either. Veronica and Valerie, some of my favorite memories are chatting with the two of you about some of the most ridiculous things. I always looked forward to coming to work; thank you both for always making me smile even when I was grouchy or upset. And thanks for helping me find my pipettes, ice boxes, and whatever else I needed on a daily basis, Valerie. I would probably still be looking for them without you. To the rest of the microenvironment group and lab, I can't possibly thank you all enough for your support.

To some of my favorite past lab members (and one current, but very distant lab member): Natalie, Kelley and Jessica. I have never met so many people that I have instantly become best friends with. The three of you, in each your own way, have helped me grow as a person and scientist. Natalie, I love laughing with you about nothing and everything. You are one of my best friends and I have enjoyed traveling and road-tripping across the country with you. Also—I still don't study pathways, even though you think that's what all biologists do. Kelley, our anniversary will always be Moffitt Research Day, and I am so glad that we met. You and Kiera have brightened my life so much. The two of you can make me laugh like no other, and we may never know "where my ball at". Jessica, you helped me weasel my way into this lab, and helped me to remain patient during a stressful time in my life (when "one day!" seemed like "one week!"). I will miss our wild nights at the Embassy Suites bar, where we can't get enough hot

tea during our late night chats. The three of you will always be so important to me, and I can't wait to travel the country to visit you all again!

To my family, Grandpa, Grandma Sherry, Aunt Barb, Uncle Scott, Kyle, Aunt Sue and Dawn: where would I be without you? I have been so lucky to have such a supportive and close extended family. You have all been so supportive of everything I have done. Studies show that if a child has five or more adults in their life in support of them they have increased chances of being successful. With all of your support, I never had a chance to not succeed. Holidays are never boring, and we can't relax to save our lives, but I wouldn't change it for anything. And of course, to my in-laws: Eleanor, Dennis, Krista, Tom, Thomas, Karlie, Doug and the other Aunt Katie: thank you for being such a great support system. I could not ask for a better extended family.

To the nerds: Liane, Adrienne, Chrissie, and Alicia. Who is still best friends with people they went to fifth grade as adults? Liane and I, that's who. We picked up Adrienne, Chrissie, and Alicia along the way and have never looked back. We are the ones who made studying look cool (or so we thought). We fostered and encouraged each other's desire and love for learning, and pushed each other to be better people in every way. We have been through everything together; hard life lessons, relationships, weddings, vacations, and really bad karaoke. I wouldn't want to experience any major life event without any of you, and I wish we all lived closer. One day we will all live on the same street as neighbors, but until then I will visit you wherever you land. I wish you could be here to celebrate with me, but I know we will make up for it later!

Last, and definitely not least: to Geri (I know you have been looking for your name!). I know I told everyone above that I couldn't have made it through grad school without them, but I

absolutely could not have made it through grad school without you. You have been there for everything, every up and every down. You have been a rock, a best friend, my coffee buddy and my PR agent. I have loved getting to know your family, and watching your kids grow into incredible adults (I can't believe I have been here that long!). I know I can be quite a PITA, but you have never complained. Thank you, for everything you have done for me.

## TABLE OF CONTENTS

List of Tables .....	iv
List of Figures .....	v
Abstract .....	vii
Chapter 1: Introduction .....	1
Cancer .....	1
The Tumor Microenvironment .....	3
Carcinogenesis and the Tumor Microenvironment.....	4
Manipulating the Tumor Microenvironment for Therapeutic Benefit.....	6
Chapter 2: Manipulating the Tumor Microenvironment for Therapeutic Benefit.....	8
Introduction.....	8
Targeting Hypoxia in the Tumor Microenvironment .....	8
Targeting Hypoxia Response Pathways.....	10
Targeting the HIF1 $\alpha$ Pathway.....	10
Targeting mTOR.....	12
Targeting UPR .....	14
Using Hypoxia to Our Advantage.....	16
Use of Bioreductive Drugs.....	16
Manipulating Hypoxia .....	18
Targeting Glucose Metabolism.....	20
Targeting Glucose Transporters.....	20
Targeting Hexokinase .....	23
Targeting Phosphofructokinases .....	25
Targeting Pyruvate Kinase M2 .....	26
Targeting Pyruvate Dehydrogenase Kinase.....	27
Targeting Lactate Dehydrogenase (LDH) .....	28
Targeting Acidosis .....	30
Targeting Proton Transport.....	30
Manipulating Tumor Microenvironment pH .....	33
Manipulating the Microenvironment for Therapeutic Benefit.....	33
Conclusion .....	35
Chapter 3: Mechanisms of Buffer Therapy Resistance .....	36
Introduction.....	36
Altered Tumor Metabolism.....	36
Tumor Acidosis and the Metastatic Cascade .....	38



Proteases and Metastatic Disease.....	40
Cellular Migration in Metastasis.....	42
Manipulating Tumor Acidosis with Systemic Buffer Therapy.....	43
Results.....	46
Efficacy of Lysine Buffer Therapy is not Universal.....	46
In vitro characterization of Lysine Buffer Therapy Resistant and Sensitive Cell Lines.....	48
Effect of pHe on Invasion Rates of Resistant and Sensitive Cells.....	50
Analysis of the Metabolic Phenotypes of Resistant and Sensitive Cells.....	52
In vivo Proteolytic Activity in Resistant and Sensitive Tumors.....	56
In vitro Protease Expression in Resistant and Sensitive Cells.....	58
The Effect of pHe on Resistant and Sensitive Cell Migration and Morphology.....	58
Discussion.....	61
Materials and Methods.....	67
Animals.....	67
Cell lines.....	67
Experimental Metastasis Model and Bioluminescent Imaging.....	67
Metabolic Profile Analysis.....	68
Electrode measurement of tumor pH.....	68
In-vivo protease activity measurements.....	68
Quantitative PCR.....	68
Invasion Assay.....	69
Microscopy Studies.....	69
Data Analysis.....	69
 Chapter 4: Evaluation of Combination Therapy and Potential Predictive Biomarkers for Hypoxia Activated Prodrugs in Pancreatic Cancer.....	70
Introduction.....	70
Tumor Hypoxia.....	70
Targeting Tumor Hypoxia.....	71
Manipulating Tumor Hypoxia.....	72
Hypoxia in Pancreatic Cancer.....	75
Results.....	76
PDAC xenografts exhibit variable sensitivity to TH-302 in vitro and in vivo.....	76
pH electrode results indicate that MiaPaCa-2 tumors exhibit “Steal”effect in response to hydralazine.....	76
Hydralazine treatment results in a reduction in tumor blood flow within 15 Minutes.....	77
MiaPaCa-2 tumors lack tonal mature vasculature.....	79
Vasculature markers identify “Steal” responsive melanoma tumors.....	80
MiaPaCa-2 tumors are moderately sensitive to TH-302, and the effect is slightly enhanced with hydralazine.....	81
Combination therapy dosing regimen optimization increases TH-302 efficacy in MiaPaCa-2 tumors.....	84

Discussion.....	85
Materials and Methods.....	88
Cell Culture.....	88
Animal Studies.....	88
pH Electrode.....	89
Ultrasound Imaging.....	90
Drug Regimens and Tumor Growth Kinetics Monitoring.....	90
Tissue Processing and Immunohistochemistry.....	91
Data Analysis.....	91
Chapter 5: Conclusion.....	92
Chapter 6: References.....	97
Appendices.....	134
Appendix A: Copyright Permission from Advances in Pharmacology.....	135
Appendix B: Copyright Permission from Neoplasia.....	136
Appendix C: Copyright Permission from Journal of Nutrition & Food Sciences.....	137
Appendix D: Copyright Permission from Journal of Cancer Science & Therapy.....	138
Appendix E: Institutional Animal Care and Use Committee Approval – Protocol R4029.....	139
Appendix F: Institutional Animal Care and Use Committee Approval – Protocol R4033.....	140
Appendix G: Individual Contributions in Authored Publications.....	141

## LIST OF TABLES

Table 2.1	Drugs Targeting Hypoxia or Hypoxia Response Pathways.....	9
Table 3.1	Common Sites of Metastatic Disease .....	40
Table 4.1	TH-302 Clinical Trials .....	73

## LIST OF FIGURES

Figure 2.1	Inhibitors of the Glycolytic Pathway .....	21
Figure 2.2	Proteins that contribute to tumor acidosis and their inhibitors .....	31
Figure 3.1	In vivo buffering of tumor pHe reduced tumor binding of GB123 .....	43
Figure 3.2	Lysine free base reduces metastases through pH buffering.....	46
Figure 3.3	Sensitivity of PC3M <sub>S</sub> to treatment with lysine buffer therapy .....	47
Figure 3.4	Resistance of B16-F10 <sub>R</sub> to treatment with lysine buffer therapy .....	48
Figure 3.5	Resistance of LL/2 <sub>R</sub> to treatment with lysine buffer therapy.....	49
Figure 3.6	Sensitivity of MDA-MB-231 <sub>S</sub> to treatment with lysine buffer therapy.....	49
Figure 3.7	Resistance of HCT116 <sub>R</sub> to treatment with lysine buffer therapy.....	50
Figure 3.8	In vitro characterization of lysine buffer therapy resistant and sensitive cell lines.....	51
Figure 3.9	Effect of pHe on invasion rates of resistant and sensitive cells.....	52
Figure 3.10	Glycolytic profile analysis of buffer therapy resistant and sensitive cells.....	54
Figure 3.11	Oxidative profile analysis of buffer therapy resistant and sensitive cells.....	55
Figure 3.12	Sensitive cells are more glycolytic than resistant cells, leading to tumor acidosis.....	56
Figure 3.13	Metabolic profile analysis of HCT116-Luc and HCT116-GFP cells .....	57
Figure 3.14	Resistant tumors have increased in vivo Cathepsin activity .....	59
Figure 3.15	Resistant tumors have increased in vivo MMP activity.....	60
Figure 3.16	Elevated MMP expression in resistant cells .....	61
Figure 3.17	Migratory patterns of LL/2 <sub>R</sub> and PC3M <sub>S</sub> cells .....	62

Figure 3.18	Morphologies in a 3D matrix in vitro .....	63
Figure 4.1	The Steal Phenomenon .....	75
Figure 4.2	pH electrode results indicate that MiaPaCa-2 tumors exhibit “Steal” Effect in response to hydralazine.....	78
Figure 4.3	Hydralazine treatment results in reduction in tumor blood flow .....	79
Figure 4.4	Hydralazine treatment results in a reduction in tumor blood flow within 15 minutes.....	80
Figure 4.5	MiaPaCa-2 tumors lack tonal mature vasculature .....	82
Figure 4.6	Vasculature markers identify “Steal” responsive melanoma tumors.....	83
Figure 4.7	Hs766t tumors are sensitive to TH-302, and the effect is not enhanced with hydralazine.....	83
Figure 4.8	SU.86.86 tumors are resistant to TH-302, and the effect is not enhanced with hydralazine.....	85
Figure 4.9	MiaPaCa-2 tumors are moderately sensitive to TH-302, and the effect is slightly enhanced with hydralazine.....	86
Figure 4.10	Combination therapy dosing regimen optimization increases TH-302 efficacy in MiaPaCa-2 tumors .....	87

## ABSTRACT

The physical tumor microenvironment contributes significantly to carcinogenesis, cancer progression and metastatic dissemination. Two main components of the tumor microenvironment, hypoxia and acidosis, are present in nearly every solid tumor and act as powerful selection forces against the tumor. Hypoxia and acidosis promote tumor heterogeneity and contribute to chemotherapy and radiotherapy resistance. This dissertation interrogates methods to target the tumor microenvironment including two novel studies describing mechanisms of buffer therapy resistance and targeting tumor hypoxia with vasodilators to enhance the efficacy of a hypoxia activated prodrug, TH-302.

In the first study, mechanisms of buffer therapy resistance were identified and detailed. Many studies have shown that the acidity of solid tumors contributes to local invasion and metastasis. Oral pH buffers can specifically neutralize the acidic pH of tumors and reduce the incidence of local invasion and metastatic formation in multiple murine models. However, this effect is not universal as we have previously observed that metastasis is not inhibited by buffers in some tumor models, regardless of the buffer used. B16-F10 (murine melanoma), LL/2 (murine lung) and HCT116 (human colon) tumors are resistant to treatment with lysine buffer therapy, whereas metastasis is potently inhibited by lysine buffers in MDA-MB-231 (human breast) and PC3M (human prostate) tumors. In the current work, I confirmed that sensitive cells utilized a pH-dependent mechanism for successful metastasis supported by a highly glycolytic phenotype that acidifies the local tumor microenvironment resulting in morphological changes. In contrast, buffer-resistant cell lines exhibited a pH-independent metastatic mechanism

involving constitutive secretion of matrix degrading proteases without elevated glycolysis.

These results have identified two distinct mechanisms of experimental metastasis, one of which is pH-dependent (buffer therapy sensitive cells) and one which is pH-independent (buffer therapy resistant cells). Further characterization of these models has potential for therapeutic benefit.

In the second study, improving the efficacy of hypoxia activated prodrug, TH-302, through induction of hypoxia was investigated. Pancreatic ductal adenocarcinomas are desmoplastic and hypoxic tumors, both of which are associated with poor prognosis. Hypoxia activated prodrugs, such as TH-302, are specifically activated in hypoxic environments and are now in a Phase III clinical trial in pancreatic cancer. Using animal models, we show that tumor hypoxia can be exacerbated using a vasodilator, hydralazine, improving TH-302 efficacy. Hydralazine reduces tumor blood flow through the “Steal” phenomenon, where atonal immature tumor vasculature fails to dilate in coordination with normal vasculature. The current study shows that MiaPaCa-2 tumors exhibit a “Steal” effect in response to hydralazine, resulting in decreased tumor blood flow and subsequent tumor pH reduction. The effect is not observed in SU.86.86 tumors with mature tumor vasculature, as measured by CD31 and smooth muscle actin (SMA) immunohistochemistry staining. Combination therapy of hydralazine and TH-302 resulted in a reduction in MiaPaCa-2 tumor volume growth after 18 days of treatment. Further optimization of hypoxia-inducing agents and dosing regimens may lead to increased TH-302 activity, potentially improving clinical outcome.

The data presented here demonstrate methods to effectively target the tumor microenvironment for therapeutic benefit. Further investigation into mechanisms of action and biomarkers for therapy response may have important implications on clinical treatment regimens for cancer patients.

# CHAPTER 1

## INTRODUCTION

### Cancer

The word “cancer” is quite deceiving as it implies cancer is a single disease. However, with increasing technological advances, we now know that “cancer” represents hundreds of different diseases. Even seemingly more specific types of cancer, such as breast cancer and lung cancer, are actually made up of many cancer subtypes. Cancer is an extremely heterogeneous disease, characterized by unregulated cell proliferation in a malignant lesion. Cancer was first described in 3000 B.C. in Egypt in the Edwin Smith surgical papyrus [1] and has been studied in great detail since then. Toxic chemicals have historically been used to kill cancer cells, often with great sacrifice to the patient’s health [2]. Upon the advent of molecular biology, cancer research focused heavily on cancer genetics and the abundance of molecular mutations that are found in tumors, spurring the birth of targeted therapies. Common mutations were identified that transform normal cells and promote malignancy, known as oncogenes. Targeted therapies, such as EGFR inhibitors in lung cancers [3], HER2 inhibitors in breast cancer [4], or B-raf inhibitors in melanoma [5], target the most prevalent oncogenes and are often efficacious initially. Each targeted therapy, however, ultimately succumbs to resistance and becomes ineffective. Resistance to targeted therapies can be innate or emerge from newly acquired mutations that occur following exposure to chemotherapy.



The emergence of resistant populations in response to chemotherapy is due in large part to tumor heterogeneity. Tumors are known to be extremely heterogeneous and contain regions of distinct genetic and phenotypic subpopulations. Bert Vogelstein, among others, has documented the heterogeneity of a tumor extensively. By studying regional heterogeneity in colorectal tumors, he proposed a model of cancer progression detailing mutations that were acquired one by one over time [6-9]. Similarly, Gerlinger and colleagues identified regionally distinct subpopulations of cells within renal cell carcinoma tumors [10]. Each region of tumor was analyzed using deep sequencing methods to identify genetic mutations that were maintained throughout the tumor, as well as genetic mutations that were unique to each population. Regional differences in the mutation load were used to model the evolution of tumor development and identify regions which ultimately metastasized to distant sites. Genetic alterations found in tumors can occur from germline mutations, environmental carcinogens or chronic inflammation, and are thought to occur over a period of years or even decades.

Tumor heterogeneity remains the biggest obstacle for targeted therapies. Targeted therapies, by design, are effective only towards tumor cells harboring a specific mutation, leaving portions of the tumor unaffected. Additionally, when administering cytotoxic targeted therapies to cancer patients, we are unintentionally applying a powerful selection force upon the tumor. Genetic instability (a hallmark of cancers) facilitates a mutator phenotype, increasing tumor heterogeneity in response to stresses, including cytotoxic therapy [11]. Resistant populations eventually emerge from heterogeneous tumors, rendering the targeted therapy ineffective [12]. Approaching cancer therapy from an evolutionary perspective and using methods like adaptive therapy may prove to be a more efficient way to use targeted therapies clinically while controlling the emergence of resistant populations [13,14].

## **The Tumor Microenvironment**

Tumors consist of much more than a population of cancer cells. The tumor microenvironment encompasses the region of the tumor and everything it contains, including various cell types, such as cancer-associated fibroblasts and immune cells, and the physical features of a tumor, such as hypoxia and acidosis. The tumor microenvironment is often overlooked when designing and using targeted therapies to treat patients despite the fact that it contributes significantly to tumor progression, malignancy, and therapy resistance. The physical characteristics of the tumor microenvironment have been studied in great detail, and unlike the variability of genetic mutations that are found in tumors, hypoxia and acidosis are present in nearly every solid tumor, making them an ideal target for therapy [15-19].

While present in nearly every solid tumor, acidosis and hypoxia can vary regionally within a tumor. Hypoxia can be spatially and temporally heterogeneous and contributes significantly to tumor progression and malignancy. Diffusion-limiting hypoxia results when the diffusion limitation of oxygen (~200  $\mu\text{m}$ ) prevents oxygenation of tumor tissue at greater distances from tumor vasculature. Perfusion limitations result from immature and chaotic tumor vasculature and cause temporal changes in tumor perfusion [20]. Hypoxia, especially intermittent hypoxia, induces extreme genotoxic stress and enables genetic mutations to occur through repression of DNA damage repair pathways [21]. Tumor hypoxia is a negative prognostic indicator and a strong predictor of metastatic potential [22]. Hypoxic tumors are also less responsive to chemotherapy and radiotherapy treatment, contributing to resistance [22].

Tumor hypoxia also promotes changes in tumor metabolism by increasing anaerobic glycolysis as an alternative way to breakdown glucose in the absence of oxygen. Overtime, upregulated glycolysis becomes a fixed phenotype and occurs even in the presence of oxygen.

This phenomenon was first characterized in the 1920's by Otto Warburg and has since been termed the Warburg Effect [23]. Acidosis quickly results in tumors due to increased excretion of lactic acid, a byproduct of aerobic glycolysis, and the inability of the tumor vasculature system to remove lactic acid waste. Tumor acidosis is clastogenic, resulting in genetic instability through induction of chromosome breaks and translocations [24]. The presence of tumor acidosis reduces drug efficacy through protonation of weak base chemotherapies, contributes to chemoresistance, and increases the metastatic potential of cancer cells [25,26].

### **Carcinogenesis and the Tumor Microenvironment**

The tumor microenvironment plays a critical role in carcinogenesis. Gatenby and Gillies have proposed a model of carcinogenesis in which tumor adaption occurs in response to microenvironmental proliferation barriers that exert evolutionary selection forces on the cancer cells [27]. They hypothesize that the common phenotypes of invasive cancers, the hallmarks of cancer [28,29], arise from clones that exhibit increased fitness in response to selective pressures from microenvironmental proliferation barriers. Initially, as tumor cells begin to grow away from the basement membrane into a hyperplastic lesion, cells encounter the normal cellular response of apoptosis. Phenotypes that allow tumor cells to remain insensitive to anti-growth signals are selected for, often through resistance to anoikis and contact inhibition. Inadequate growth promotion occurs when growth factors and serum become limiting as tumor cells move away from the basement membrane. Self-sufficiency in growth signals is selected to increase the fitness of the tumor cells, and is often achieved through up-regulation of growth factor signaling pathways. As cells continue to grow and divide, entry into senescence becomes the next microenvironmental proliferation barrier. Tumors most commonly overcome this through upregulation of telomerase to select for limitless replicative potential. As cells continue to grow

from the basement membrane, oxygen becomes a limiting factor and hypoxia results. Unable to catabolically consume glucose substrates through the oxygen-dependent tricarboxylic acid cycle (TCA), or oxidative phosphorylation (OXPHOS), clones that have increased glycolytic flux become selected for and outgrow clones lacking mechanisms to support increased glycolysis. Acidotic waste from upregulated glycolysis floods the tumor microenvironment and becomes stagnant, due to chaotic and immature tumor vasculature, dropping the tumor pH significantly. Acidosis, which is toxic to normal cells selects for cells that are resistant to acid-mediated toxicity. Finally, ischaemia becomes a microenvironmental proliferation barrier, which selects for sustained angiogenesis as well as invasive and metastatic clones.

It is important to note that the order of the microenvironmental barriers are fluid and do not need to occur in the order proposed. For example, entry of cell into senescence may occur before cells detach from the basement membrane. The objective of the model is to consider carcinogenesis from an evolution dynamics perspective. The tumor microenvironment is the adaptive landscape that applies selective pressures upon tumor cells, and the fitness of clones to the current microenvironmental selection pressure determines their outgrowth. This model also supports a common observance of significant heterogeneity within a tumor, most likely due to the outgrowth of numerous clones with the variable tumor microenvironment.

More recently, Gillies, Verduzco and Gatenby have proposed a unifying model of carcinogenesis that further describes the evolutionary selection pressure exerted by the tumor microenvironment upon a tumor [30,31]. In addition to increasing genomic instability and mutation load of a tumor, hypoxia and acidosis themselves are potent evolutionary selection forces that alter the landscape of a tumor. Together, they increase the rate of evolution of a

tumor and increase tumor heterogeneity, ultimately leading to increased malignancy and resistance to therapy.

### **Manipulating the Tumor Microenvironment for Therapeutic Benefit**

The presence of hypoxia and acidosis in virtually every tumor, along with their influence on cancer progression and metastasis make them ideal targets for therapy. Manipulation of the tumor microenvironment has the potential to prevent tumor progression, inhibit metastatic disease and increase the efficacy of currently available targets. Developing therapies that target cancer phenotypes, rather than genotypes, has significant advantages over conventional targeting therapies.

The risk of developing resistance is reduced when targeting phenotypes rather than genotypes. Convergent evolution occurs frequently in tumors, and genetic instability and heterogeneity increases the chances that cancer cells will select for mutations that overcome inhibition by chemotherapy [32]. This is evident in the number of mutations that are found in a single cell signaling pathway. For example, self-sufficiency in growth signals is a common phenotype of cancers and is a hallmark of cancer [28,29]. The number of mutations that have been identified that can lead to self-sufficiency in growth signals is astronomical. Mutations can occur in the receptor tyrosine kinase themselves, either in the extracellular domain or the intracellular signaling domain, leading to constitutive pathway activation. Downstream signaling proteins can also be mutated to constitutively activate a cell growth pathway, negating the need for the receptor tyrosine kinase. Inhibition of one portion of a cellular signaling pathway will ultimately lead to mutations in other portions of the pathway. This has been observed clinically in patients treated with erlotinib, an inhibitor of EGFR [3]. Despite initial response to treatment, patients eventually develop resistance to erlotinib and become unresponsive to treatment. To

date, 12 mechanisms of resistance to erlotinib have been identified, confirming the complexity of targeting cancer genotypes [33].

Targeting cancer phenotypes will be efficacious on larger populations of patients, instead subpopulations of patients harboring a single genetic mutation. Targeting the tumor microenvironment is an ideal therapeutic approach. Phenotypes such as tumor hypoxia and acidosis are commonly found in solid tumors and contribute significantly to cancer progression and malignancy. This dissertation will describe current therapies that are being investigated preclinically and clinically to inhibit the two main physical features of the tumor microenvironment: hypoxia and acidosis. Additionally I will describe two aspects of my doctoral work focused on manipulating the tumor microenvironment for therapeutic benefit: 1) Identifying mechanisms of buffer therapy resistance, and 2) Manipulating tumor hypoxia to increase the efficacy of hypoxia activated prodrugs in pancreatic tumors.

## **CHAPTER 2**

### **MANIPULATING THE TUMOR MICROENVIRONMENT FOR THERAPEUTIC BENEFIT**

#### **Note to Reader**

Portions of this chapter have been previously published in *Advances in Pharmacology*, 2012, 65:63-107 [34], and are utilized with permission of the publisher.

#### **Introduction**

In chapter 1, I introduced a microenvironmental model of carcinogenesis [27,35]. Two of the microenvironmental characteristics, tumor hypoxia and acidosis have been studied extensively to elucidate their role in tumor initiation and progression (described in detail below). As hypoxia and acidosis are present in virtually all human solid tumors, targeting these two phenotypes, the “causes and consequences” of the tumor microenvironment, is an effective way to reach a large population of patients to overcome tumor growth and metastasis. In this chapter, I describe developmental drugs to target various aspects of hypoxia, cellular response to hypoxia and tumor metabolism. Finally, I detail methods that are currently being investigated preclinically and clinically to manipulate the tumor microenvironment for therapeutic benefit.

#### **Targeting Hypoxia in the Tumor Microenvironment**

Hypoxia is a common phenotype of solid tumors. As tumors grow, proangiogenic factors stimulate new vessel growth within a tumor. However, these new vessels tend to be immature

and chaotic, and hence lead to poor perfusion [36]. Tumors found to contain hypoxic regions typically respond poorly to therapy in the clinic [20]. Hypoxia can be difficult to target due to its spatial and temporal heterogeneity within tumors and the fact that hypoxic volumes are the most poorly perfused. Nonetheless, successful approaches to target hypoxia have been developed, and some of these are in clinical trials. These approaches can be broadly described as (1) targeting hypoxia response pathways; (2) drugs that require hypoxia for their activity and thus efficacy and (3) methods to manipulate hypoxia to our advantage to increase efficacy of hypoxia-activated prodrugs (**Table 2.1**).

**Table 2.1** Drugs Targeting Hypoxia or Hypoxia Response Pathways

<b>Drug</b>	<b>Target</b>	<b>Stage of Development</b>
Topotecan	Topo I/HIF1 $\alpha$ expression	FDA approved (ovarian, cervical, SCLC)
EZN-2968	HIF1 $\alpha$ expression	Phase I/Pilot study
PX-478	HIF1 $\alpha$ expression/protein stability	Phase I
Rapamycin	mTOR	FDA approved for non-oncogenic indications
CCI779 (temsirolimus)	mTOR	FDA approved (renal cell carcinoma, mantle cell lymphoma)
RAD001(everolimus)	mTOR	FDA approved (renal cell carcinoma, pancreatic neuroendocrine tumors & non-oncogenic indications)
Metformin	AMPK/mTOR/cell cycle	FDA approved for non-oncogenic indications
Bortezomib (PS-341)	Proteasome/UPR	FDA approved (mantle cell lymphoma, multiple myeloma)
STF-083010	IRE1/UPR	Preclinical
Salicaldehydes	IRE/UPR	Preclinical
Tirapazamine (TPZ)	Hypoxia	Clinical trials completed
TH-302	Hypoxia	Phase I-III
Banaxantrone (AQ4N)	Hypoxia	Phase I
Apaziquone (E09)	Hypoxia	Phase I-III
PR-104	Hypoxia	Phase I-II



## Targeting Hypoxia Response Pathways

Tumors typically have lower oxygen concentrations ( $pO_2$ ) than levels detected in normal tissue [37]. As a tumor grows outward, away from blood vessels, the ability to receive oxygen from diffusion through tissue diminishes quickly leading to diffusion-limited (or chronic) hypoxia. Additionally, perfusion-limited (or acute) hypoxia can result from variable blood flow through chaotic and immature vessels that are characteristic of tumors. Hypoxia can be a significant source of stress for cancer cells and several survival and response pathways have been identified that allows cancer cells to overcome oxygen stress.

### *Targeting the HIF1 $\alpha$ Pathway*

Modulation of the hypoxia response in cells is orchestrated by transcription factors, hypoxia inducible transcription factors, HIF1 $\alpha$  and/or HIF2 $\alpha$ . Under normoxic conditions, HIF1 $\alpha$  is inactivated via proteasomal degradation, regulated by the VHL ubiquitin ligase [38,39]. In response to hypoxia, HIF1 $\alpha$  is not degraded and the resulting stabilized protein will heterodimerize with HIF1 $\beta$  (a.k.a. the aryl hydrocarbon receptor nuclear translocator, ARNT) and activate promoters containing hypoxia response elements (HREs). Transcriptional targets of HIF1 $\alpha$  can be found in glycolytic, angiogenic, survival, and migration pathways [40]. Constitutive HIF1 $\alpha$  stabilization has been observed in many cancers and is correlated with aggressive disease, poor prognosis, and drug resistance, making HIF1 $\alpha$  an attractive drug target [41-44]. This is an active area of research and there are numerous investigational drugs aimed at inhibiting HIF1 $\alpha$  with a number of approaches: for example, targeting HIF1 $\alpha$  mRNA expression, protein translation, protein stability, and transcriptional activity. Following, we illustrate some of these approaches. More exhaustive discussion of this subject can be found at [45]. Topotecan is an FDA approved drug that is indicated for ovarian, cervical cancers, and small cell lung

carcinoma. The primary mechanism of action is through inhibition of topoisomerase I which induces genotoxic stress through DNA double strand breaks [46]. Screening of the NCI Diversity Set of chemical compounds for small molecule inhibitors led to the discovery of a second mechanism of topotecan activity through inhibition of HIF1 $\alpha$  expression [47]. Further topotecan studies confirmed inhibition of HIF1 $\alpha$  expression, concluding that translation of HIF1 $\alpha$  is inhibited in a topoisomerase 1-dependent mechanism by topotecan [48]. Tumor xenograft models treated with topotecan have decreased HIF1 $\alpha$  levels, diminished angiogenesis, and reduced tumor growth [49]. Furthermore, patients treated with topotecan had low to undetectable levels of HIF $\alpha$  in tumor biopsies, correlating with decreased levels of vascular endothelial growth factor (VEGF) and GLUT1 [50]. Seven of 10 patients treated with topotecan to receive dynamic contrast enhanced (DCE)-MRI exhibited decreased blood flow and permeability through their tumors after one treatment.

Abolishing expression of HIF1 $\alpha$  has been shown to be an effective way to inhibit tumor growth, inspiring the development of methods to target mRNA expression of HIF1 $\alpha$  as an alternative to targeting HIF1 $\alpha$  stability. An antisense oligonucleotide designed to inhibit HIF1 $\alpha$  expression has moved into clinical trials [51]. EZN-2968 was developed by Enzon Pharmaceuticals, Inc. using locked nucleic acid (LNA) oligonucleotide technology to reduce HIF1 $\alpha$  expression [52,53]. EZN-2968 was confirmed to selectively inhibit HIF1 $\alpha$  mRNA expression *in vitro*, resulting in a lasting decrease in HIF1 $\alpha$  protein levels, followed by a reduction in expression of HIF1 $\alpha$  target genes. EZN-2968 also showed activity in a tumor xenograft model by repressing tumor growth. Phase 1 clinical studies treating hematologic patients with EZN-2968 have recently concluded (NCT00466583) and have been followed by a pilot trial that is currently recruiting patients with liver metastasis (NCT01120288).

PX-478 is an orally available small molecule that has been shown to inhibit HIF1 $\alpha$  activity by reducing HIF1 $\alpha$  levels [54]. Tumor xenograft experiments using a variety of tumor cell lines showed that treatment with PX-478 reduced tumor growth or tumor regression which correlated with decreased levels of HIF1 $\alpha$  and its target genes GLUT1 and VEGF. The half-life of PX-478 in murine plasma is short at 50 min, although concentrations capable of inhibiting HIF1 $\alpha$  expression can be found for 8 h. Imaging of tumor xenografts with DCE and diffusion-weighted (DW)-MRI showed that treatment with PX-478 reduced tumor blood vessel permeability within 2 h of treatment and returned to normal 48 h after treatment [55]. Mechanistic studies have revealed that PX-478 may have multiple mechanisms of action in the inhibition of HIF1 $\alpha$  by hindering both transcription and stability of HIF1 $\alpha$  protein [56]. PX-478 can also contribute to clinical efficacy by acting as a radiosensitizer in prostate cancer cell lines and in in vivo tumor models [57,58]. Recently, phase I clinical trials investigating the safety and preliminary efficacy of PX-478 in patients with advanced solid tumor or lymphomas were completed (NCT00522652). Results from the phase I trial, presented at the 2010 ASCO Annual meeting, showed stable disease (SD) in ~40% of participants with mild toxicities [59].

### *Targeting mTOR*

The mammalian target of rapamycin (mTOR) is a kinase that is activated during cell stresses, including nutrient and energy depletion, triggering a signaling cascade regulating metabolism and many cell survival mechanisms [60,61]. mTORC1, a subunit of a complex nucleated by mTOR, has been shown to be important for tumorigenesis following activation of AKT [62]. Exposure to hypoxia in normal cells promotes activation of the tuberous sclerosis protein 1 complex (TSC1/2), which in turn negatively regulates the mTOR complex [63]. Additional evidence indicates that inhibition of the mTOR complex due to hypoxia can be

accomplished through interaction with promyelocytic leukemia (PML) tumor suppressor or disruption of mTORC1 binding to RHEB [64,65]. It is hypothesized that hypoxia mediated inhibition of mTOR is a selective mechanism for mutations that are beneficial for cell growth in hostile environments [66]. Alternatively, constitutively active mTOR has been observed in advanced breast cancer. In addition, loss of mTOR repressors, such as PTEN and TSC1/2, can result in unregulated mTOR activity [67,68]. While the exact role mTOR plays in carcinogenesis is not fully understood, mTOR inhibitors have been successful on the bench, and have moved into the clinic.

Rapamycin, a metabolite isolated from bacteria, was first identified in the 1970s to be a powerful antifungal drug [69]. Rapamycin was quickly determined to have antitumor activity, and was discovered to selectively target mTOR allosterically in the early 1990s [70,71]. Rapamycin also has potent immunosuppressive activity and is approved for transplant patients to prevent organ rejection as well as anti-restenosis after heart surgery due to its anti-angiogenic properties, but is not an approved medication for the treatment of cancer. Analogs of rapamycin, or “rapalogs,” are constantly being designed to be more specific to mTOR and have better pharmacologic properties and have been successful in the clinic. Currently, CCI779, or temsirolimus, is approved for treatment of RCC and mantle cell lymphoma, and is being investigated clinically for the treatment of other cancers, such as leukemia, non–small cell lung cancer (NSCLC), and breast cancer [72-74]. RAD001, or everolimus, has been approved for RCC and pancreatic neuroendocrine tumors, as well as an antirejection medication following organ transplant [75,76]. In addition to single agent drugs, rapalogs are being investigated in coordination with drugs that target other signaling pathways to improve efficacy, such as PI3K or AKT [77-79].

The antidiabetic drug metformin and its analogs buformin and phenformin have recently been identified as having potential anticancer activity. Metformin reduces blood glucose levels through decreasing hepatic gluconeogenesis and activation of AMPK (AMP-activated protein kinase) and is commonly used clinically for the treatment of type 2 diabetes [80-82]. AMPK can regulate activity of mTOR through activation of TSC1/2 [83]. Studies of diabetic patients receiving metformin revealed significantly reduced cancer risk compared to cohorts receiving other diabetic medications [84,85]. *In vitro* studies later confirmed that metformin represses growth of breast cancer cells through an AMPK-dependent signaling and inhibition of mTOR mechanism [86,87]. Metformin treatment seems to inhibit other cellular processes such as the cell cycle through reduction of cyclin D1 and diminishing the transcription of GRP78, an estrogen receptor chaperone protein that is elevated in cancers and involved in Unfolded Protein Response (UPR) signaling [88,89]. Metformin is currently being investigated clinically to determine if it is best used as a treatment or a preventative medication.

#### *Targeting UPR*

Hypoxia inhibits the ability of the endoplasmic reticulum (ER) to properly fold and organize proteins. The UPR is activated in the ER under hypoxia stress, which functions to maintain ER homeostasis or initiate apoptosis. Three proteins found at the ER membrane, PERK (PKR-like ER kinase), IRE1 (inositol requiring 1), and ATF6 (activating transcription factor 6), act independently to signal stresses leading to UPR activation [90]. Response by the UPR to hypoxia is important for tumor growth, and aberrant UPR signaling due to the absence of PERK or IRE1 results in increased regions of hypoxia and reduced growth rates [91,92]. Activation of the UPR response results in both reduction of translation and inhibition of protein maturation pathways as well as a detoxification process known as ER-associated degradation (ERAD) and

induction of autophagy [93]. In addition to activation of UPR in response to hypoxia, other cellular stresses often found in solid tumors can lead to UPR activation. Such stresses include calcium homeostasis, redox status, and glucose deprivation, making UPR an important cellular response mechanism in cancer, and also an attractive pathway to target clinically.

The ERAD response to cellular stresses is activated by the UPR and results in priming misfolded proteins to be shuttled out to the cytoplasm for proteasomal degradation [94]. Blocking the ERAD response through proteasome inhibitors like bortezomib (PS-341) has been a successful strategy for tumors with high ER stress such as multiple myeloma [95,96]. Recent research suggests that hypoxia sensitizes cells to ER stress resulting from bortezomib treatment, leading authors to suggest pairing bortezomib with normoxia targeting drugs to improve therapeutic response [97]. Such combinations have been investigated in murine models, and have shown to repress tumor growth when bortezomib was used in coordination with a HDAC6 specific inhibitor, ACY-1215, in a multiple myeloma model [98]. Clinical trials are also ongoing, investigating the efficacy of combining bortezomib treatment with other chemotherapies, such as mitoxantrone (topoisomerase II inhibitor), mapatumumab (antibody specific for TRAIL death receptor), and vorinostat (HDAC inhibitor).

IRE1 has two enzymatic domains, a kinase domain and an endonuclease domain [99,100]. Crystal structures have shown that IRE1 dimerizes in a juxtaposed configuration that allows for autophosphorylation resulting in increased endonuclease activity [101,102]. Screening for potential inhibitors of IRE1 using a cell-based reporter system identified STF-083010 [103]. Treatment of multiple myeloma cells with ER stresses resulted in mRNA cleavage of XBP1 by IRE1, which was abrogated with treatment of STF-083010 [104]. STF-083010 was shown to selectively inhibit the endonuclease activity of IRE1 without affecting

kinase activity. Although *in vivo* antitumorigenic responses were observed, more research will need to be performed to optimize an IRE1 inhibitor using STF-083010 as a scaffold. Another high-throughput screening search found salicylaldehyde analogs to be inhibitors of IRE1 [105]. Similar to STF-083010, salicylaldehydes inhibit IRE1 endonuclease activity *in vitro* and *in vivo*, increasing the interest to develop more potent and selective inhibitors targeting IRE1.

## **Using Hypoxia to Our Advantage**

### *Use of Bioreductive Drugs*

Bioreductive prodrugs are a class of drugs that are inert in tissues with normal pO<sub>2</sub> but are able to undergo chemical reduction in tissues with severe hypoxia to release cytotoxic warheads, selectively targeting cancer cells within hypoxic regions. In general, there are five different chemical scaffolds that have been used to generate bioreductive prodrugs (nitro groups, quinones, aromatic N-oxides, aliphatic N-oxides, and transition metals), all of which are able to be reduced in the absence of oxygen. One of the earliest reports of the use of bioreductive quinones to selectively target hypoxia is the use of mitomycin C in the 1960s [106,107]. During the last half century, bioreductive drugs scaffolds have been improved upon making them more selective and potent in hypoxic tumors.

Tirapazamine, or TPZ, is one of the most advanced bioreductive drugs through the clinical trials process. TPZ is built off of an aromatic N-oxide bioreductive scaffold [108]. During hypoxia, TPZ undergoes an intracellular one-electron reduction to a radical anion, then further converted to either a hydroxyl radical or an oxidizing radical, ultimately resulting in DNA damage [109-111]. TPZ creates DNA interstrand cross-links which stall replication forks and induce DNA breaks that require homologous recombination repair [112]. TPZ has been extensively studied clinically in combination with cisplatin and radiation in patients with

squamous cell carcinoma, head and neck cancer, and lung cancer with moderate to inconclusive results [113-116]. Further analysis showed that TPZ was being metabolized too quickly, and was not effectively penetrating tumor tissues [117,118]. Consequently, TPZ analogs are currently being developed with the goal of improving drug solubility, cytotoxicity, selectivity, and tissue penetration characteristics [119].

TH-302 is built upon a scaffold of a 2-nitroimidazole and is a nitrogen mustard prodrug that is selectively reduced under hypoxia ( $<0.5\% \text{ O}_2$ ) [120]. As TH-302 is reduced, the prodrug splits and releases its cytotoxic warhead, bromo-isophosphoramidate mustard (Br-IPM). As Br-IPM is released into hypoxic tissue, it cross-links with DNA, killing cells in the hypoxia compartment as well as neighboring cells with its bystander effect [121,122]. TH-302 was shown to have efficacy *in vitro* and *in vivo* in a wide subset of cancer cell lines and xenografts and was further found to have favorable drug-like properties and pharmacokinetic profiles [120,123,124]. TH-302 entered phase I clinical trials as a single agent drug in patients with advanced solid tumors and has also been tested in combination with doxorubicin in patients with advanced soft tissue sarcoma, gemcitabine in patients with pancreatic cancer; docetaxel for patients with prostate or lung cancers [125,126]. TH-302 was generally well tolerated, but some patients experienced skin and mucosal dose-limiting toxicities. Recently, phase I/II clinical trials of TH-302 as a single agent concluded with SD or better detected across a number of cancer types. Current clinical trials are investigating the efficacy of TH-302 as a single agent or in combination therapy for cancers, including melanoma, multiple myeloma, RCC, pancreatic carcinoma, and phase III trials have begun in patients with sarcoma. TH-302 is more thoroughly described in Chapter 4 of this dissertation.



Banoxantrone, or AQ4N, is an N-oxide bioreductive prodrug that was developed to selectively target hypoxic regions of tumors [127]. The reduction under hypoxia releases a cytotoxic alkylaminoanthraquinone metabolite (AQ4) which induces DNA damage through inhibition of topoisomerase II. AQ4N has been shown to be efficacious in murine models of breast cancer when combined with chemotherapy or radiation therapy [128-130]. Phase I clinical trials have investigated the activity of AQ4N either as a single agent or in combination with radiation therapy [131,132]. AQ4N was well tolerated by patients and is now being tested in clinical trials to evaluate the efficacy of AQ4N (NCT00394628, NCT00109356, and NCT00090727).

Two other bioreductive drugs, apaziquone (E09) and PR-104, have been successful on the bench top and have moved into clinical studies [133,134]. While bioreductive drugs have been especially successful in preclinical studies, and have shown some success in the clinic, no bioreductive prodrug has been approved by the FDA to date. Current research is aimed at improving bioreductive prodrug selectivity, stability, and cytotoxicity. Additionally, research is ongoing to develop bioreductive prodrugs that are non-genotoxic and instead target other cellular processes. For example, 2-nitroimidazole-5-ylmethyl is a 2-nitroimidazole that releases 5-bromoisoquinoline after reduction, targeting poly(ADP-ribose) polymerase 1 (PARP1) [135].

### **Manipulating Hypoxia**

While the data from hypoxia activated prodrugs (HAPs) in the clinic are promising, it can be reasoned that they may be more efficacious if tumor hypoxia can be selectively and transiently increased at the time of treatment. Thus, inducing hypoxia in tumors can be an efficient way of increasing the efficacy of drugs that target hypoxia. There are a number of mechanisms available with which to exacerbate tumor hypoxia selectively, including

metabolically (e.g., pyruvate or DCA), or by reducing oxygen delivery (e.g., antiangiogenic agents or vasodilators).

It has recently been shown that tumor hypoxia can be increased following intravenous injection of pyruvate [136,137], whose mechanism of action may involve inducing cells to increase respiration [137]. EPRI, a spectroscopic imaging technique that measures in vivo oxygen concentrations, of tumors in mice following an intravenous injection of hyperpolarized <sup>13</sup>C pyruvate revealed a significant decrease in tumor oxygenation that reached a maximum at 1 h, and returned to normal within 5 h [136]. Knowledge of a tumor's oxygenation status is important for treatment plans, as pyruvate-induced hypoxia reduced the ability of radiotherapy to kill cancer cells even after tumor oxygenation had returned to normal levels. DCA, an inhibitor of PDK, has also been reported to initiate a metabolic switch in cancer cells from glycolysis to oxidative phosphorylation [138]. Induction of oxidative phosphorylation by DCA increased reactive oxygen species, pH, and apoptotic proteins in HeLa cells. Additionally, the metabolic switch observed after DCA treatment correlated with an increased sensitivity of HeLa cells to cisplatin, suggesting that manipulation of a tumor's metabolism may be therapeutically successful.

Tumor oxygenation can also be manipulated by controlling oxygen delivery with antiangiogenic or antivascular agents. Angiogenesis is a common phenotype (“Hallmark”) of cancer that is regulated by HIF1 $\alpha$  signaling [29]. Tumors support an induction of angiogenesis by producing angiogenic growth factors such as VEGF and platelet-derived growth factor (PDGF). Several antiangiogenic inhibitors that target the immature angiogenic vasculature have been approved, including sorafenib, a VEGFR and PDGFR inhibitor, avastin (bevacizumab), an antibody targeting VEGF, and sunitinib, a VEGFR and PDGFR inhibitor [139]. Although

resistance to antiangiogenic drugs has become a major obstacle in clinical cancer treatment [140], their use to acutely increase hypoxia in combination with HAPs has not yet been published. Alternatively, there are agents, such as combretastatin, that will target mature vessels, and these are also known to increase tumor hypoxia [141]. Another characteristic of the immature tumor vasculature is a lack of tone. Thus, vasodilators, such as hydralazine, induce a systemic drop in blood pressure, which is not matched by the tumor vasculature, causing a transient decrease in perfusion within the tumor [142]. This “steal” phenomenon has been demonstrated using Doppler Ultrasound to measure decreased tumor blood flow [143]. The decrease in perfusion leads to increases in acidosis and hypoxia; both have been shown using pH electrodes or MRS, for acidosis and pO<sub>2</sub> electrodes for hypoxia [144-147].

### **Targeting Glucose Metabolism**

Aerobic glycolysis has long been known to be a common hallmark of solid tumors. This metabolic switch has been proposed to provide an advantage to growing tumors by allowing adaptation to low oxygen environments. This leads to increased acidification of the local tumor microenvironment, allowing for evasion of the immune system and increased metastatic potential [35,148]. In the next section, we describe drugs that are in preclinical or clinical studies that target glucose metabolism of tumors (**Figure 2.1**).

#### *Targeting Glucose Transporters*

Glucose, a major carbon source for cells, is a 6-carbon ring structure converted to pyruvate canonically along the Embden-Meyerhof glycolytic pathway. Entry of glucose into cells occurs by facilitated diffusion through a family of 14 membrane-bound proteins called glucose transporters (GLUTs). GLUT1, the founding member of the GLUT family, was isolated from erythrocytes in 1977 [149]. Upregulation of GLUT1 and GLUT3 expression has been

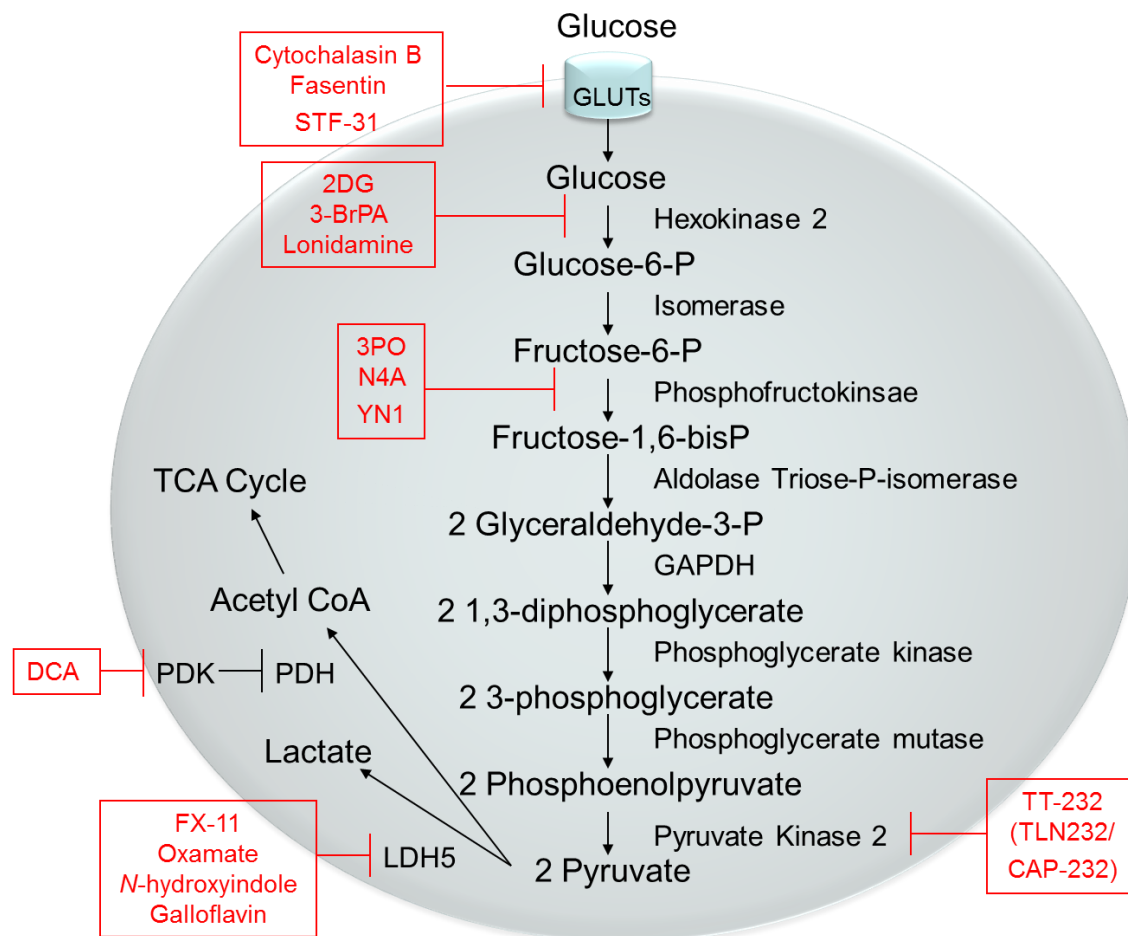


**Figure 2.1.** Inhibitors of the Glycolytic Pathway. The figure depicts the glycolytic pathway from glucose entry into cells through production of pyruvate, which is converted either to lactate or to acetyl coA for entry into the TCA cycle. Movement of metabolic intermediates through the pathway is designated by arrows. Enzymes in the glycolytic pathway are placed next to the arrow leading from their substrate to their product. Inhibitors of glycolytic enzymes or glucose transporters appear in boxes.

described in many cancers, and may be a key step in tumor progression. Increased expression of GLUTs correlate with poor prognosis and short survival of patients with ovarian, breast, and squamous cell carcinomas [150-152]. GLUT1 ( $K_m = 6.9$  mM) and GLUT3 ( $K_m = 1.8$  mM) each have a high affinity for glucose, and are thought to be the main transport mechanisms for glucose into cells [153-155]. Importantly, Hatanaka showed in 1974 that glucose uptake by cells is a rate-limiting step in glycolysis. Subsequent work by other groups determined that transformed

cells with increased expression of GLUTs at the plasma membrane is a strong independent prognostic indicator for FDG uptake and glucose consumption [156-159].

Increased expression of GLUT1 and GLUT3 during tumor progression allows for unregulated metabolism of glucose, making it an intriguing therapeutic target. Recent research described the cytotoxic and chemosensitizing properties of anti-GLUT1 antibodies in numerous lung and breast cancer cell lines reconfirming the importance of glucose uptake for survival [160]. Decades of research have resulted in the discovery of many other GLUT inhibitors, including Cytochalasin B and select tyrosine kinase inhibitors [161,162].

High-throughput screening for drugs capable of sensitizing cells that evade FAS ligand-induced apoptosis have identified fasentin, a small molecule inhibitor that binds to the intracellular channel of GLUT1, reducing glucose transport [163]. Further studies uncovered altered expression of genes involved in glucose metabolism following treatment of FAS-resistant prostate and leukemia cells with fasentin and FAS ligand [164]. Ultimately, fasentin alone was unable to induce cell death in FAS-ligand resistant cells, despite a rapid, albeit, partial reduction in glucose uptake following fasentin treatment.

Renal cell carcinoma (RCC), known for harboring inactivating mutations in the von Hippel-Lindau (VHL) ubiquitin ligase gene, was identified as a candidate for chemical synthetic lethality screening for GLUT inhibitors [165]. VHL mutations often coincide with a reorganized metabolic profile, wherein the tumor becomes highly glycolytic and relies on high levels of GLUT1 expression. One class of compounds, led by STF-31, caused necrotic cell death in RCC cells lacking functional VHL. *In silico* modeling revealed a potential docking site for STF-31 located in the central channel of GLUT1, and further functional studies confirmed inhibition of GLUT1 by STF-31. FDG-PET scans confirm reduced glucose uptake in RCC tumors treated

with STF-31, corresponding with retarded tumor growth. Lack of toxicities resulting from treatment with STF-31 encourages further research into its therapeutic potential and widespread efficacy in other tumors overexpressing GLUT1.

### *Targeting Hexokinase*

As glucose enters the cytosol, hexokinase phosphorylates the sixth carbon, effectively trapping glucose intracellularly and priming it for catabolism. Hexokinase-2 is frequently overexpressed in cancers, overcoming silencing methylation found on its promoter in normal tissues [166]. Expression of hexokinase is transcriptionally regulated by both p53 and hypoxia-inducible factor 1 $\alpha$  (HIF1 $\alpha$ ) [167]. Glucose analogs, specifically 2-deoxyglucose, can be radiolabeled to image tumors with increased glucose uptake ( $^{18}\text{F}$ FDG), and have also been studied as inhibitors of glycolysis [168,169]. These analogs enter cells normally through GLUT1 or GLUT3 transporters and are phosphorylated by hexokinase. As with glucose, the 6-phospho form of these analogs are unable to exit cells, and are feedback inhibitors of hexokinase activity. However, unlike glucose, the phosphorylated glucose analogs are unable to be rapidly catabolized through the remainder of the glycolytic pathway, that is, phosphofructokinase, and can build up to high levels intracellularly, where they prevent further glucose metabolism. Although there have been some successes using deoxyglucose *in vitro* and in animal models as a glycolytic inhibitor, clinical successes have not extended past utilization as an imaging contrast agent to visualize tumors or as a radio-sensitizing agent [170,171].

3-bromopyruvate (3-BrPA) has been identified as a potent inhibitor of glycolysis through its promiscuous inhibition of hexokinase-2 as well as glyceraldehyde-3-phosphate dehydrogenase (GAPDH). 3-BrPA has been widely studied as an alkylating agent, but its first anticancer properties were identified in 2001 as an inhibitor of hexokinase-2 [172-174].

Selectivity appears to depend on its uptake by overexpressed monocarboxylate transporter, SLC5A8 [174]. In addition to its use as a single agent, recent research has focused on combining 3-BrPA with other chemotherapies to overcome ATP-requiring multidrug resistance (MDR) mechanisms. Nakano et al. used 3-BrPA to sensitize MDR-expressing tumors to daunorubicin or doxorubicin treatment [175]. Similar work by Zhou et al. confirms that intracellular ATP is essential for drug resistance, and that disruption of cellular energy levels through inhibition of hexokinase-2 by 3-BrPA resensitized MDR cells to therapy [176].

Lonidamine was first identified as an inhibitor of aerobic glycolysis through inhibition of hexokinase-2 in tumor cells in 1981 [177,178]. As with 3-BrPA, inhibition of hexokinase-2 by lonidamine induced apoptosis [179]. Lonidamine acts as a single agent and has been extensively studied as a treatment for MDR [180,181]. Already approved for use as an anticancer chemotherapy in Europe, phase II clinical trials began in the United States in 2005 treating patients with benign prostatic hyperplasia (BPH) [179,182]. Despite reports of some cancer patients receiving 40 times the dose than patients in the US trial, and indications that prostate volumes were reduced during treatment, the US phase II trial was terminated due to liver toxicities and no subsequent trials have begun [182,183]. In an effort to harness the therapeutic efficacy of lonidamine against MDR and reduce toxicities due to dosage, Milane et al. have developed epidermal growth factor receptor (EGFR)-targeted nanoparticles encapsulating lonidamine and paclitaxel [183,184]. Orthotopic MDR-positive breast cancer xenografts treated with targeted drug-containing nanoparticles showed reduced tumor growth compared to treatment with blank nanoparticles. Transient weight losses were observed in all groups. Liver toxicities were highest in animals treated with soluble paclitaxel alone or soluble paclitaxel + lonidamine, and were less severe when drugs were bound to nanoparticles. Hematologic

analyses also revealed reduced toxicity following treatment with drug combinations encapsulated within nanoparticles. Overall, lonidamine is a promising hexokinase-2 inhibitor that may show clinical benefit either alone or in combination with other chemotherapies.

#### *Targeting Phosphofructokinases*

Phosphofructokinase-1 (PFK-1) catalyzes the phosphorylation of fructose-6-phosphate to fructose-1,6-bisphosphate in a rate-limiting step in the glycolytic pathway. Regulation of PFK-1 activity is reduced as a result of oncogene activation, such as Ras or Src, through elevated levels of fructose-2,6-bisphosphate's physiologic activator of PFK-1 [185,186]. Phosphofructokinase-2 (PFK-2), as well as the p53 target TIGAR, is a regulator of the steady-state level of intracellular fructose-2,6-bisphosphate, and the PFKFB3 isozyme has been identified to be overexpressed in leukemias and solid tumors [187-189]. Small molecule inhibitors targeting the substrate-binding domain of PFKFB3 have been identified as antineoplastic agents [189]. *In vitro* inhibition of recombinant PFKFB3 revealed 3PO (3-(3-Pyridinyl)-1-(4-Pyridinyl)-2-Propen-1-one) as a lead compound that inhibits PFKFB3 but does not affect activity of PFK-1. 3PO was further shown to inhibit normal cell cycling in several solid tumor and hematologic cell lines further inhibiting tumor growth in xenograft models of lung, breast, and leukemia by suppression of glycolytic flux [189].

To improve upon clinical limitations of 3PO, such as solubility and high preclinical doses, Akter et al. has engineered nanoparticle drug delivery systems for 3PO [190]. Encapsulating 3PO within a hydrophilic shell through conjugation to block copolymers improved 3PO bioavailability. 3PO conjugated block copolymers were also engineered with a hydrazone bond that is cleaved in acidic conditions ( $\text{pH} < 7.0$ ) to preferentially target acidic tumor microenvironments. *In vitro* experiments with 3PO containing micelles resulted in



significant cell death across several cell lines providing encouragement for future work in preclinical models.

In a separate study, N4A and YN1 were identified to be competitive inhibitors of PFKFB3 [191]. While treatment of cells with these novel compounds resulted in decreased glycolytic flux followed by cell death, selectivity of the drugs was not ideal, and further optimization of the drug scaffold is currently underway.

#### *Targeting Pyruvate Kinase M2*

Pyruvate kinase (PK) catalyzes the transfer of a phosphate from phosphoenolpyruvate to ADP in the final step of aerobic glycolysis, resulting in one molecule each of ATP and pyruvate. Of the four pyruvate kinase isoforms, PKM1 is expressed in most tissues. PKM2 is a splice variant of PKM1 that is primarily expressed in embryonic development, but is also reported to be the main isoform expressed in tumors [192]. PKM2 expression has been associated with the Warburg Effect, carcinogenesis, and tumor growth. Due to increased expression of PKM2, cancer patients typically have higher levels of PKM2 in plasma and saliva, and this is being investigated in a clinical trial to determine if salivary levels of PKM2 can be used as a biomarker for malignancy (NCT01130584).

TT-232 (TLN-232/CAP-232) is a somatostatin structural analog that has been shown to significantly reduce tumor growth in murine models, and has entered clinical trials for refractory metastatic RCC and melanoma (NCT00422786 and NCT00735332). TT-232 has antiinflammatory effects through its interaction with somatostatin receptor 4 (SSTR4), a G proteincoupled receptor, and antitumor effects mediated through its inhibition of PKM2 [193,194]. Unlike somatostatin, TT-232 is able to exhibit antitumor effects without the antisecretory activity that is required for somatostatin's efficacy in neuroendocrine tumors and

pancreatitis [195]. In addition to inhibition of PKM2, treatment of cells with TT-232 inhibits proliferation, induces cell cycle arrest, and initiates apoptosis [196,197]. Phase I clinical trials of TT-232 were successfully completed without significant adverse events, allowing entry into phase II trials.

#### *Targeting Pyruvate Dehydrogenase Kinase*

Following the conversion of phosphoenolpyruvate to pyruvate by PK, further oxidation of pyruvate is enabled by mitochondrial pyruvate dehydrogenase (PDH), which catalyzes the oxidative decarboxylation of pyruvate to acetyl-CoA, which can then enter the tricarboxylic acid (TCA) cycle. PDH is negatively regulated at three serine phosphorylation sites by pyruvate dehydrogenase kinase (PDK), which shifts glucose from oxidative to glycolytic metabolism [198].

Dichloroacetate (DCA) has been used clinically over the past several decades for the treatment of lactic acidosis and mitochondrial disorders [199]. DCA is an inexpensive, orally available drug that targets PDK [200-202], and has recently been shown to have anticancer effects both *in vitro* and *in vivo* [138,203]. The Michelakis group hypothesized that inhibition of PDK with DCA could shift glucose metabolism from glycolytic to oxidative, eliminating excessive lactic acid production observed in cancer cells [204]. Indeed, treatment of lung, glioblastoma, and breast cancer cells reversed cell metabolism from glycolytic to oxidative; and in doing so increased ROS production, decreased mitochondrial membrane potential, and sensitized cells to apoptosis. *In vivo* rodent studies demonstrated the antitumor properties of DCA by reducing overall tumor volumes and inducing apoptosis in a lung cancer xenograft model [204]. Further preclinical studies have shown DCA to have similar proapoptotic effects on endometrial cancer cells as well as sensitizing prostate cancer cells to radiation therapy

[203,205]. Numerous clinical trials are currently recruiting, or underway, to administer DCA as a single agent, or in combination with other chemotherapies or radiation, in a wide range of cancers. The first published data from clinical trials with DCA as an anticancer therapy was recently published [206]. Resected glioblastoma tissue from 49 patients treated with DCA confirmed mitochondrial depolarization in vivo. Five patients with either newly diagnosed or recurrent glioblastoma were placed on a treatment regimen of DCA with standard therapies, temozolomide (TMZ) and radiation therapy, after surgical tumor debulking. During a 15-month follow-up, toxicities were moderate, with peripheral neuropathy being the only toxicity noted with ~80% of patients remaining clinically stable 15 month after the onset of therapy.

#### *Targeting Lactate Dehydrogenase (LDH)*

Lactate dehydrogenase (LDH) catalyzes the interconversion of pyruvate and lactate. LDH is a tetrameric protein made from two different (heart and muscle) subunits. LDH5 (a.k.a. LDH-A or M<sub>4</sub>) is usually expressed in muscle tissue and has a low K<sub>m</sub> for pyruvate, while LDH1 (a.k.a. H<sub>4</sub>) is more ubiquitously expressed and has a lower K<sub>m</sub> for lactate. During the redox reaction of pyruvate to lactate, NADH is oxidized to NAD<sup>+</sup>, replenishing intracellular levels of NAD<sup>+</sup> and allowing glycolysis to become self-sufficient. LDH5 subunits are transcriptionally regulated by HIF1 $\alpha$  and hence levels of LDH5 are increased in HIF1 $\alpha$ -positive cancers [207,208]. Recently, LDH5 has been shown to be important for tumor initiation, although the exact mechanism is currently unclear [209-211].

Gossypol, a cotton seed extract, has been studied as an antifertility drug that inhibits sperm LDH, and further experimentation has revealed cross inhibition of gossypol analogs to LDH5 [212]. More recent gossypol analog studies focusing on 8-deoxyhemigossylic derivatives that target the NADH and pyruvate binding sites of LDH identified 3-dihydroxy-6-methyl-7--

(phenylmethyl)-4-propylnaphthalene-1-carboxylic acid, or FX11, as a preferential inhibitor of LDH5 [213]. Treatment of human lymphoma cells, P493, with FX11 correlated with knockdown of LDH5 by siRNA by increasing oxygen consumption, ROS production, decreasing ATP levels, and cell death [214]. Similar results were observed in RCC and breast cell lines, with the sensitivity to FX11 being highest in cells with a more glycolytic phenotype. *In vivo* studies also indicated that FX11 inhibits both carcinogenesis and tumor progression of lymphoma and pancreatic tumors [214]. It was notable that these treatments were not myelosuppressive or toxic, despite the presence of LDH-A in normal tissues. Although a promising candidate drug to target the glycolytic phenotype of tumors, FX11 is not yet in clinical trials.

The most recent research for novel LDH5 inhibitors began in an attempt to fabricate a drug suitable for entry into the clinic. From this research, a series of N-hydroxyindole-based inhibitors were generated to have specificity for LDH5 over LDH1 [215]. *In vitro* experiments showed promising  $K_i$  values in the low micromolar range for some of the compounds synthesized. Additionally, cellular assays resulted in reduced lactate production and retarded cellular proliferation. Virtual screening of the National Cancer Institute (NCI) Diversity Set by another group identified galloflavin as a novel LDH inhibitor [212]. Galloflavin was further characterized and shown to bind preferentially to free enzyme without blocking either the pyruvate or NADH binding sites. Enzymatic assays using purified LDH1 and LDH5 showed that galloflavin acts as an inhibitor of both isoforms. Cellular assays confirmed *in vivo* activity of galloflavin with reduced lactate production, a reduction of cellular ATP levels, and decreased cellular proliferation. Preliminary murine experiments suggest that galloflavin could be a well-tolerated drug that should be developed further.

## Targeting Acidosis

The microenvironment of solid tumors is known to be more acidic (pH 6.5–6.9) than the physiological pH of normal tissue (pH 7.2–7.5), which can be attributed to a tumor's increased glycolytic flux and poor vasculature perfusion [15,16]. Acidic microenvironments have been shown to increase the invasiveness of a tumor, leading to increased metastasis [26,216,217]. In this section, we will describe drugs that target acidosis in tumors and systematic approaches to reduce acidosis in the tumor microenvironment (**Figure 2.2**).

### *Targeting Proton Transport*

Metabolically produced hydrogen ions (acid) can be exported from cells by a variety of mechanisms including, inter alia, sodium-hydrogen exchange (NHE), anion exchangers (AEs), vacuolar ATPases (V-ATPases), and membrane-bound carbonic anhydrases (CAs) [218]. NHE and AE are ubiquitously expressed and have proven to be poor anticancer drug targets, either through inefficacy or through toxicity, and these have been reviewed [219]. Following, we will discuss some of the newer, less well-explored members of this class of transporters. CAs are metalloenzymes that catalyze the interconversion of carbon dioxide and water to bicarbonate and protons. Mammalian carbonic anhydrases ( $\alpha$ -CAs) can be cytosolic, mitochondrial, secreted, or membrane-bound. The primary function of mammalian CAs is to maintain the acid–base balance of cells, tissue, and blood. As aerobic glycolysis becomes the primary means of energy production for a tumor cell, the ability to regulate physiological pH<sub>i</sub> becomes paramount to maintain cellular processes such as proliferation as well as inhibition of apoptosis [220,221]. CAIX and CAXII are two transmembrane CAs that have been identified to be associated with tumor progression and metastasis [222-224]. As a transcriptional target of HIF1 $\alpha$ , CAIX expression is upregulated in hypoxic tissue and has been shown to be a poor prognostic marker

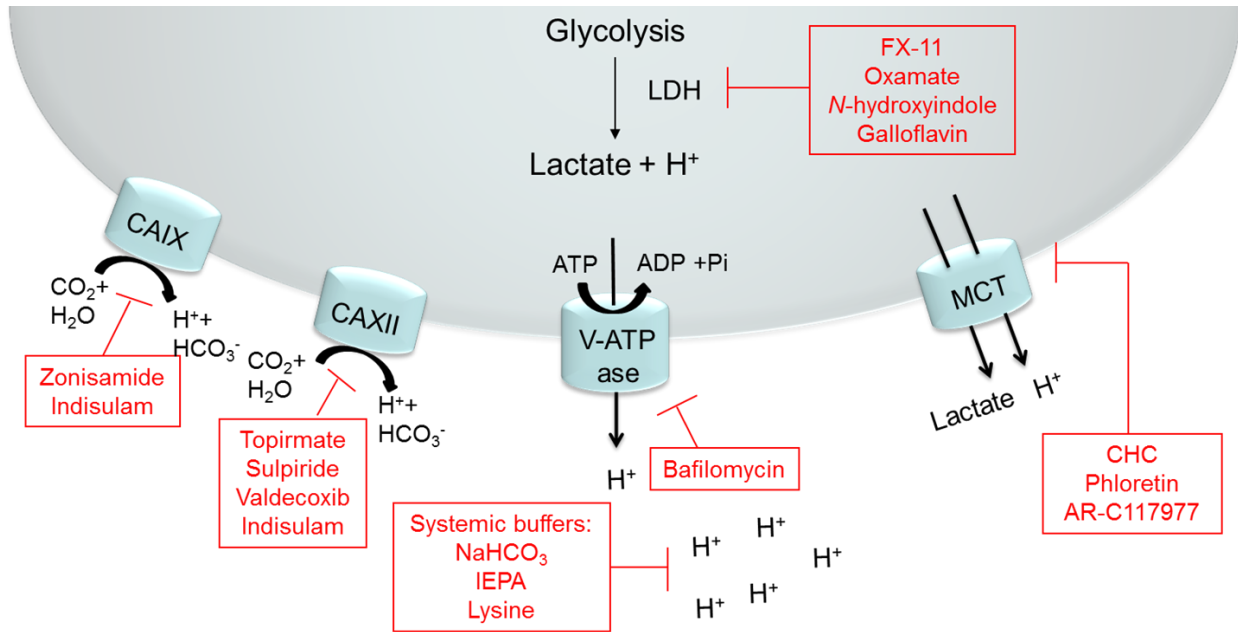


**Figure 2.2.** Proteins that contribute to tumor acidosis and their inhibitors. The figure depicts proteins and transporters that contribute to extracellular acidosis in a tumor due to increased lactate production from increased glycolytic flux. Included are CAIX and CAXII, carbonic anhydrases that catalyze the interconversion between carbon dioxide and water to bicarbonate and protons; and V-ATPases and MCTs, which allow transport of H<sup>+</sup> into the extracellular environment. Inhibitors of the proteins that contribute to tumor acidosis appear in boxes.

in several cancer types, including breast cancer [225]. CAXII is also overexpressed in tumors and is associated with disease progression and response to therapy [223,226]. As carbon dioxide is hydrated, HCO<sub>3</sub><sup>-</sup> is moved intracellularly to maintain pHi while protons are pumped into the extracellular environment of a tumor, decreasing the pHe [226] promoting an aggressive metastatic environment [227,228]. Members of α-CA require zinc for activity, making them susceptible to inhibition by sulfonamides, which coordinates with the zinc ion found in the active sites of CAs. Sulfonamide analogs, such as topiramate, sulpiride, and valdecoxib, have been shown to potently inhibit CAXII, while zonisamide has been identified to be an effective inhibitor of CAIX (Greenberger et al., 2008; Li et al., 2005). Perhaps the most studied sulfonamide analog, indisulam, has high affinity for CAIX and CAXII, in addition to seven other

CAs [229,230]. Indisulam inhibits CAIX in nanomolar quantities and shows efficacy against tumor xenografts in vivo. In addition to CAIX inhibition, indisulam induced sequelae, such as disruption of the G1/G2 phases of the cell cycle and expression changes of genes related to cell adhesion, cell signaling, and altered glucose metabolism [231-233].

Clinical trials for the treatment of solid tumors with indisulam have been ongoing for the past decade. Five phase I clinical trials have been conducted focusing on optimizing the dosing regimen of indisulam to patients with solid tumors [234-238]. Fatigue and mucositis were noted as adverse events during the trial, and reversible neutropenia and thrombocytopenia were dose-limiting toxicities. Phase II trials have been completed on patients with platinum-pretreated NSCLC in a multicenter study [239]. While some patients experienced a positive response to indisulam, the effect was not long term. Objective responses to indisulam therapy were not achieved during this trial, which may be attributed to inherent difficulties of being a second-line therapy to platinum-pretreated NSCLC [240]. Further trials are being conducted using indisulam as both a single agent and as combination therapy for different tumor types.

Another membrane-bound transporter involved with acidification of the tumor microenvironment is V-ATPase [241,242]. In tumor cells, V-ATPases can prevent intracellular acidification by transporting protons into lysosomal compartments that are released into extracellular space, or by directly pumping protons into the tumor microenvironment [243]. In addition to promoting tumor metastasis by acidifying the tumor microenvironment, overexpression of V-ATPases following chemotherapy treatment appears to be a drug resistance mechanism [244,245]. In 1988, bafilomycins were identified to be potent inhibitors of V-ATPases [246]. Since this discovery, several generations of V-ATPase inhibitors have been developed and investigated and can be classified into five families of V-ATPase inhibitors [247].

While targeting V-ATPases is desirable as an anticancer target to reduce metastatic potential and drug resistance, clinical relevance is unknown due to likely toxicities [248-251].

The monocarboxylate transporter 1, MCT1, a membrane-bound transporter is required for lactate (coupled with a proton) to move across the plasma membrane. MCT1 has been documented to have dysregulated expression in colorectal, breast, and cervical carcinomas [252-254]. Inhibition of MCT1 reduces intracellular pH and induces apoptosis, making it an attractive target for antitumorigenic therapy [255]. Several small molecule inhibitors of MCT1 have been identified including *o*-cyano-4-hydroxycinnamate (CHC), phloretin, and AR-C117977 [255,256]. Currently, no MCT1 inhibitors are being investigated clinically.

#### *Manipulating Tumor Microenvironment pH*

Orally distributed systemic buffers have been shown to be an effective way to increase pHe of a tumor [257]. Continuous oral delivery of sodium bicarbonate to tumor bearing mice have been shown to increase selectively the pHe of a tumor and are effective at reducing the rate and size of metastasis, without changing the volume of the primary tumor [258,259]. In addition to reducing metastasis, buffering with sodium bicarbonate increased breast tumors sensitivity to doxorubicin and mitoxantrone, chemotherapies known to be ineffective in acidic tumor environments [25,258,260]. A similar reduction in metastasis was achieved using orally available imidazole(IEPA) or lysine buffers in murine experimental metastasis models [261,262]. Buffer therapy will be more thoroughly detailed in Chapter 3 of this dissertation.

#### **Manipulating the Microenvironment for Therapeutic Benefit**

Combination therapy has been a long-standing strategy for the treatment of cancer patients. Drug resistance to single agent regimens is a major obstacle in the clinic and combination therapy aims to target more of a heterogeneous tumor, reducing the ability of a



tumor to develop resistance. The commonality of phenotypic characteristics of the tumor microenvironment between patients encourages the targeting of the microenvironment in combination with other cytotoxic chemotherapies. In the earlier sections, I detailed a number of approaches to target the tumor metabolic phenotype as well as describing strategies to manipulate hypoxia (exacerbation of hypoxia metabolically or by reducing oxygen delivery) for therapeutic benefit. In this section, we will describe additional combination therapies that manipulate the metabolic or physiologic phenotype of cancers.

2DG, the glucose analog hexokinase inhibitor, has been unsuccessful as a single agent chemotherapy in the clinic, but has recently been of interest as a sensitizer of cancer cells to other chemotherapies or radiation therapy [263-266]. Targeting metabolic pathways or DNA integrity through ionizing radiation (IR) or treatment with drugs like metformin in combination with 2DG treatment can lead to significant antitumor effects [267,268]. Clinical studies have verified that combination therapy of 2DG with IR is safe for patients, and reduced toxicity associated with IR in some patients [269,270]. Preclinical studies using 2DG as a sensitizer are promising; however, clinical studies investigating the efficacy need to be completed before 2DG sensitizing treatment becomes routine.

VEGF inhibitors, and antiangiogenic inhibitors in general, have similarly unintended effects on the tumor microenvironment, resulting in normalization of the tumor vasculature. Vascular normalization, first described by Rakesh K. Jain, is a maturation of existing immature vessels within a tumor when neoangiogenesis is inhibited [166,271,272]. Vascular maturation results in better oxygen delivery and tumor perfusion, relieving interstitial tumor pressure which is hypothesized to provide better drug delivery to patients and reduce resistance to chemotherapy [272]. Treatment of tumor bearing mice with VEGF inhibitor DC101 resulted in tumor vascular

remodeling, where vasculature became nonleaky and more organized [273]. Further studies have been conducted to study the timing of vascular normalization with optimal sensitivity to radiation treatment [274,275]. Vascular normalization has been observed in patients with nonmetastatic rectal adenocarcinoma receiving bevacizumab [276-278].

Although tumor reduction was not observed, microvessel density and vascular permeability decreased and histological analysis confirmed the presence of mature vasculature within tumors. Preclinical and clinical studies have provided support for the vascular normalization hypothesis; however, more studies need to be completed to fully optimize the normalization window to improve efficacy of this treatment.

## **Conclusion**

Initially a barrier during carcinogenesis, the tumor microenvironment during the later stages of carcinogenesis provides an advantage for a tumor to outcompete normal tissue, becoming more aggressive and metastatic. Additionally, common characteristics of a tumor microenvironment provide a haven of protection for a tumor against chemotherapies. The immature and chaotic vasculature that exacerbates hypoxia within a tumor also provides minimal perfusion through a tumor for effective drug therapy, and extracellular acidosis due to preferential metabolism through aerobic glycolysis creates an environment that effectively traps weakly basic drugs from moving intracellularly. Extensive research has been focused on targeting the tumor microenvironment, providing clinicians with chemotherapies that target the glycolytic pathway, acidosis, hypoxia, and hypoxia response pathways (**Table 2.1**).

Manipulation of the tumor microenvironment has been an effective strategy for the treatment of a wide range of patients and will continue to be an important area of drug discovery in the future.

## CHAPTER 3

### MECHANISMS OF BUFFER THERAPY RESISTANCE

#### **Note to Reader**

Portions of this chapter have been previously published in *Neoplasia* 2014, 16:354-364 [279]; and 2013, 15:1125-1137 [280]; *Advances in Pharmacology* 2012, 65:63-107 [34]; *Journal of Cancer Science & Therapy* 2011, Suppl 1:S1-004; and *Journal of Nutrition & Food Sciences* 2012, S2 [281] and are utilized with permission of the publisher.

#### **Introduction**

##### *Altered Tumor Metabolism*

Otto Warburg first described an increased rate of aerobic glycolysis followed by lactic acid fermentation in cancer cells in 1924, later termed the *Warburg Effect* [23]. Almost a century of research has confirmed Warburg's initial observation, solidifying increased glycolytic flux as a common cancer phenotype [29]. Elevated expression of glycolytic genes are observed in ~70% of human cancers [282]. Warburg hypothesized the metabolic shift away from oxidative phosphorylation was due to mitochondrial dysfunction, yet this has not been substantiated [283]. While interest in cancer metabolism peaked in the middle part of the twentieth century, interest waned with the advent of molecular biological techniques in the 1970s. In 1976, Sidney Weinhouse famously declared that "***Since our perspectives have broadened over the years, the burning issues of glycolysis and respiration in cancer now flicker only dimly***" [284]. The

development of  $^{18}\text{F}$ -fluorodeoxyglucose ( $^{18}\text{F}$ FDG)-PET imaging to visualize increased glucose uptake in tumors and metastasis has rekindled interest in cancer metabolism, and is commonly used clinically for diagnosis and disease monitoring [285].

At first glance, the switch of glucose metabolism from oxidative phosphorylation to aerobic glycolysis seems paradoxical. Aerobic glycolysis is a significantly less efficient method to generate ATP from glucose than oxidative phosphorylation. For tumor cells that likely have reduced access to nutrients and are proliferating quickly, effective use of available nutrients is paramount. Significant effort has focused on understanding the altered metabolic phenotype and its benefit to proliferating tumor cells.

Aside from ATP production, many biochemical intermediates are produced from glucose metabolism that contribute to biomass production. Anabolic pathways are essential pathways for proliferating cells, and are likely one of the key reasons glucose is metabolized so differently than normal cells. Following phosphorylation by hexokinase, glucose-6-phosphate (G-6-P) can be shuttled through the pentose phosphate shunt for nucleotide synthesis, producing NADPH (nicotinamide adenine dinucleotide phosphate, reduced) during the process. Movement of G-6-P through the pentose phosphate shunt is facilitated in part by tumoral expression of pyruvate kinase M2 (PKM2), the final enzyme in glycolysis that catalyzes the transfer of phosphate from phosphoenolpyruvate (PEP) to ATP and producing pyruvate [192]. Importantly, PKM2 is a less efficient enzyme than its isoform PKM1 that is expressed in normal tissue, and is negatively regulated by oncogenic tyrosine kinase signaling pathways [192,286]. A reduction in efficiency during the final steps of glycolysis creates a bottleneck in the glycolytic pathway, and redirects G-6-P into the pentose phosphate pathway, allowing for nucleotide synthesis, an essential requirement for proliferating cells.

An alternate hypothesis has been proposed by Epstein et al to explain the Warburg Effect from an energetic perspective [287]. They propose that increased aerobic glycolysis in cancer cells serves to meet rapidly changing energetic demands from membrane pumps. Oxidative phosphorylation, while extremely efficient, is very slow to increase throughput to meet acute increases in energetic demand. They propose that cancer cells use oxidative phosphorylation to maintain the baseline energy demands, while using glycolysis to feed ATP to membrane pumps on demand during proliferation and migration. This hypothesis is supported by the localization of key glycolytic enzymes near the membrane of cells, and a rapid increase in glycolytic flux upon stimulation of membrane transporters.

Any pyruvate that is produced during glycolysis has several potential metabolic fates. Through aerobic glycolysis, pyruvate is converted to lactate by lactate dehydrogenase, which will be discussed more thoroughly below. Alternatively, pyruvate can pass through the mitochondrial membrane, where it is converted into acetyl-CoA by pyruvate dehydrogenase. Entry into the TCA cycle requires further conversion to citrate, which can also be shuttled back into the cytoplasm under high ATP/ADP and NADH/NAD<sup>+</sup> conditions found in proliferating cells [192,288], and converted into acetyl-CoA. Once in the cytoplasm, acetyl-CoA is used for amino acid and lipid synthesis, essential anabolic pathways for proliferating tumor cells. In addition to biomass production, the alternative metabolic pathways described above, generate NADPH. NADPH is required for macromolecular synthesis and is an important regulator of the cellular redox state which is often disrupted in tumors [289].

#### *Tumor Acidosis and the Metastatic Cascade*

Lactate is the canonical product of aerobic glycolysis, produced from pyruvate by lactate dehydrogenase. Lactate production is the most common fate of glucose, and accounts for as

much as 90% of glucose taken in by glioblastoma cells [290]. Lactate has traditionally been considered a waste product of glycolysis and is shuttled extracellularly with  $H^+$ , to maintain intracellular pH ( $pH_i$ ). Tumors frequently upregulate membrane proton pumps to export excess intracellular acid, including monocarboxylate and proton transporters, sodium-hydrogen exchangers (NHE), anion exchangers (AEs), vacuolar ATPases (V-ATPases), and membrane-bound carbonic anhydrases (CAs) [218,253,291]. One such transporter, carbonic anhydrase-9 (CA-IX) is a negative prognostic indicator in many cancers [292,293]. Proton and lactic acid export, combined with poor vascular perfusion, cause the tumor to become highly acidic (pH 6.5 - 6.9) relative to the physiological pH of normal tissues (pH 7.2-7.5) [15,16]. Acidic microenvironments have been shown to increase cellular motility and invasiveness of a tumor, leading to increased metastasis [26,216,217].

Progression to metastatic disease remains the highest mortality risk for cancer patients, despite significant efforts to therapeutically target metastatic lesions [29,294]. Metastatic disease involves the movement of cancer cells from the primary tumor into secondary growths in distant organs. The process, known as the metastatic cascade, involves a series of steps involving: 1) acquisition of an invasive phenotype and invasion into the local stroma around the primary tumor site; 2) intravasation into vasculature; 3) survival of circulating tumor cells (CTCs) in the vasculature; 4) extravasation into the secondary organ; and 5) colonization and growth in the secondary organ site to form a successful metastasis. While metastatic disease is a fairly common clinical phenomenon, metastasis is a highly inefficient process. The vast majority of cancer cells that begin movement away from the primary tumor will die throughout the process, and  $< 0.01\%$  will succeed to form full fledged metastasis in secondary organs [294]. Interestingly, the latency period for the metastatic cascade varies widely across cancer types. For instance,

breast cancer metastasis usually occurs over years, even decades; while lung or melanoma patients suffer metastatic dissemination much faster and is sometimes present at diagnosis. In fact, the recurrence-free survival rate for patients with stage I breast cancer is 94% [295], while stage I lung adenocarcinoma patients are around 75% [296] and melanoma patients usually reoccur within 2 years [297,298]. Another phenomenon commonly observed in metastatic disease is the frequency with which cancers commonly metastasize to the same secondary organs. Metastatic disease is often confined to specific secondary organs, which is dependent on the primary cancer type. For example, breast cancers typically metastasize to the brain, bone, liver and lungs; while colorectal and pancreatic cancers metastasize to the liver and lungs (**Table 3.1**). The complexity of the metastatic cascade, including latency and secondary organ site variability, has encouraged significant efforts to find similarities in the mechanisms of metastasis across tumor types with the ultimate goal of treating or preventing metastatic disease.

**Table 3.1** Common Sites of Metastatic Disease

<b>Cancer Type</b>	<b>Site of Metastatic Disease</b>	
Breast Cancer	Bone, lungs, liver & brain	[299-303]
Prostate Cancer	Bone	[304]
Lung Cancer	Brain, bone, & liver	[305]
Colorectal Cancer	Liver & lungs	[306]
Melanoma	Lungs, brain, skin & liver	[307]

*Proteases and Metastatic Disease*

A class of enzymes, proteases, has received significant attention due to their widespread role in the metastatic cascade. Acidity and proteases are tightly linked when described in the “acid-mediated invasion” hypothesis which proposes that acidification of the tumor

microenvironment can be associated with cathepsin release to trigger matrix remodeling [291]. This dissertation will focus specifically on two classes of proteases, matrix metalloproteinases (MMPs) and cysteine cathepsins. MMPs are zinc-dependent endopeptidases. Their overexpression has been observed in a number of tumors and is a predictor of progression to metastatic disease [308-310]. MMPs are transcribed as pro-enzymes that must be activated, either by proteolytic cleavage or chemical modifications, which can occur intracellularly or extracellularly after secretion [308,311]. MMPs are regulated through multiple levels; through gene expression, compartmentalization intracellularly and extracellularly, activation of pro-enzyme to active enzyme, and by the presence of tissue inhibitors of metalloproteinases (TIMPs) [285]. MMPs breakdown components of the extracellular matrix (ECM), and have been shown to participate in every step of the metastatic cascade [308]. Due to the extensive involvement of MMPs in the metastatic cascade, and the ability to target MMP enzymes with small molecules [312], clinical trials began in earnest in the 1990s. Unfortunately, clinical use of MMP inhibitors (MMPi) were largely considered a failure for a variety of reasons [313]. First, timing of MMPi administration in the process of cancer progression is essential for efficacy, and clinical trials were not designed with this in mind [260,314]. Pre-clinical models showing efficacy of MMPi were treated during the early stages of cancer development and progression, while clinical trials were conducted in end-stage patients with widespread disease [315-317]. Second, broad inhibitor activity towards multiple MMPs resulted in dose-limiting toxicities in trials, which may be alleviated with more specific inhibitors [312,314].

Another type of protease, cysteine cathepsins, are lysosomal in origin but can be excreted into the tumor microenvironment, where they degrade the ECM [318-320]. Cysteine cathepsins, like MMPs, have been implicated in cancer progression and metastasis through their interaction



in complex networks and protein signaling pathways [321,322]. Regulation of cysteine cathepsins occurs at the gene expression level [323], localization intracellularly and extracellularly, activation of pro-enzymes to activate the enzymatic activity, and through endogenous inhibitors [322]. Of particular interest to the work in this thesis, Cathepsin B expression and activity has been shown to be regulated by pH. The pH of the tumor microenvironment regulates the secretion of Cathepsin B into the microenvironment, which has been linked to tumor progression [324,325].

Recently, Rothberg et al. characterized the impact of the acidic tumor microenvironment on the release of active Cathepsin B from MDA-MB-231 cells into the pericellular tumor microenvironment [280]. Live-cell proteolytic imaging techniques [326] were used to confirm increased degradation of DQ-collagen IV upon exposure to acidic culture. A fluorescent activity-based probe, GB-123 [327], that binds active Cathepsin B confirmed pericellular localization of active Cathepsin B under acidic conditions. To determine if Cathepsin B activity is regulated by  $\text{pH}_e$  *in vivo*, GB-123 was used to quantify Cathepsin B activity in tumors. Mice bearing orthotopic MDA-MB-231 tumors were provided tap water or 200 mM bicarbonate (to raise the  $\text{pH}_e$  of the tumors). Tap treated mice had significantly more GB-123 within their tumors, confirming that acidic tumor conditions increase Cathepsin B activity *in vivo* (**Figure 3.1**), and that treatment with buffer therapy can reduce Cathepsin B activity by increasing  $\text{pH}_e$ .

#### *Cellular Migration in Metastasis*

Cell migration through tissue can occur through different mechanisms, either as single cells or in a collective fashion [328,329]. Cell migration patterns have been further classified based on cellular morphology of rounded and elongated cell types in 3D culture systems as well as *in-vivo* tumor models [330]. Additionally, tumor acidity and expression of proton pumps have

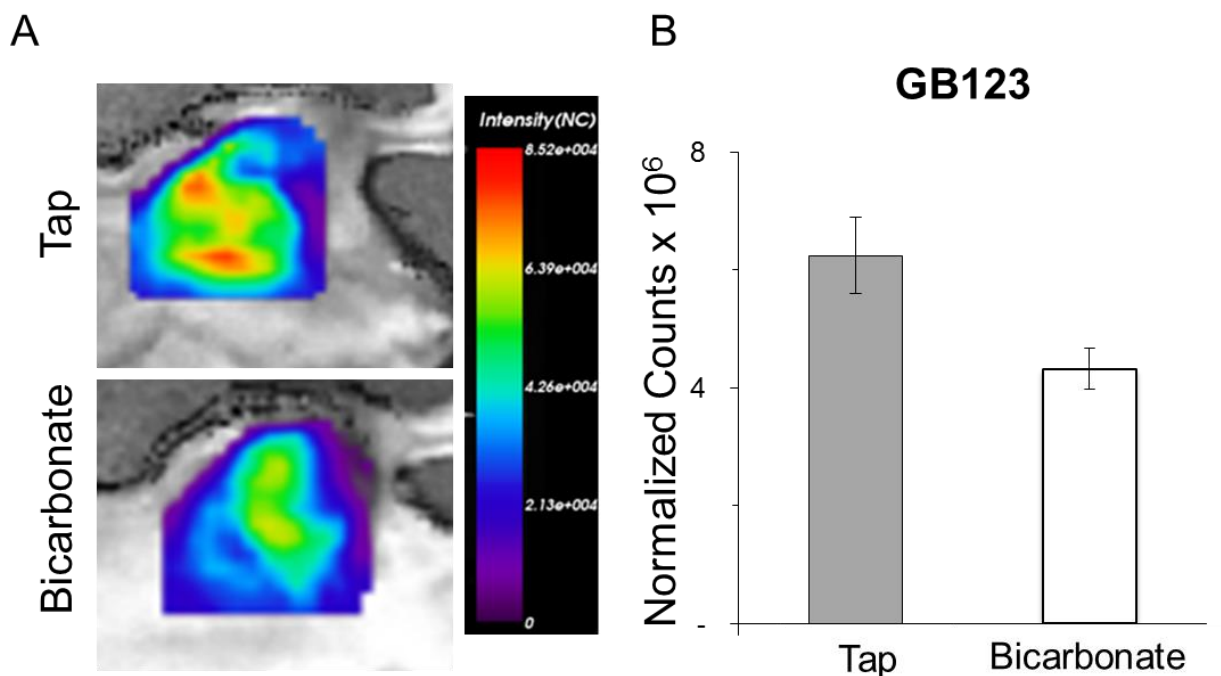


**Figure 3.1** *In vivo* buffering of tumor  $\text{pH}_e$  reduced tumor binding of GB123. (A) Enlarged representative fluorescent images of MDA-MB-231 orthotopic tumors showing retention of GB123 18 hours post-injection. (B) Average normalized counts of GB123 retained in MDA-MB-231 orthotopic tumors  $\pm$  SEM; a one-tailed unpaired *t* test was used to determine significance,  $p = 0.03$

been associated with increased cellular migration and invasion in breast and melanoma cell lines [331-333].

#### *Manipulating Tumor Acidosis with Systemic Buffer Therapy*

As acidosis is a common phenotype in solid tumors, we have developed a strategy to neutralize acidity using orally ingested buffers [257]. We have shown previously that treatment of mice with orally available buffers is efficacious in reducing spontaneous and experimental metastasis by increasing extracellular pH ( $\text{pH}_e$ ) due to higher buffering capacity of blood [259]. This is a targeted effect, as it only brings into balance the pH of tissues that were previously out of the physiological range [257]. Increased tumor  $\text{pH}_e$  following treatment with oral buffers has been confirmed through MRI and microelectrodes [259,261]. Sodium bicarbonate ( $\text{pK}_a=6.4$ ), 2-

imidazole-1-yl-3-ethoxycarbonylpropionic acid (IEPA) ( $pK_a=6.9$ ), and free-base lysine ( $pK_a=10$ ) have all been shown to be effective in reducing metastases *in-vivo* [259,261,334].

Initial studies focused on the reduction on metastasis formation following treatment with buffer therapy, as there was no observable reduction in tumor volume reduction [259]. Further studies using a genetically engineered prostate cancer model [Transgenic Adenocarcinoma of the Mouse Prostate (TRAMP)], however, show that carcinogenesis can be inhibited by buffer therapy [262]. The timing of buffer therapy initiation proved to be imperative for optimal efficacy. When TRAMP pups were administered buffer therapy early, at 4 weeks of age, development of prostate tumors was potently inhibited. If buffer therapy was delayed until the TRAMP mice were 10 weeks of age, the therapy was ineffective in preventing tumor formation. Importantly, mice that were treated at 10 weeks of age still benefited from treatment with buffer therapy, as metastatic formation was significantly inhibited. Future studies to optimize buffer therapy regimens are necessary to fully understand the potential for clinical efficacy of buffer therapy.

Treatment with buffer therapy is non-toxic, as mice maintain their weight, blood pH, renal function and immune cell distribution throughout the course of treatment [259,261,334]. While non-toxic, treatment with sodium bicarbonate may be of concern for patients suffering from hypertension, due to the excess sodium counter-ion that is simultaneously dosed with bicarbonate. Treatment with alternate buffers, such as lysine, tris, or IEPA, would overcome this limitation, though likely at a higher cost of treatment. Of the currently available buffers, lysine is the most efficacious as it has the highest  $pK_a$  of the three [257].

To confirm that buffer therapy reduces metastasis formation through buffering, the buffering capacity of free-base lysine was significantly reduced by lowering the pH from pH

10.0 to pH 8.4 (below the second pKa) prior to treatment of mice. Mice were then injected with luciferase expressing PC3M cells via tail vein injection in an experimental metastasis model. Metastatic formation was measured weekly by bioluminescent imaging, which showed that reducing the buffering capacity of lysine rendered the therapy significantly less effective in preventing metastatic formation than lysine pH 10 (**Figure 3.2**) [281]. This experiment confirms that buffering capacity is required for efficacy of buffer therapy in reducing metastatic formation.

Notably, the efficacy of buffer therapy is not universally observed. Metastases in two cell lines; MDA-MB-231, human breast adenocarcinoma; and PC3M, prostate adenocarcinoma; are both inhibited by buffer therapy, while B16-F10 cells, murine melanoma, and LL/2 cells, murine lung carcinoma, were resistant to the same treatment [259,261,334]. The success of buffer therapy suggests that, at least in sensitive cells, there is a metastatic mechanism that has an acidic pH optimum. This study investigates the mechanisms of buffer therapy resistance. The observation that buffering is not universally efficacious led us to hypothesize that resistant and sensitive lines utilize different metastatic mechanisms, one that is pH-independent and one that is pH-dependent. Metabolic profiling confirms that buffer-sensitive lines have a much more robust glycolytic phenotype, compared to resistant lines, and that this is coupled to increased tumor acidification. In contrast, resistant lines constitutively expressed proteases in a pH-independent fashion, compared to sensitive lines whose protease activities were low and pH-dependent. Acidic pH<sub>e</sub> results in morphological changes in sensitive cells, while resistant cells were unaffected. We propose that sensitive cells activate proteases and alter their morphology by acidifying their microenvironment, which can be inhibited by buffer therapy and that resistant cells have constitutively active protease release.

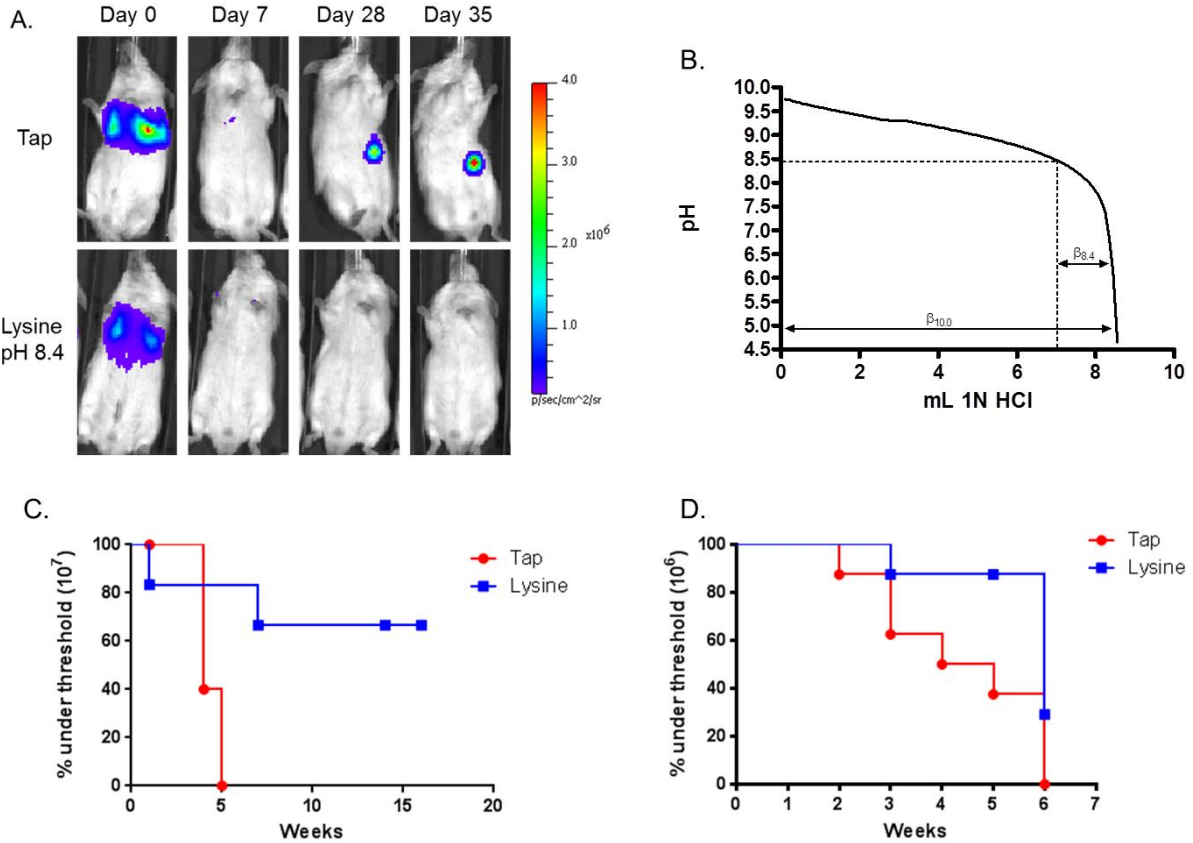


**Figure 3.2** Lysine free base reduces metastases through pH buffering. SCID mice were divided into two cohorts: tap water and lysine, which received supplementation of lysine free base in drinking water at pH 8.4. Both groups were injected with bioluminescent PC3M cells one week following initiation of treatment. (A) Representative bioluminescent images of mice receiving tap water or lysine pH 8.4 throughout the course of the experiment. (B) Lysine was titrated to pH 8.4 using HCl (1N), a pH at which the pH buffering capacity is significantly reduced ( $\beta_{10.0} = 8.5 \text{ mEq}$  vs  $\beta_{8.4} = 1.5 \text{ mEq}$ ). Lethal burden thresholds for survival curves were set at 3-fold background signal (Rose criterion), which was set by the measuring the bioluminescent signal one week post injection. (C) Survival curve of mice treated with lysine pH 10.0 showed a significant increase in overall survival compared to tap water ( $p = 0.004$ ). (D) Survival curve of mice treated with “de-buffered” lysine pH 8.4 showed a reducing in survival benefit compared to the control group ( $p = 0.04$ ). Log-rank (Mantle-Cox) tests were used to determine significance of survival data.

## Results

### *Efficacy of Lysine Buffer Therapy is not Universal*

We have previously shown that experimental metastasis of PC3M cells was inhibited by 200 mM lysine (pH = 10.1) (performed by Arig Ibrahim Hashim) (**Figure 3.3**) [281,334].

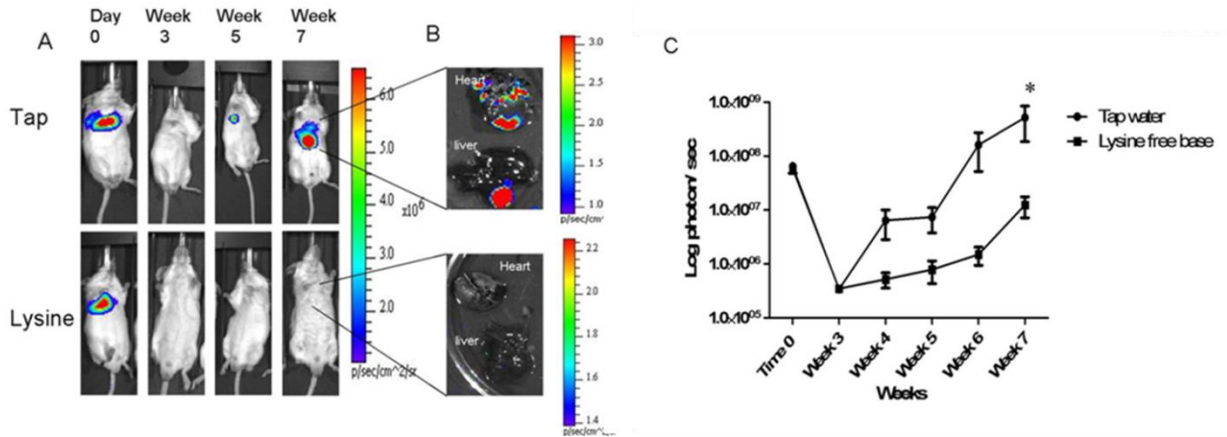


**Figure 3.3** Sensitivity of PC3M<sub>5</sub> to treatment with lysine buffer therapy. (A) Representative bioluminescent images of PC3M<sub>5</sub> metastasis in SCID mice. (B) *Ex vivo* bioluminescent imaging of PC3M<sub>5</sub> metastasis. (C) Graphic representation of bioluminescent imaging of PC3M<sub>5</sub> metastasis. Data is reported as log photons/sec ± SEM. s, sensitive

Importantly, we have shown previously that neutralized lysine (pH = 8.4) was much less effective in preventing metastases than lysine (pH = 10.1), showing the effect was due to buffering capacity (**Figure 3.2**) [281]. In the current study, we sought to identify additional lysine-sensitive and -resistant cell lines using experimental metastasis models. Mice were pretreated with 200mM lysine or tap water for one week prior to intravenous injection of Firefly-luciferase expressing cells in an experimental metastasis model. Metastasis formation was monitored weekly or bi-weekly with bioluminescent imaging, and presence of metastasis was confirmed with *ex vivo* imaging post-mortem and histological analysis. Consistent with previous work, B16-F10 metastasis were unaffected by lysine treatment (**Figure 3.4**) [259]. LL/2 cells were similarly unresponsive to lysine treatment, showing no difference in metastasis formation or survival benefit with treatment (**Figure 3.5**). MDA-MB-231 cells experienced significantly lower metastatic burden following therapy ( $p < 0.05$ ), which translated into a significant survival benefit ( $p < 0.05$ ) (**Figure 3.6**). HCT116 cells had not previously been tested using an experimental metastasis model, but had shown a reduction in local invasion in a window-

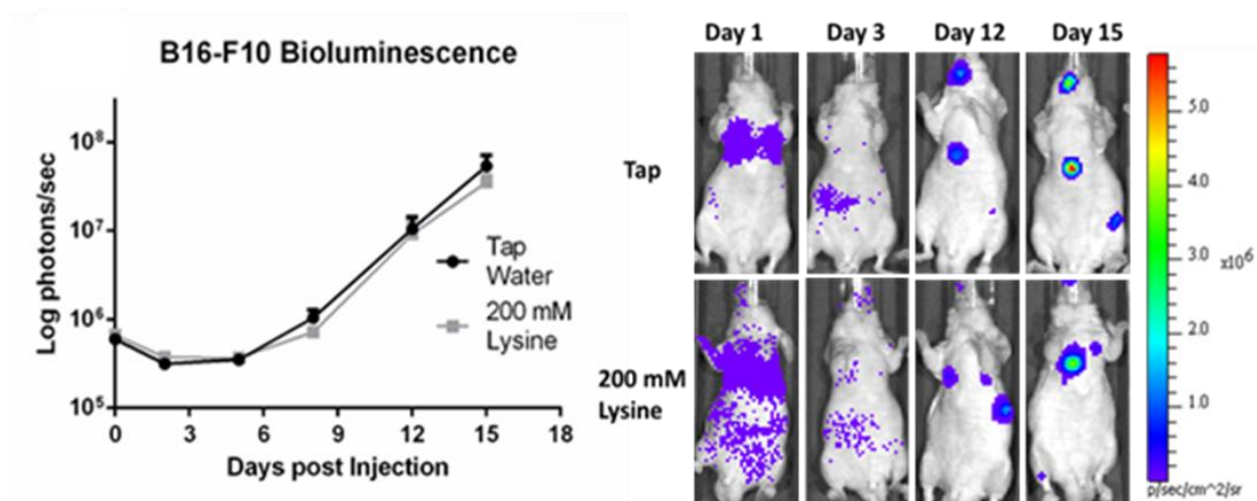


**Figure 3.4** Resistance of B16-F10<sub>R</sub> to treatment with lysine buffer therapy. Effect of lysine was determined by pre-treating SCID-beige mice for a week before tail vein injection of B16-F10<sub>R</sub> cells stably expressing Firefly-luciferase in an experimental metastasis model. Treatment of 200 mM lysine was administered continuously throughout the experiment. Bioluminescent imaging of B16-F10<sub>R</sub> metastasis (Tap  $n = 10$ , Lysine  $n = 10$ ) shows buffer therapy is ineffective (left). Representative bioluminescent images of one mouse per cohort are shown throughout the course of the experiment (right). Metastasis formation was measured by bioluminescent imaging, reported as log photons/sec  $\pm$  SEM. <sub>R</sub>, resistant

chamber model when treated with 200mM bicarbonate [291]. In contrast to those results, treatment of mice with lysine had no effect on HCT116 metastatic formation or survival (**Figure 3.7**). From this point on, cells will be identified as resistant or sensitive to lysine buffer therapy with subscripts (Resistant<sub>R</sub>; Sensitive<sub>S</sub>).

*In vitro characterization of Lysine Buffer Therapy Resistant and Sensitive Cell Lines*

We subsequently performed *in vitro* studies to identify potential mechanisms of resistance. Profiling cell lines *in vitro* confirmed that cultured cells resemble cells grown *in vivo*, giving us confidence that mechanisms identified *in vitro* translate *in vivo*. For example, growth rates of resistant cells (B16-F10<sub>R</sub>, LL/2<sub>R</sub> and HCT116<sub>R</sub>) were significantly higher compared to sensitive cells (PC3M<sub>S</sub> and MDA-MB-231<sub>S</sub>) ( $p < 0.001$ ) (**Figure 3.8A**). The *in vitro* growth curves closely followed *in vivo* growth rates, with B16-F10<sub>R</sub> and LL/2<sub>R</sub> expanding significantly faster

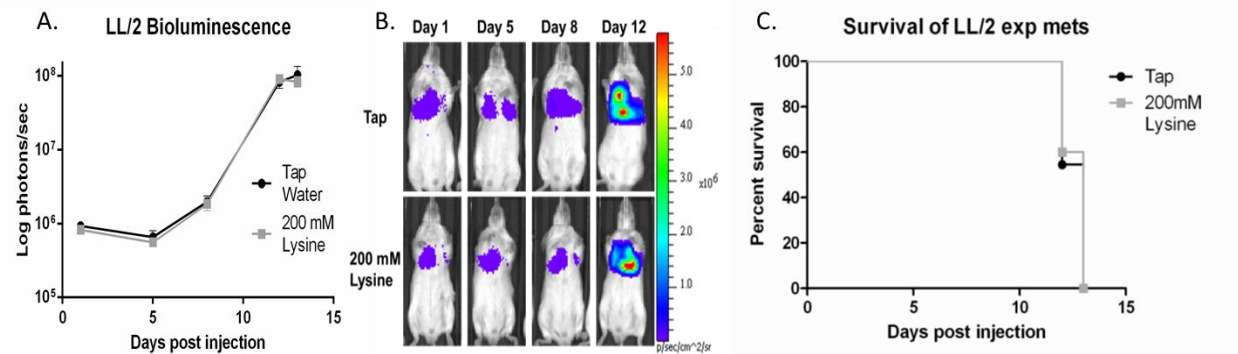


**Figure 3.5** Resistance of LL/2<sub>R</sub> to treatment with lysine buffer therapy. Effect of lysine was determined by pre-treating SCID-beige mice for a week before tail vein injection of LL/2<sub>R</sub> cells stably expressing Firefly-luciferase in an experimental metastasis model. Treatment of 200 mM lysine was administered continuously throughout the experiment. (A) Bioluminescent imaging of LL/2<sub>R</sub> metastasis (Tap *n* = 10, Lysine *n* = 10) shows buffer therapy is ineffective. (B) Representative bioluminescent images of one mouse per cohort are shown throughout the course of the experiment. (C) Kaplan Meier curve showing survival of experimental metastasis model of LL/2<sub>R</sub>. Metastasis formation was measured by bioluminescent imaging, reported as log photons/sec ± SEM. R, resistant

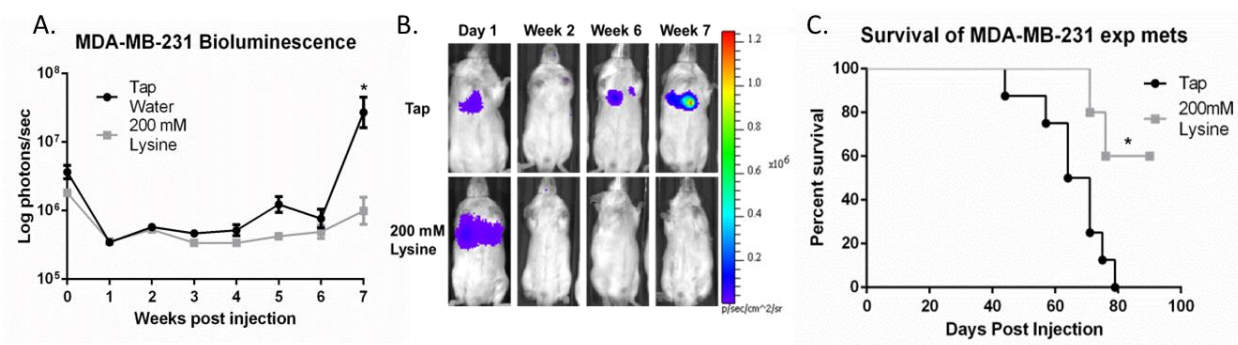


**Figure 3.6** Sensitivity of MDA-MB-231<sub>S</sub> to treatment with lysine buffer therapy. Effect of lysine was determined by pre-treating SCID-beige mice for a week before tail vein injection of MDA-MB-231<sub>S</sub> cells stably expressing Firefly-luciferase in an experimental metastasis model. Treatment of 200 mM lysine was administered continuously throughout the experiment. (A) Bioluminescent imaging of MDA-MB-231<sub>S</sub> metastasis (Tap *n* = 5, Lysine *n* = 8) shows buffer therapy is effective. (B) Representative bioluminescent images of one mouse per cohort are shown throughout the course of the experiment. (C) Kaplan Meier curve showing increased survival of MDA-MB-231<sub>S</sub> upon treatment with lysine. Metastasis formation was measured by bioluminescent imaging, reported as log photons/sec ± SEM. \* *p* < 0.05; S, sensitive



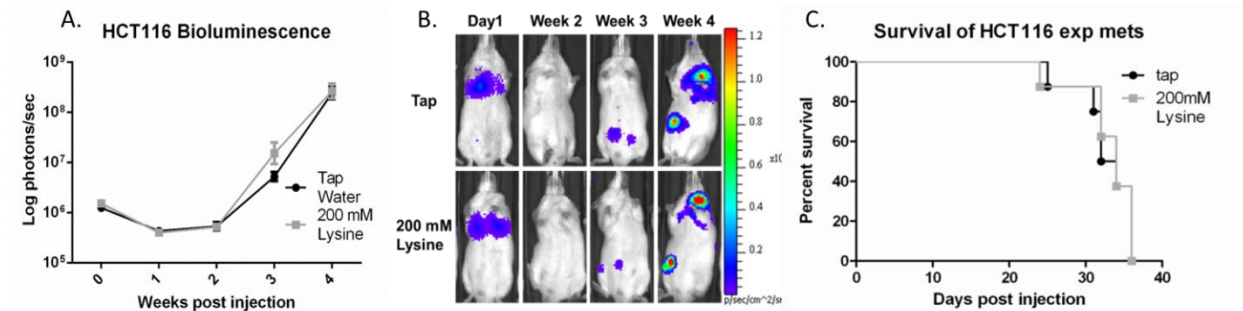


**Figure 3.7** Resistance of HCT116<sub>R</sub> to treatment with lysine buffer therapy. Effect of lysine was determined by pre-treating SCID-beige mice for a week before tail vein injection of HCT116<sub>R</sub> cells stably expressing Firefly-luciferase in an experimental metastasis model. Treatment of 200 mM lysine was administered continuously throughout the experiment. (A) Bioluminescent imaging of HCT116<sub>R</sub> metastasis (Tap  $n = 8$ , Lysine  $n = 10$ ) shows buffer therapy is ineffective. (B) Representative bioluminescent images of one mouse per cohort are shown throughout the course of the experiment. (C) Kaplan Meier curve showing survival of experimental metastasis model of HCT116<sub>R</sub>. Metastasis formation was measured by bioluminescent imaging, reported as log photons/sec  $\pm$  SEM. R, resistant

than PC3M<sub>S</sub> and MDA-MB-231<sub>S</sub> ( $p < 0.0001$ ) (compare Figures 3.3-3.6 with Figure 3.8A), and HCT116<sub>R</sub> growing at an intermediate rate (Figures 3.7 and 3.8A). While culturing cells, it was apparent that there were differences in the size of the resistant and sensitive cells, which may contribute to increased metastasis through increased extravasation from the vasculature. Cell size was measured while free in suspension to estimate their size in circulation, showing resistant cells were significantly smaller than sensitive cells ( $p < 0.05$ ) (Figure 3.8B), which may allow for more rapid extravasation during metastasis.

#### *Effect of $pH_e$ on Invasion Rates of Resistant and Sensitive Cells*

Buffer therapy selectively increases the  $pH_e$  of tumors, hence, we sought to determine the effect of pH on invasion *in vitro* [259,261]. Cells were fluorescently labeled with 10  $\mu$ g/ml of DilC<sub>12</sub>(3) prior to seeding in the apical chamber of a Boyden chamber system in serum-free media. pH 6.8 or pH 7.4 media containing serum (as a chemo-attractant) was placed in the basal

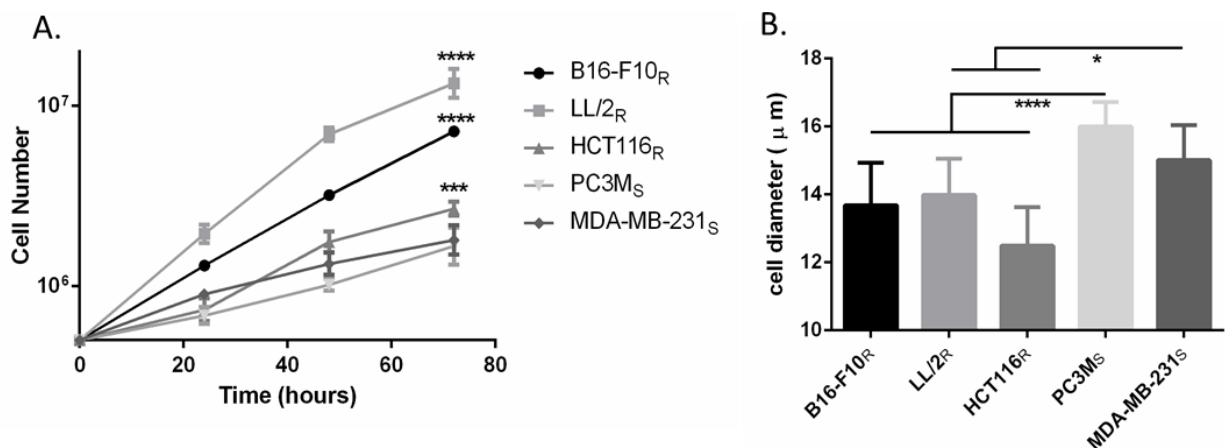


**Figure 3.8** *In vitro* characterization of lysine buffer therapy resistant and sensitive cell lines. (A) Average cell growth curves measured over 72 hours indicates significant growth rate differences between resistant and sensitive cells and correlate with *in vivo* tumor growth rates. Data shown as mean cell number  $\pm$  SD. (B) Cell diameter measurements of single cells in suspension show resistant cells are significantly smaller than sensitive cells. Data shown as mean cell diameter ( $\mu\text{m}$ )  $\pm$  SD. \*  $p < 0.05$ ; \*\*\*  $p < 0.001$ ; \*\*\*\*  $p < 0.0001$ ; <sub>R</sub>, resistant; <sub>S</sub>, sensitive.

chambers. A FluoroBlok™ membrane below a layer of matrigel enabled me to kinetically measure cell invasion over 48 hours using a fluorescent reader. Uptake of fluorescent dye had no adverse effect on cell proliferation (data not shown). Invasion rates were measured for each cell line and analyzed to determine the differential rate of invasion between each pH condition, in order to self-normalize for differences in uptake of the fluorescent dye across cell lines. Resistant cells, B16-F10<sub>R</sub>, LL/2<sub>R</sub>, and HCT116<sub>R</sub> showed no significant change in their rates of invasion between pH 6.8 and pH 7.4 (**Figure 3.9**). MDA-MB-231<sub>S</sub> cells, however, had a significantly increased rate of invasion at pH 6.8, relative to pH 7.4, when compared to B16-F10<sub>R</sub> ( $p < 0.05$ ), LL/2<sub>R</sub> ( $p < 0.05$ ), and HCT116<sub>R</sub> ( $p < 0.005$ ) (**Figure 3.9**). While not statistically significant, PC3M<sub>S</sub> cells followed the same trend as MDA-MB-231<sub>S</sub> cells of having an increased rate of invasion at pH 6.8 relative to pH 7.4 (**Figure 3.9**). As growth rates are suppressed under these acute acidic conditions for each cell line (data not shown), we conclude that the increased

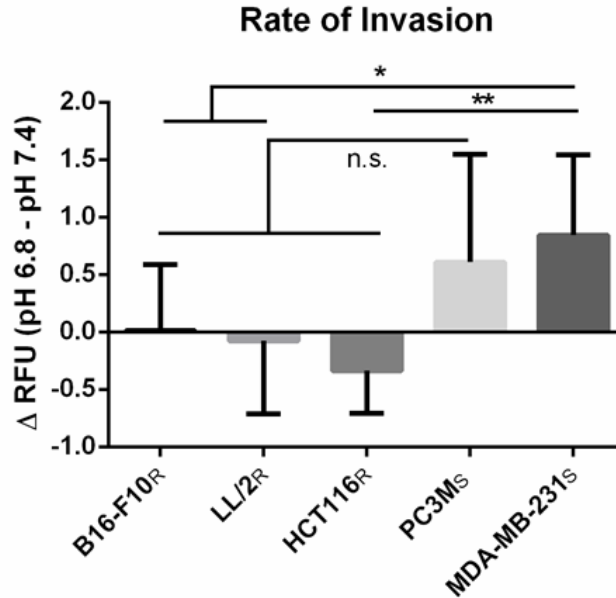


**Figure 3.9** Effect of  $pH_e$  on invasion rates of resistant and sensitive cells. *In vitro* invasion assay using a Boyden chamber coated with Matrigel. Fluorescently labeled cells were measured every 6 hours for 48 hours for invasion through Matrigel layer. Data shown is the result of two biologic experiments ( $n = 6$ /sample) normalized to wells lacking serum attractant ( $n = 2$ /sample). Data is presented as the mean difference in the rate of invasion of cells cultured in pH 6.8 and cells cultured in pH 7.4  $\pm$  SD. The rate of invasion of sensitive cells increases in pH 6.8 compared to resistant lines. \* $p < 0.05$ ; \*\* $p < 0.005$ ; R, resistant; S, sensitive.

invasion rate in sensitive cell lines is a real phenomenon, and not the result of growth rate differences. Together, these data suggest that resistant and sensitive cells utilize different invasive mechanisms, pH-independent and pH-dependent mechanisms, respectively.

#### *Analysis of the Metabolic Phenotypes of Resistant and Sensitive Cells*

The Warburg Effect is a common phenomenon in solid tumors that contributes to acidification of the tumor microenvironment. Originally, we hypothesized resistant lines would produce acid at a higher rate, implying that increasing the buffer load could overcome buffer resistance. To test this, we examined the effect of 400 mM bicarbonate on experimental B16-F10<sub>R</sub> metastasis formation and observed no effect (data not shown); suggesting resistant cells were not merely producing acid at a higher rate. This was verified by metabolic profiling of

resistant and sensitive cells using a Seahorse XF® analyzer which measures real-time H<sup>+</sup> production and oxygen consumption rate over a monolayer of cells in a transient microchamber. Metabolic profiling assays were performed in parallel and normalized assay data to either cell number or protein concentration, to confirm that normalized results were not an artifact of cell size differences (data not shown). To determine glycolytic activity, a “glycolytic stress test” was performed, which includes measuring extracellular acidification rates (ECAR) following sequential addition of glucose to measure basal glycolysis, a mitochondrial poison (oligomycin) to estimate total glycolytic capacity, and 2-deoxyglucose to measure non-glycolytic ECAR. Interestingly, sensitive cells had significantly higher basal glycolytic rates, compared to resistant cells ( $p < 0.0001$ ) (**Figure 3.10A**). Glycolytic reserve is calculated by measuring the difference in the maximal glycolytic capacity, after treatment with oligomycin, and basal glycolysis. Possibly as a consequence of their high basal rates, the sensitive cells showed significantly lower amounts of glycolytic reserve, compared to resistant cells ( $p < 0.0001$ ), suggesting that they are near maximum glycolytic capacity in their basal metabolic state (**Figure 3.10B**).

The rate of decrease in O<sub>2</sub> can be converted to an oxygen consumption rate, OCR. The “mitochondrial stress test” initially determines basal respiration. We observed that resistant cells had significantly higher basal OCR compared to sensitive cells ( $p < 0.05$ ) (**Figure 3.11**). We suspect that the higher basal OCR in resistant cells is most likely related to the energy demands of a higher proliferation rate (**Figure 3.8**). Treatment with an inhibitor of the F<sub>0</sub> subunit of mitochondrial ATP synthase, oligomycin, provided OCR attributed directly to ATP production. These data showed that buffer therapy resistant cells had significantly higher OCR that attributed to ATP production ( $p < 0.0001$ ) (**Figure 3.11**). These mitochondrial stress test data suggest that resistant cells rely on mitochondrial oxidative metabolism (OXPHOS) for their energy needs.

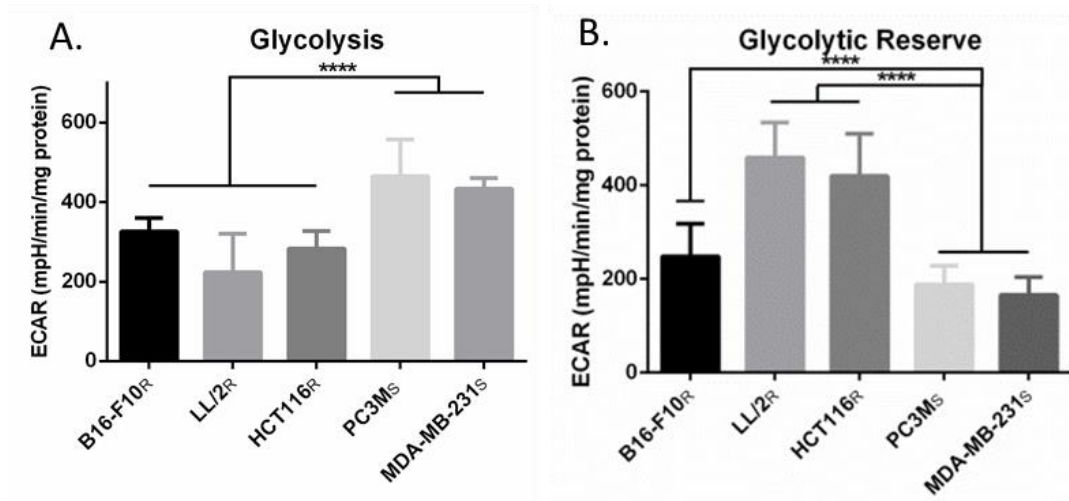


**Figure 3.10** Glycolytic profile analysis of buffer therapy resistant and sensitive cells. *In vitro* extracellular acidification rate (ECAR) of resistant and sensitive cells, measured using Seahorse XF-96 Instrument. Metabolic data are presented as mean  $\pm$  SD. (A) ECAR measurements in response to 5.55 mM glucose stimulation indicate basal glycolytic activity of cells. Sensitive cells are significantly more glycolytic than resistant cells. (B) The increase in ECAR of cells in response to treatment with 1  $\mu$ M oligomycin minus basal glycolytic activity indicates the glycolytic reserve of cells. Sensitive cells have significantly reduced glycolytic reserve compared to resistant cells. \*\*\*\* $p < 0.0001$ ; R, resistant; S, sensitive.

Metabolic analysis of OXPHOS and glycolytic pathways in resistant and sensitive cells showed distinct metabolic profiles. This can be directly shown by expressing data as basal OCR/ECAR ratios, which are self-normalized and showed that sensitive cells were significantly ( $p < 0.005$ ) more glycolytic than resistant cells (**Figure 3.12A**). These differences in metabolic profiles were related to the ability of buffer therapy to inhibit metastasis (**Figures 3.3-3.7**), and correlate with distinct phenotypic differences in their *in vivo* and *in vitro* proliferation rates (**Figure 3.8A**), and size (**Figure 3.9A**).  $pH_e$  measurements of PC3M<sub>S</sub> and B16-F10<sub>R</sub> tumors (performed by Heather H. Cornell) support the metabolic evidence presented, with PC3M<sub>S</sub> tumors being more acidic than B16-F10<sub>R</sub> tumors (**Figure 3.12B**). Previous studies, using MRS imaging with the pH indicator 3-aminopropylphosphonate (3-APP) and fluorescent ratio imaging with SNARF-1,

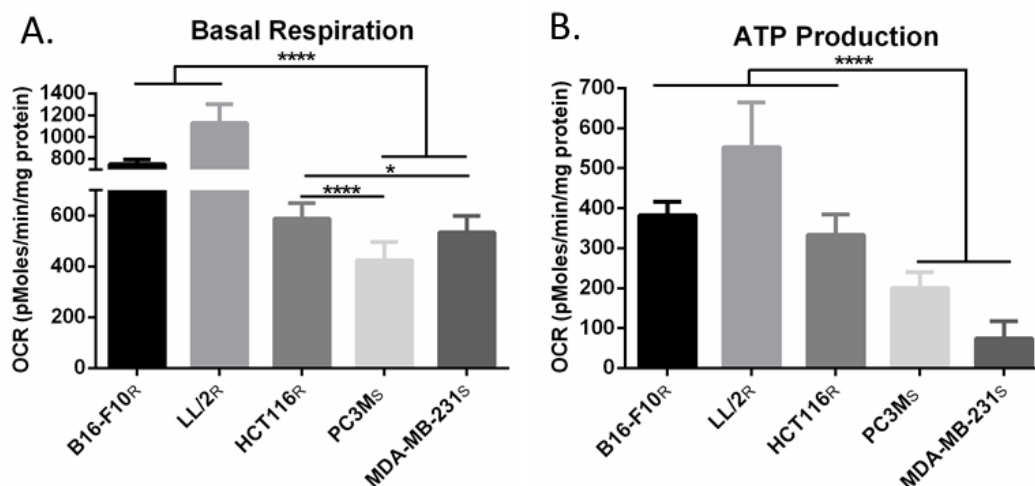


**Figure 3.11** Oxidative profile analysis of buffer therapy resistant and sensitive cells. *In vitro* oxygen consumption rate (OCR) of resistant and sensitive cells, measured using Seahorse XF-96 Instrument. Metabolic data are presented as mean  $\pm$  SD. (A) Basal OCR measurements show significantly higher oxidative phosphorylation flux in resistant cells compared to sensitive cells. (B) OCR contributing to production of ATP during oxidative phosphorylation is measured by the difference of basal OCR and the OCR of cells after treatment with 1  $\mu$ M oligomycin, a mitochondrial ATP synthase inhibitor. The amount of OCR contributing to the production of ATP by oxidative phosphorylation is significantly higher in resistant cells compared to sensitive cells. \* $p < 0.05$ ; \*\*\*\* $p < 0.0001$ ; R, resistant; S, sensitive.

have shown that MDA-MB-231 tumors are similarly acidic and can be manipulated with buffer therapy to increase the tumor pH [259]. We have previously observed sensitivity of HCT116-GFP cells to bicarbonate in window-chamber studies [291], but observed clear resistance of HCT-116<sub>R</sub>-Luc cells in our current studies (**Figure 3.7**). Interestingly, HCT116-GFP cells had a different metabolic profile than the HCT116<sub>R</sub>-Luc cells used in the *in vivo* experimental metastasis model herein, suggesting the presence of two phenotypically distinct populations of these cells, supported by differences in their OCR/ECAR ratios ( $p < 0.0001$ ) (**Figure 3.13**). Importantly, DNA fingerprinting confirmed that both lines used were HCT116 colorectal cells (data not shown). Notably, the glycolytic HCT-116-GFP cells were inhibited by buffer therapy [291]; whereas the oxidative HCT-116-luc cells were not (**Figure 3.7**).

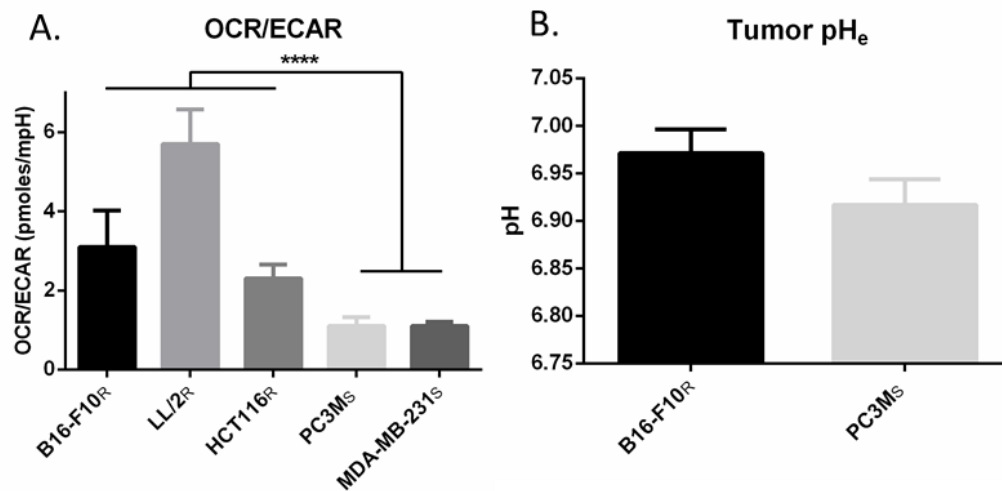


**Figure 3.12** Sensitive cells are more glycolytic than resistant cells, leading to tumor acidosis. (A) The OCR/ECAR ratio of cells during basal metabolism indicates that sensitive cells are significantly more glycolytic than resistant cells. (B) Intratumoral pH measurements of subcutaneous tumors using pH electrodes shows that increased glycolytic activity of sensitive cells, PC3M<sub>S</sub>, contributes to a more acidic tumor microenvironment than resistant tumors, B16-F10<sub>R</sub>. pH data are presented as mean of independent measurements (B16-F10<sub>R</sub>  $n = 10$ ; PC3M<sub>S</sub>  $n = 5$ )  $\pm$  SEM. \*\*\*\* $p < 0.0001$ ; R, resistant; S, sensitive

#### *In vivo Proteolytic Activity in Resistant and Sensitive Tumors*

Invasion kinetics and metabolic profiling suggest that resistant cells invade via a mechanism that is pH-independent. Proteases have been identified as key enzymes involved in the metastatic cascade. Prior data have shown that low pH significantly stimulated the release of active cathepsin-B from buffer-sensitive MDA-MB-231 cells in 2-D and 3-D culture [259,335]. Hence, we hypothesize that resistant cells may release active proteases in a constitutive, pH-independent fashion. To investigate this, mice bearing tumors were imaged using fluorescent indicators that are activated by protease activity. ProSense 750EX and MMPsense 680 fluoresce upon cleavage by Cathepsins B, L, S and Plasmin (ProSense 750EX) or MMPs -2, -3, -9 and -13 (MMPsense 680). Using a tomographic near-IR fluorescence imaging system, FMT2500, activated probes were imaged 24 hours post-probe injection followed by fluorescent signal

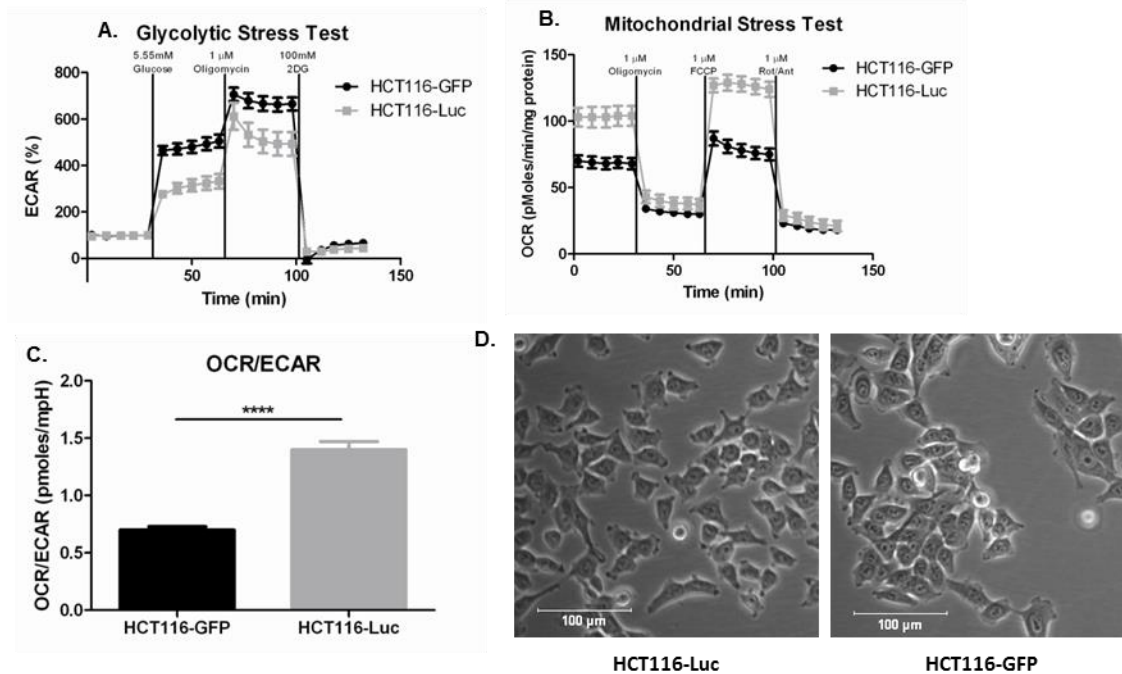


**Figure 3.13** Metabolic profile analysis of HCT116-Luc and HCT116-GFP cells. Glycolytic and mitochondrial stress tests show different metabolic profiles of HCT116-Luc and HCT116-GFP cells. (A) Extracellular acidification rates (ECAR) of cells after stimulation of glycolysis with glucose (5.55 mM), oligomycin (1  $\mu$ M) and glycolysis inhibitor 2DG (100 mM). (B) Oxygen consumption rates (OCR) of cells before treatment with oligomycin (1  $\mu$ M), FCCP (1  $\mu$ M) and Rotenone (1  $\mu$ M) and Antimycin A (1  $\mu$ M). (C) OCR/ECAR ratio of cells during basal metabolism. (D) Representative brightfield microscopy images of HCT116-Luc and HCT116-GFP cells in pH 7.4 culture conditions. Data shown as mean  $\pm$  SD. Scale bars represent 100  $\mu$ m. \*\*\*\* $p < 0.0001$

integration over the tumor region of interest (ROI). B16-F10<sub>R</sub> tumors were not used due to high melanin levels that quench fluorescence. Thus, the *in vivo* protease activity was measured in the most resistant (LL/2<sub>R</sub>) and the most sensitive (PC3M<sub>S</sub>) cell lines (**Figure 3.3** and **Figure 3.5**). Quantification of activated ProSense 750EX in LL/2<sub>R</sub> tumors showed significantly higher cysteine cathepsin activity compared to PC3M<sub>S</sub> under control conditions ( $p < 0.0001$ ) (**Figure 3.14**). Although treatment reduced ProSense 750EX activation in LL/2<sub>R</sub> tumors ( $p < 0.05$ ), activity still remained significantly higher than PC3M<sub>S</sub> cells under either pH condition (**Figure 3.14**) [318]. Conversely, MMPsense 680 was visibly activated in both LL/2<sub>R</sub> and PC3M<sub>S</sub> tumors



in control mice (**Figure 3.15**). Buffer treatment increased MMP activity in LL/2<sub>R</sub> tumors ( $p < 0.05$ ), and reduced MMP activity 2-fold in PC3M<sub>S</sub> tumors, but was not statistically significant (**Figure 3.15**). Resistant LL/2<sub>R</sub> tumors had higher intrinsic cathepsin activity than did PC3M<sub>S</sub> tumors and elevated MMP activity following buffer therapy. Therefore, we can conclude that resistant lesions have more protease activity compared to sensitive lesions, which may be contributing to buffer therapy resistance.

#### *In vitro Protease Expression in Resistant and Sensitive Cells*

To confirm *in vivo* protease activity results, cell cultures exposed to media at pH 7.4 or pH 6.8 were analyzed for MMP-2, -3, -9, and -13 (MMPs that activate MMPsense 680) mRNA expression. We chose to focus on MMP expression due to the significant increase of MMP activity observed upon treatment with lysine in LL/2<sub>R</sub> tumors (**Figure 3.15**). Both LL/2<sub>R</sub> and PC3M<sub>S</sub> cells exhibited an increased expression of MMP-3 and -13 at pH 6.8 (**Figure 3.16A**). To further compare differences, transcript expression was analyzed in LL/2<sub>R</sub> cells normalized to PC3M<sub>S</sub> cultures. LL/2<sub>R</sub> cells have higher MMP expression compared to PC3M<sub>S</sub> cells for each of the transcripts analyzed, with the exception of MMP-9 (**Figure 3.16B**). Importantly, there were no differences in fold change of each transcript relative to PC3M<sub>S</sub> when exposed to acidic or physiological conditions, showing that higher proteolytic expression of resistant cells was pH-independent. MMP transcript analysis confirms our hypothesis that buffer therapy resistant lines are constitutively proteolytic *in vitro* (**Figure 3.16**) as well as *in vivo* (**Figure 3.14 and Figure 3.15**).

#### *The Effect of $pH_e$ on Resistant and Sensitive Cell Migration and Morphology*

Recent research has focused on identifying different modes of migration and invasion during metastasis [328]. To understand migratory differences between LL/2<sub>R</sub> and PC3M<sub>S</sub>,

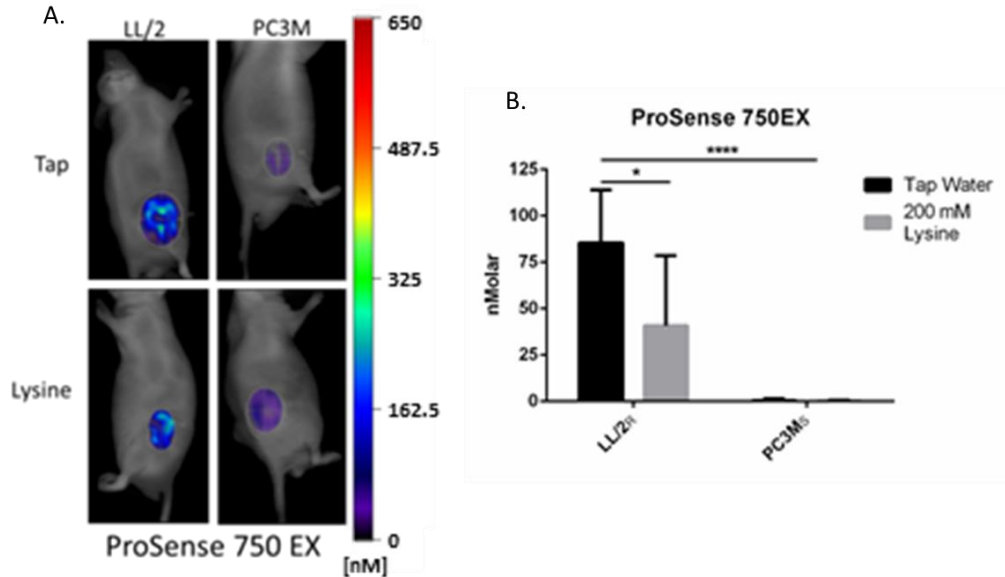


**Figure 3.14** Resistant tumors have increased *in vivo* Cathepsin activity. Mice bearing LL/2<sub>R</sub> (Tap  $n = 7$ , Lysine  $n = 8$ ) and PC3M<sub>S</sub> (Tap  $n = 7$ , Lysine  $n = 5$ ) tumors were injected with an activatable probe, ProSense 750EX, which reports Cathepsin activity. (A) Representative images of fluorescent tomographic imaging showing cathepsin activity through ProSense 750EX signal in LL/2<sub>R</sub> and PC3M<sub>S</sub> tumors in mice receiving either tap water or lysine buffer. (B) Quantitation of ProSense 750EX activated signal in tumors, normalized to tumor size. Data are presented as mean nanomolar concentration  $\pm$  SD. \* $p < 0.05$ ; \*\*\*\* $p < 0.0001$ ; R, resistant; S, sensitive.

cell motility was monitored in a wound healing assay by imaging cells for 18 hours following wound formation. Percent relative wound density was calculated by measuring the density of cells that migrated into the original wound. LL/2<sub>R</sub> cells were significantly more migratory than PC3M<sub>S</sub> cells cultured in physiologic pH ( $p < 0.0001$ ) (**Figure 3.17**). Interestingly, exposure to low pH had differential effects on cell migration for each of the cell lines. LL/2<sub>R</sub> migration across the wound was significantly retarded under acidic conditions ( $p < 0.01$ ), while PC3M<sub>S</sub> cell migration was significantly accelerated under acidic conditions ( $p < 0.0001$ ) (**Figure 3.17**). Additionally, sensitive and resistant cells exhibited different modes of migration. PC3M<sub>S</sub> cells moved across the wound as a mass following leading cells, suggestive of a collective cell

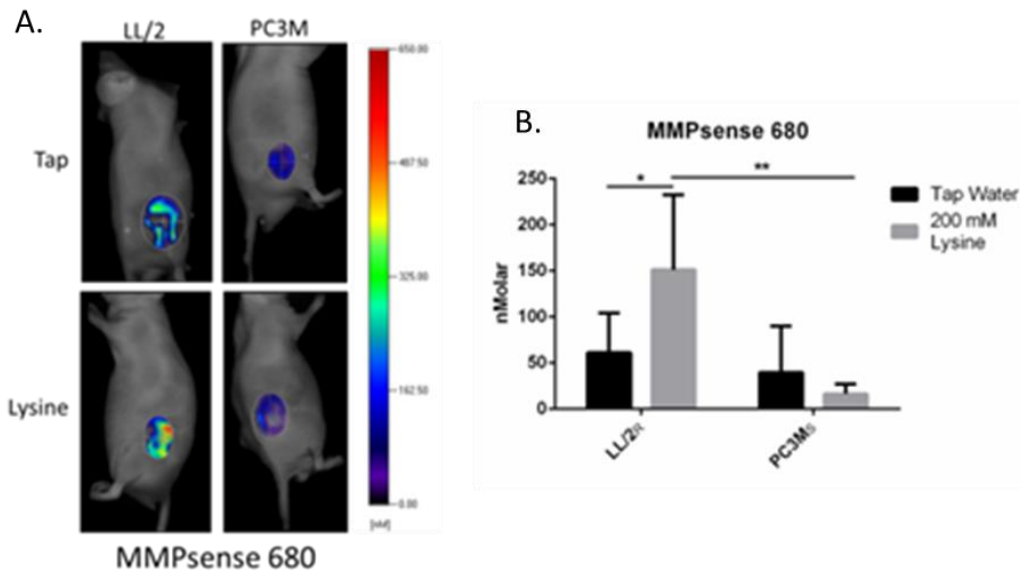


**Figure 3.15** Resistant tumors have increased *in vivo* MMP activity. Mice bearing LL/2<sub>R</sub> (Tap  $n = 7$ , Lysine  $n = 8$ ) and PC3M<sub>S</sub> (Tap  $n = 7$ , Lysine  $n = 5$ ) tumors were injected with an activatable probe, MMPsense 680, which reports MMP activity. (A) Representative images of fluorescent tomographic imaging showing MMP activity through MMPsense 680 signal in LL/2<sub>R</sub> and PC3M<sub>S</sub> tumors in mice receiving either tap water or lysine buffer. (B) Quantitation of MMPsense 680 activated signal in tumors, normalized to tumor size. Data are presented as mean nanomolar concentration  $\pm$  SD. \* $p < 0.05$ ; \*\* $p < 0.01$ ; R, resistant; S, sensitive.

migration phenotype, while LL/2<sub>R</sub> cells moved as single cells, which is characteristic of single-cell or multicellular streaming invasive phenotypes (data not shown). While studying the movement of cells in a 2D culture environment is useful, 3D cultures more closely resemble physiological obstacles encountered during metastasis. Using phalloidin staining, we studied the morphology of LL/2<sub>R</sub> and PC3M<sub>S</sub> cells in a thick (500-1000  $\mu\text{m}$ ) layer of Matrigel® under physiological or acidic conditions. In a 3D matrix LL/2<sub>R</sub> and PC3M<sub>S</sub> cells have distinctly different cellular morphologies. PC3M<sub>S</sub> cells have an elongated phenotype with multiple protrusions into the local matrix (**Figure 3.18**). In response to acidic conditions, PC3M<sub>S</sub> cells maintained an elongated phenotype although completely void of the protrusions that were observed under physiological conditions, which may allow for greater invasive potential. In

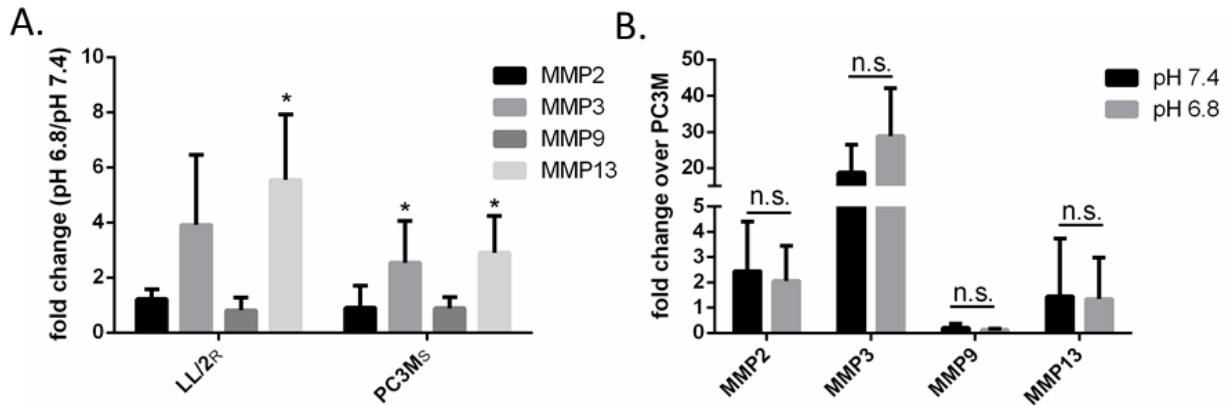


**Figure 3.16** Elevated MMP expression in resistant cells. Quantitation of MMP expression in sensitive and resistant cells grown in physiological or acidic pH media for 24 hours. Transcripts were normalized to  $\beta$ -actin expression before analysis. (A) Ratio of expression of MMP-2, -3, -9, and -13 in LL/2<sub>R</sub> and PC3M<sub>S</sub> cultured in acidic media relative to cells cultured in physiological media. (B) Ratio of expression of MMP-2, -3, -9, and -13 in LL/2<sub>R</sub> cells relative to expression in PC3M<sub>S</sub> cells cultured in acidic and physiological media. Data are the average of three independent experiments and is reported as mean  $\pm$  SD. \* $p < 0.05$ ; R, resistant; S, sensitive

contrast, LL/2<sub>R</sub> cells had a rounded morphology that, consistent with the phenotypes we characterized above, remain unchanged from physiologic to acidic pH (**Figure 3.18**).

## Discussion

In our previous studies, we demonstrated that an acidic microenvironment is critical for carcinogenesis and tumor invasion. Furthermore, we have found that systemic buffers reduce intra- and peri-tumoral acidity, inhibit carcinogenesis in transgenic mice, and inhibit metastatic growth in a wide range of cell lines *in vivo* [259,262,291]. However, as with most therapeutic regimens, efficacy of buffer therapy was not universally observed. The current work focused on identifying molecular and metabolic phenotypes of resistant cells, with an expectation that such data could identify additional biomarkers to stratify tumors for their response to buffer therapy. Using a panel of cells representing different cancers, we have characterized two responsive cell lines, PC3M<sub>S</sub> and MDA-MB-231<sub>S</sub>, and three resistant cell lines, B16-F10<sub>R</sub>, and LL/2<sub>R</sub>, and

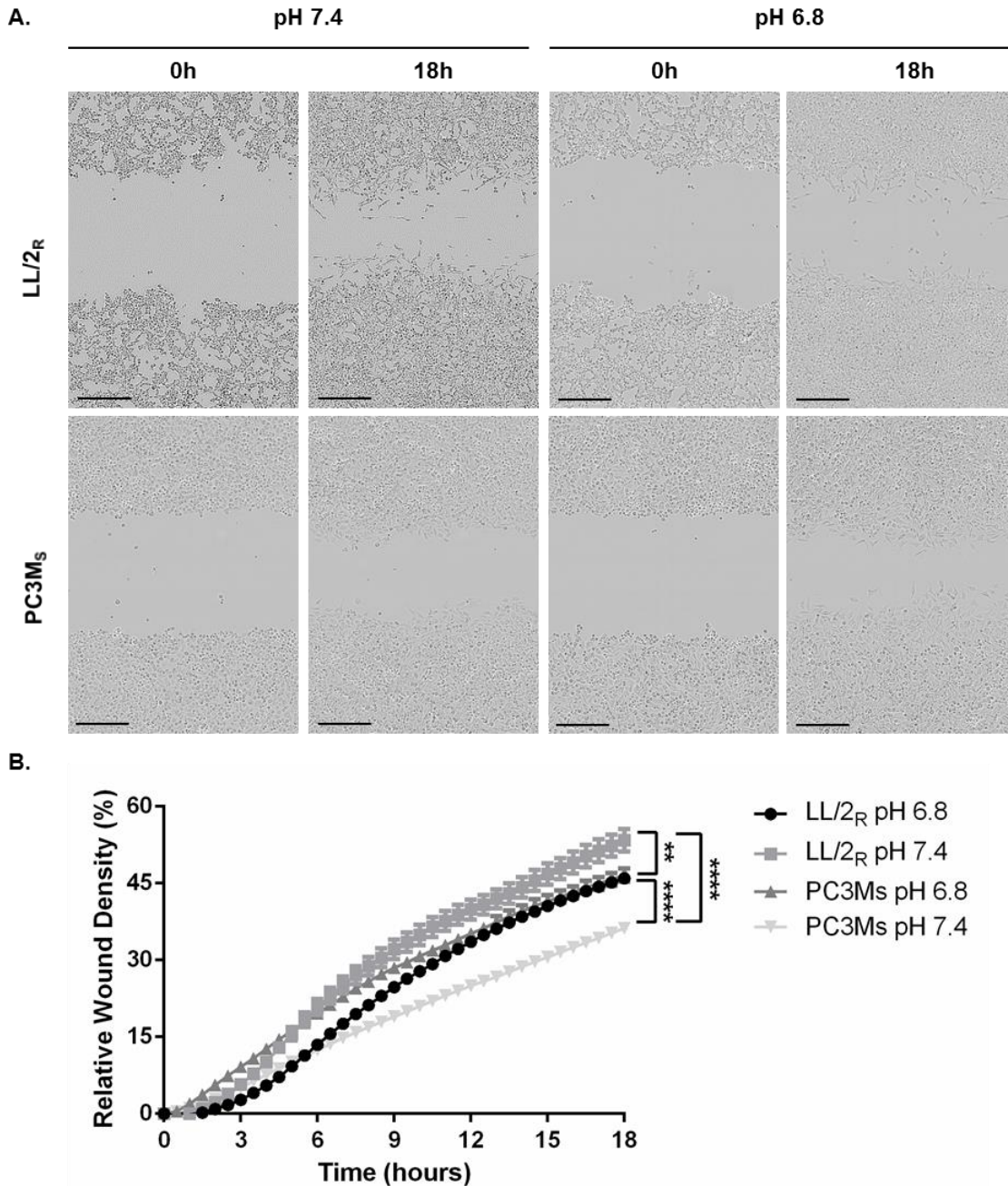


**Figure 3.17** Migratory patterns of LL/2<sub>R</sub> and PC3M<sub>S</sub> cells. 700- to 800- $\mu$ m wounds were created in confluent cell cultures exposed to physiologic or acidic media 24 hours before wound formation, and during the duration of the experiment. Samples were imaged in 30-minute intervals for 18 hours. (A) Representative microscopy images of LL/2<sub>R</sub> (upper panel) and PC3M<sub>S</sub> (lower panel) show movement across a wound at 0 and 18 hours in pH 7.4 or pH 6.8 media. Scale bars represent 300  $\mu$ m. (B) Percent relative wound density was determined by measuring the density of cells within the original wound site at each of the time points imaged. Data are shown as the mean  $\pm$  SEM and are representative of three independent experiments. \*\* $p < 0.01$ ; \*\*\*\* $p < 0.0001$ ; <sub>R</sub>, resistant; <sub>S</sub>, sensitive.

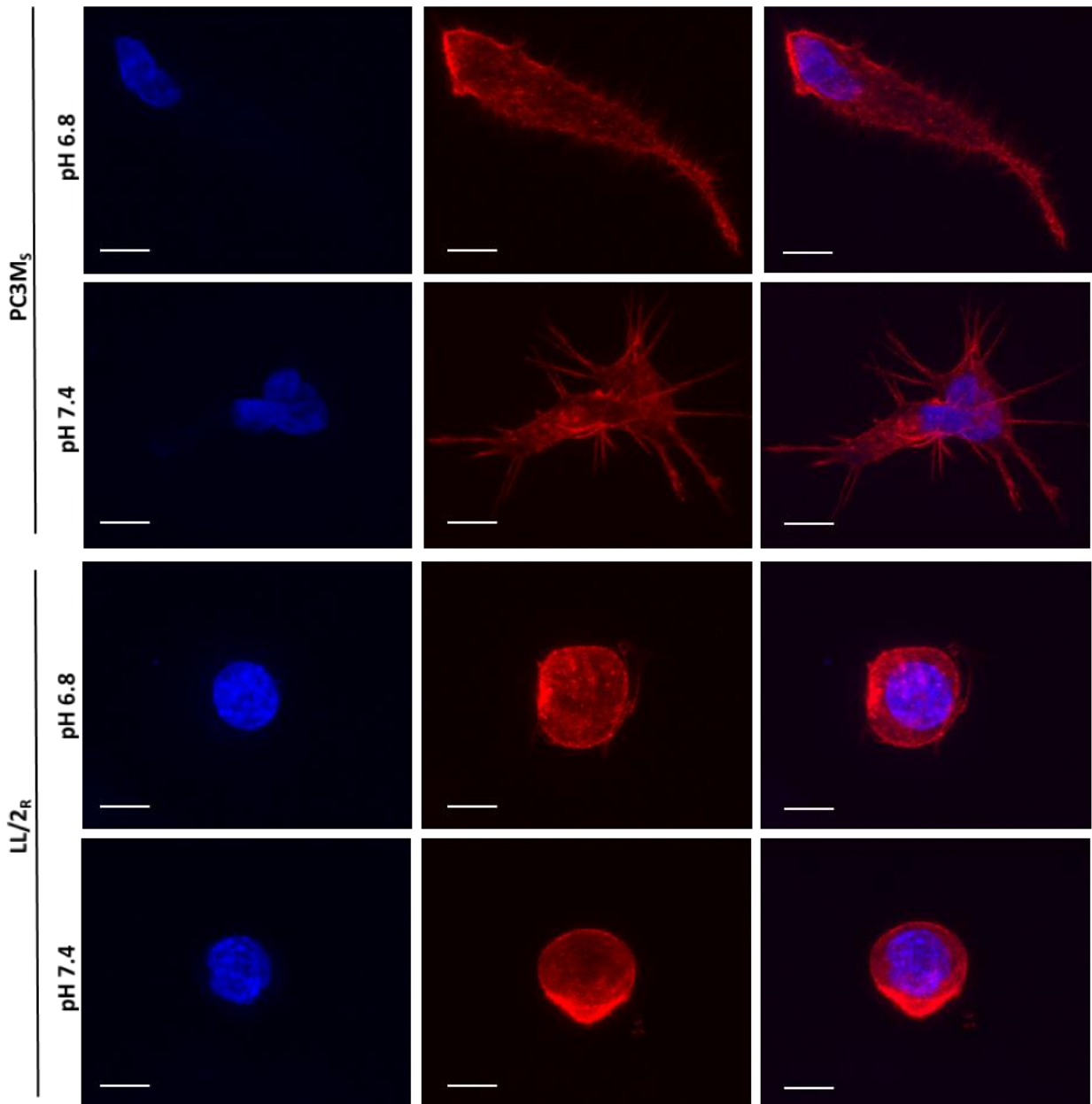


**Figure 3.18** Morphologies in a 3D matrix *in vitro*. LL/2<sub>R</sub> and PC3M<sub>S</sub> cells were seeded onto a thick (500-1000  $\mu\text{m}$ ) layer of polymerized Matrigel and invaded into the matrix over a period of 72 hours in pH 6.8 or pH 7.4 media. Single cells were imaged using confocal microscopy for morphological studies. Representative images of PC3M<sub>S</sub> cells (upper panel) and LL/2<sub>R</sub> cells (lower panels) show a 3D reconstruction of at least 20 slices. Phalloidin (F-actin) is shown in red, Hoeschst nuclear stain is shown in blue. Scale bars represent 10  $\mu\text{m}$ . <sub>R</sub>, resistant; <sub>S</sub>, sensitive.

HCT116<sub>R</sub>. In addition to faster growth rates *in vivo* and *in vitro*, resistant cells were significantly smaller in diameter than sensitive cells, which may allow increased access to invade the extracellular space, either through more efficient extravasation or secondary site colonization. Faster growth and smaller size may be enough to render resistant cells too aggressive for buffer therapy to be effective.

Further exploration, however, has revealed a number of other important molecular and metabolic parameters that could contribute to resistance. Kinetic invasion assays suggest that there are distinct mechanisms used for invasion by these two groups. Sensitive line invasion is pH-dependent, allowing buffer therapy to intercept metastasis by neutralizing acidity *in vivo*. Resistant cell line invasion, on the other hand, is pH-independent, bypassing the need for acidosis to metastasize.

Metabolic alterations contribute to acidification of tumor microenvironments. Metabolic profiling showed that sensitive cells were unequivocally more glycolytic than the resistant cells. Cells with elevated glycolysis produce more acidic tumors. Previously, we have confirmed that buffer therapy is an effective method of increasing the pH<sub>e</sub> of tumors, which diminishes the ability of sensitive, but not resistant cells, to invade locally and metastasize [259,261,334]. While resistant tumors were less acidic than highly glycolytic sensitive tumors, they were nonetheless more acidic relative to normal tissues, likely due to poor perfusion. Neutralizing the tumor acidity in these tumors had less of an effect on their metastatic potential because they have upregulated mechanisms to bypass the need for acid-stimulated invasion. Expression, release, and enzymatic activity of proteases are regulated by acidosis. While sensitive cells, PC3M<sub>S</sub>, have measureable expression of MMPs, resistant cells, LL/2<sub>R</sub>, have consistently higher expression of MMPs regardless of pH. Expression of MMPs correlated with protease activity *in-*

*in vivo*. Interestingly, LL/2<sub>R</sub> tumors had a significant increase in MMP activity in response to treatment, suggesting buffer therapy could exacerbate the metastatic burden, although increases in metastatic formation in mice receiving buffer therapy was not observed. Protease activation in resistant tumors is not adversely affected by buffer therapy, and allows resistant lines to circumvent inhibition of metastasis by buffer therapy. Similar results were observed in a parallel study [335], in which acidic pH increased pericellular active cysteine cathepsins *in vitro*, which was reduced following buffer therapy treatment *in vivo* (**Figure 3.1**). Furthermore, resistant and sensitive cells exhibited distinct morphological differences in 3D culture systems. Interestingly, acidic conditions resulted in the loss of protrusions in 3D culture of PC3M<sub>S</sub>, which may contribute to their increased invasiveness in acidosis. Resistant and sensitive cells consistently had differential responses to changes in extracellular pH, regardless of the inclusion or absence of Matrigel matrix (migration, invasion and morphology studies), suggesting that the changes observed were due to pH alterations, rather than cell signaling pathways such as integrin signaling.

Although buffer therapy is not universally effective in reducing metastases, it does have potential advantages over targeted cytotoxic chemotherapies that are in current clinical practice. Tumors are heterogeneous, containing genetically distinct regional sub-populations that originate over a lifetime of tumor growth [9,10,336]. Intrinsic or acquired resistance to chemotherapy is a major obstacle of targeted therapies clinically, and will continue to remain so for the foreseeable future [12]. In contrast, treatment of solid tumors with buffer therapy targets tumor acidity, a common phenotypic consequence of tumor somatic evolution [27,337]. In addition to enhancing local invasion and metastatic potential, tumor acidosis contributes to drug resistance through ion-trapping of weakly basic chemotherapeutics, preventing active drug from reaching therapeutic



doses within cells [25,258,260]. Therefore, buffer therapy may also be useful as an adjuvant to traditional chemotherapies. Notably, a clinical trial of buffer therapy in cancer patients has recently been initiated (NCT01846429).

In the current studies, buffer therapy was initiated prior to inoculation to prevent progression to metastatic disease. Previous studies show buffer therapy has little effect on reducing primary tumor growth, but significantly reduces spontaneous metastasis formation [259]. Similarly, in a transgenic prostate cancer model, buffer therapy prevented development of prostate adenocarcinoma when therapy was initiated immediately following weaning (4 weeks of age) [262]. Interestingly, if therapy was initiated later (10 weeks of age) development of prostate cancer was delayed, but was not inhibited, while progression to metastatic disease was still prevented with treatment. Our data shows that buffer therapy is an effective method of halting tumor progression and metastasis formation, but also indicates that the timing of therapy initiation is instrumental for maximal efficacy. Future studies on optimization of buffer therapy delivery and treatment schedules are necessary to harness the full potential of buffer therapy clinically.

Identifying distinct metastatic mechanisms of sensitive and resistant tumors allows for the identification of predictive biomarkers of buffer therapy response. FDG-PET screening may be an ideal method of screening patients to assess their glycolytic phenotype to predict response to buffer therapy. Clinically, FDG-PET imaging is used to diagnose up to 90% of primary tumors, indicating that the vast majority of patients have glycolytic tumors that may benefit from treatment with buffer therapy [338]. Further screening of additional cell lines for responsiveness to buffer therapy will help solidify potential biomarkers or alternative treatments for resistant tumors. A current limitation of our research was the use of five cell lines originating from

different cancers. Deeper analysis into panels of cell lines originating from the same primary organ site will surely provide more insight and will need to be studied in the future. Such observations are commencing with the identification of two populations of HCT116 cells that have distinctly different metabolic and invasive behaviors.

## **Materials and Methods**

### *Animals*

Animals were housed according to IACUC protocol at the USF Vivarium within Moffitt Cancer Center. 4-6 week old SCID-beige (Charles River) or nu/nu mice (Harlan) were used in experimental metastasis models or for fluorescent imaging of subcutaneous tumors, respectively.

### *Cell lines*

PC-3M-Luc6 clone, B16-F10-G5 clone and LL/2-M38 clone luciferase expressing cells were obtained from Xenogen Caliper. MDA-MB-231 and HCT116 cells (ATCC) stably expressing luciferase were generated using lentiviral transduction. Cells were cultured in typical incubation conditions (37°C and 5% CO<sub>2</sub>). Cell counts and diameters were measured with the Countess Automated Cell Counter (Invitrogen).

### *Experimental Metastasis Model and Bioluminescent Imaging*

Experimental metastasis models and bioluminescent imaging was performed as described previously [334]. SCID-beige mice were pretreated with 200 mM Lysine or tap water for one week prior to injection, and continued throughout the study.  $1 \times 10^6$  cells were injected intravenously in 100  $\mu$ L PBS. Mice were imaged immediately after injection by bioluminescent imaging to confirm successful injections. Metastasis formation is inferred from bioluminescent signal, which is reported as mean log photons emitted/second  $\pm$  SEM. MDA-MB-231 growth rate doubling times (DT) were determined by fitting three parameter Gompertz function

[339,340]. Statistical significance using Log-DT as a descriptor for the groups was determined using one-sided Anova test.

#### *Metabolic Profile Analysis*

Metabolic profiles were determined using the Seahorse Extracellular Flux (XF-96) analyzer (Seahorse Bioscience) as described previously [334]. Briefly, assay media was supplemented with 11 mM glucose, 0.5 mM sodium pyruvate and 2 mM glutamine for mitochondrial stress tests (MST) and glucose free media for glycolysis stress tests (GST). Cells were treated with 1  $\mu$ M oligomycin, FCCP, Rotenone and Antimycin during MST. GST treatments include 11 mM glucose, 1  $\mu$ M oligomycin and 100 mM 2DG. ECAR and OCR values were standardized to mg/protein and reported as the mean  $\pm$  SD.

#### *Electrode measurement of tumor pH*

pH measurements were performed as described previously [261]. Briefly, a reference electrode was placed in a non-tumor site. A needle microelectrode (OD 0.8 mm with a beveled end) was inserted into the center of the tumor, and was held in place until readings stabilized. pH was measured at three locations and reported as mean  $\pm$  SEM.

#### *In-vivo protease activity measurements*

nu/nu mice were provided with either tap water or 200mM free base lysine seven days prior to inoculation (Sigma Aldrich).  $1 \times 10^6$  LL/2 and PC3M cells were injected as bilateral subcutaneous flank injections in PBS solution. 24 hours prior to imaging, mice were injected with activatable fluorescent probes, MMPsense680 and Prosense750EX (Perkin Elmer), intravenously. *In-vivo* measurements were obtained using the FMT2500 (Perkin Elmer) tomographic imaging system. Fluorescent signal from each probe was quantified based on an internal standard. Data was reported as mean  $\pm$  SD.

### *Quantitative PCR*

RNA was isolated from cell pellets using RNeasy Mini Kit (Qiagen). qPCR reactions were carried out with iScript One-Step RT-PCR kit with SYBR Green (Bio-Rad) using Applied Biosystems StepOne PCR system (Applied Biosystem). MMP-2 and MMP-9 primers were obtained from S. Chellepan (Moffitt Cancer Center)(Supplemental Table 1). Data was analyzed using  $\Delta\Delta C_t$ , with the gene of interest normalized to  $\beta$ -actin.

*Invasion Assay:* Cells were pre-labeled with 10  $\mu$ g/ml of DilC<sub>12</sub>(3) (BD Biosciences) before seeding cells in serum free media into the apical chambers of the BD BioCoat™ Tumor Invasion System (BD Biosciences). Media containing serum was used as a chemo-attractant in the basal chambers. Fluorescence readings were obtained every 6 hours using BioTek Synergy HT plate reader (BioTek Instruments).

### *Microscopy Studies*

Cell migration assays were conducted using a 96-well plate WoundMaker™ (Essen BioScience) to create homogenous 700-800  $\mu$ m wounds. Images were recorded every 30 minutes and wound properties, including % Relative Wound Density (%RWD, shown below), were measured with IncuCyte Software (Essen BioScience).

$\%RWD(t) = 100 \times [w(t) - w(0)] / [c(t) - c(0)]$ ; where  $w(t)$  = Density of wound region at time,  $t$ ; and  $c(t)$  = Density of cell region at time,  $t$ .

Migration videos were recorded with a JuLi microscope using a 10x objective lens (NanoEnTek) and generated with ImageJ software. Cell morphology studies were performed as previously described [330]. Confocal images were obtained with an Olympus FV1000 MPE multiphoton laser scanning microscope through a 60x LUM Plan FI/IR 0.9N.A. water immersion lens

(Olympus). 405 diode and Red HeNe lasers were used to excite the samples. Images were prepared using FV10-ASW Version 03.00.01.15 software (Olympus).

#### *Data Analysis*

Data was analyzed using GraphPad Prism v6.02 (GraphPad Software, Inc.) & Matlab (MathWorks, Inc.). Statistics were performed using an unpaired two-tailed student's t-test with Welch's correction. Data is reported as mean  $\pm$ SD or  $\pm$ SEM.

**CHAPTER 4**

**EVALUATION OF COMBINATION THERAPY AND POTENTIAL PREDICTIVE  
BIOMARKERS FOR HYPOXIA ACTIVATED PRODRUGS IN PANCREATIC  
CANCER**

**Note to Reader**

Portions of this chapter have been previously published in *Advances in Pharmacology*, 2012, 65:63-107 [34] and are utilized with permission of the publisher.

**Introduction**

*Tumor Hypoxia*

Tumor hypoxia is found in solid tumors of all cancer types. As tumors outgrow their vasculature, the diffusion limit of oxygen from a blood vessel (~200  $\mu\text{m}$ ) becomes a limiting factor, resulting in insufficient oxygen and nutrient delivery to the tumor tissue. Angiogenesis, one of the hallmarks of cancer [28,29], is initiated upon detection of hypoxia, but often generates immature and chaotic vasculature in the tumor [272,341]. Disorganized and immature vasculature results in tumor hypoxia that is extremely heterogeneous both temporally and spatially. Diffusion-limiting hypoxia occurs in regions with mature, patent vasculature, but lack well organized capillary beds to supply all regions of the tumor tissue. Perfusion-related hypoxia occurs from inconsistent tumor blood flow within a tumor, resulting in regions of low oxygenation [20]. Hypoxia is a potent selection force on cancer cells, contributing to tumor

heterogeneity and propagating cancer phenotypes such as pro-survival [66,342] and altered metabolism [343]. Hypoxia inhibits DNA damage repair pathways [22] and increases reactive oxygen species (ROS) [344] resulting in genomic instability and promoting tumor progression [345].

Tumor hypoxia is an indicator of poor prognosis in patients [346-348]. Reduced tumor oxygenation, whether measured using oxygen electrodes, upregulation of hypoxia markers or exogenous markers of hypoxia, consistently correlates with reduced overall survival in patients [349]. Tumor hypoxia, in addition to selecting for a more aggressive cancer phenotype, contributes to chemotherapy and radiation therapy resistance [350,351]. Hypoxia-associated chemotherapy resistance can be mediated by: a lack of drug delivery to the tumor due to poor perfusion [350], hypoxia-induced resistance to apoptosis [352], and decreased cell proliferation of the hypoxic cell fractions [353]. Poor perfusion in tumors decreases chemotherapy penetration into tumors, reducing the effectiveness of treatment [354,355]. Radiation therapy requires the presence of oxygen to generate DNA-damage inducing free radicals, extinguishing the cytotoxic effect of treatment in areas of low oxygenation [352,356,357]. Additionally, hypoxic cell signaling pathways, orchestrated by HIF1 $\alpha$ , can promote survival during radiation therapy [358-360].

### *Targeting Tumor Hypoxia*

Significant efforts have focused on developing clinical agents to reduce hypoxia in tumors or target cells residing in the hypoxic niche (reviewed in detail in Chapter 2). Recently, efforts to target the hypoxic compartments of tumors therapeutically have been pursued, most notably through the use of hypoxia-activated prodrugs (HAPs). HAPs are relatively inert in tissues with normal oxygenation (pO<sub>2</sub>), but are reduced by select one-electron oxidoreductases

under hypoxic conditions to release cytotoxic or cytostatic effectors. A second generation HAP, TH-302 is assembled on a 2-nitroimidazole hypoxia-sensitive trigger and is selectively activated under extreme hypoxia (< 0.05% O<sub>2</sub>) to release a cytotoxic warhead, bromo-isophosphoramidate (Br-IPM) [120]. Similar 2-nitroimidazoles, such as pimonidazole [361] and EF5 [362], are routinely used *in vivo* to identify regions of tumor hypoxia through immunohistochemistry, but lack the cytotoxic warhead of TH-302. TH-302 cytotoxicity has been evaluated extensively *in vitro* [124] and is highly effective in preclinical mouse models [121,363]. Under hypoxic conditions, TH-302 undergoes 1e<sup>-</sup> reduction mediated by CYPOR, releasing Br-IPM [124]. Br-IPM, an alkylating agent, induces DNA damage and cell-cycle arrest in hypoxic cells, and exhibits a bystander effect by killing cells in adjacent normoxic tissues [124].

TH-302 is being investigated clinically for several cancers including pancreatic, sarcoma, multiple myeloma, glioma, kidney, liver, and non-small cell lung cancers (**Table 4.1**). TH-302 has been studied extensively in pancreatic patients with metastatic or unresectable disease. Recently, a phase I/II trial showed that TH-302, in combination with gemcitabine, significantly increased progression-free survival by 2.4 months for pancreatic patients compared to patients receiving gemcitabine alone ( $p = 0.008$ ) [364]. TH-302 has since advanced to phase III clinical trials, which are currently recruiting participants (NCT01746979). TH-302 has also progressed to phase III clinical trials in metastatic or locally advanced unresectable soft tissue sarcoma patients (NCT01440088).

#### *Manipulating Tumor Hypoxia*

As tumor hypoxia is required for TH-302 activity, and TH-302 exhibits a bystander effect by killing cells in adjacent normoxic tissues [121], we hypothesize that TH-302 efficacy could be improved by transiently increasing the hypoxic fraction in solid tumors. *In silico* models and



**Table 4.1** TH-302 Clinical Trials

Clinical Trial Registry Number	Cancer Type		Clinical Phase
NCT00495144	Advanced Solid Tumors	C	1/2
NCT00742963	+/- Doxorubicin in Advanced Soft Tissue Sarcoma	C	1/2
NCT01440088	+/- Doxorubicin in Unresectable or Metastatic Soft Tissue Sarcoma	A	3
NCT01746979	+ Gemcitabine in Untreated Unresectable Pancreatic Adenocarcinoma	R	3
NCT01522872	+/- Bortezomib in Multiple Myeloma	R	1/2
NCT01864538	Advanced Melanoma	R	2
NCT01381822	+/- Sunitinib in RCC, GIST and Pancreatic Neuroendocrine Tumors	A	1/2
NCT01497444	+ Sorafenib in Unresectable Kidney or Liver Cancer	R	1/2
NCT01833546	Solid Tumors and Pancreatic Cancer (Japan)	R	1
NCT01149915	Advanced Leukemia	C	1
NCT01721941	+ Doxorubicin in Hepatocellular Carcinoma	N	1
NCT01485042	+ Pazopanib in Advanced Solid Tumors	A	1
NCT02020226	Cardiac Safety Study in Advanced Solid Tumors	R	1
NCT01403610	+/- Bevacizumab in High Grade Glioma	R	2
NCT02093962	+/- Pemetrexed in Non-squamous NSCLC	R	2
NCT01144455	+/- Gemcitabine in Previously Untreated Pancreatic Adenocarcinoma	A	2
NCT00743379	+ Gemcitabine, Docetaxel OR Pemetrexed in Advanced Solid Tumors	A	1/2
NCT02047500	+ Gemcitabine AND Nab-Paclitaxel in Previously Untreated Pancreatic Cancer	R	1

A = Active; C = Complete; R = Recruiting; N = Not yet recruiting

experimental evidence show the most effective approach to decrease tumor  $pO_2$  is to increase cellular respiration [365]. This was effective in colon carcinoma cells (RKO) in which pharmacological inhibition of HIF-1 $\alpha$  with echinomycin increased oxygen consumption, decreased tumor  $pO_2$  and increased the activity of the HAP, tirapazamine [366]. This treatment resulted in a chronically hypoxic environment that could lead to further hypoxic adaptation of the tumor cells and HAP side effects. In contrast, we propose that transient and acute exacerbation of hypoxia, in combination with TH-302, would be more effective with fewer side-effects. Prior

work has observed that exogenous pyruvate increases the hypoxic fraction in squamous cell carcinoma (SCC) tumors [136] through a transient increase in oxygen consumption (unpublished observations). We have observed that exogenous pyruvate increased efficacy of TH-302 in pre-clinical SCC and PDAC models (unpublished observations and [367]). To explore alternative pharmacologic methods to transiently exacerbate hypoxia and hence enhance the anti-tumor properties of TH-302, we herein investigate the “Steal” phenomenon.

The “Steal” phenomenon has been extensively documented in cancer models [368]. The “Steal” phenomenon occurs when vasodilators, such as hydralazine, cause healthy blood vessels to dilate leading to decreased systemic blood pressure (**Figure 4.1**). Tumor vasculature is often immature and atonal, lacking the ability to constrict or dilate. Hence, during systemic vasodilation, there is a physiological reduction in blood pressure that cannot be matched by the tumor microenvironment and vasculature. The resulting pressure difference creates a transient decrease in tumor perfusion [369-371], increase in tumor hypoxia [372], and increase in tumor acidosis [144,373-375]. Hydralazine has been shown to reduce tumor blood flow within 30 minutes and lasts for 4 to 6 hours [376]. Interestingly, low doses of hydralazine (0.1 mg/kg) increase tumor blood flow, but higher doses (2.5 – 10.0 mg/kg) are effective to reduce tumor perfusion by 80-90% [143]. Hydralazine has been used to enhance the activity of first generation hypoxia-targeted chemotherapies [377,378] and hyperthermia [379,380] by increasing tumor hypoxia, but has not been investigated using current HAPs, including TH-302. In this study we hypothesized that hydralazine could be used acutely to reduce perfusion and increase hypoxia within the tumor microenvironment, thus enhancing the efficacy of TH-302 in pancreatic tumor models.

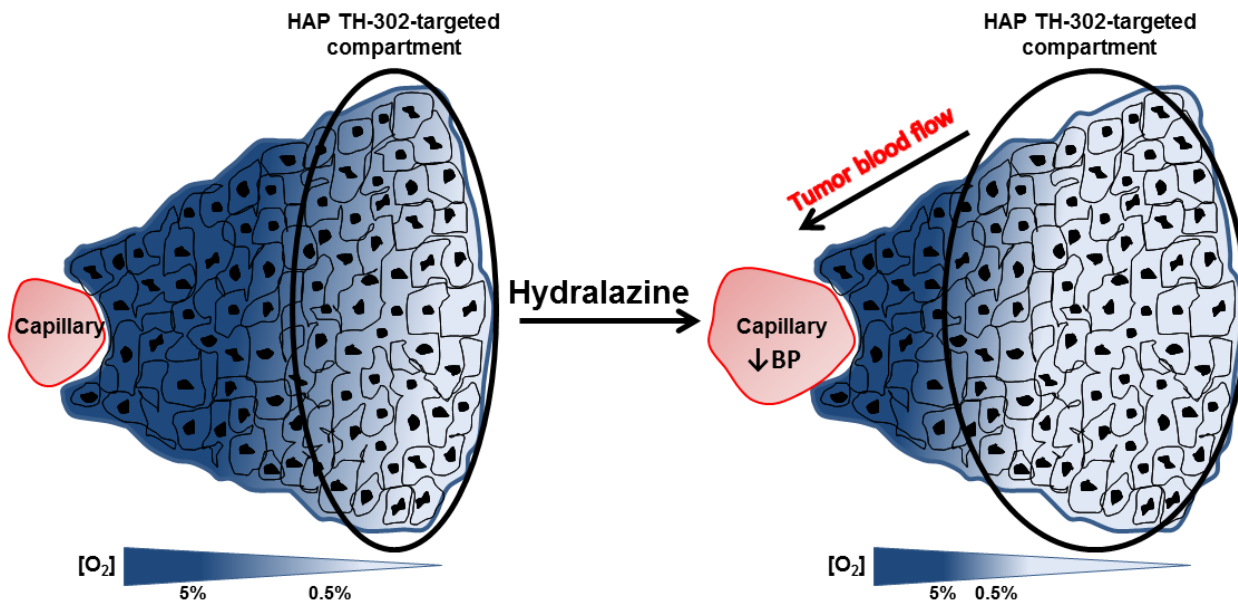


Figure adapted from J. Wojtkowiak

**Figure 4.1** The Steal Phenomenon. Treatment with hydralazine, a vasodilator, cause healthy patent vasculature to dilate resulting in a systemic reduction in blood pressure. Tumor vasculature is often immature and atonal, lacking the ability to constrict or dilate. During systemic vasodilation, there is a physiological reduction in blood pressure that cannot be matched by the tumor microenvironment and vasculature. The resulting pressure differentials creates a transient decrease in tumor perfusion, resulting in increased hypoxia. We hypothesize that increased hypoxia following hydralazine treatment will expand the region of TH-302 activation, increasing TH-302 efficacy in pancreatic xenograft models.

### *Hypoxia in Pancreatic Cancer*

Pancreatic ductal adenocarcinoma (PDAC) patients have extremely poor prognoses, with a 5-year survival rate of approximately 6%. Survival remains low due to a lack of early detection while PDAC is still localized and ineffectiveness of traditional chemotherapies to control PDAC progression. These low survival rates demonstrate the need to develop novel treatment strategies. Pathologically, PDAC tumors are extremely heterogeneous and contain a dynamic desmoplastic stromal compartment, both of which contribute to tumor progression and chemotherapy resistance [381,382]. Desmoplastic stroma is proliferative fibrotic tissue that promotes tumor progression and metastasis [382]. In addition to being a mechanical barrier for drug penetration, desmoplastic stroma contributes profoundly to tumor hypoxia; a common

physiological trait of PDAC tumors that is also associated with both chemotherapy and radiotherapy resistance [350,357,383]. Hypoxic tumor tissues have also been shown to have increased metastatic potential [346] and a majority of PDAC tumors present as metastatic late-stage disease.

## Results

### *PDAC xenografts exhibit variable sensitivity to TH-302 in vitro and in vivo*

Previous studies have shown variable response of three PDAC cell lines, Hs766t, MiaPaCa-2 and SU.86.86, to TH-302 monotherapy both *in vitro* and *in vivo*. Treatment of cells cultured under anoxic conditions with TH-302 show that MiaPaCa-2 cells are the most sensitive ( $IC_{50} = 2.1 \pm 0.7 \mu\text{mol/L}$ ); SU.86.86 responding moderately ( $IC_{50} = 12 \pm 1.2 \mu\text{mol/L}$ ); and Hs766t the least sensitive ( $IC_{50} = 60 \pm 7.5 \mu\text{mol/L}$ ) [124]. Interestingly *in vivo*, tumor xenograft models using the same cell lines show different responses to TH-302 monotherapy. Hs766t responded the most favorably to TH-302 treatment [121], with complete inhibition of tumor growth, while MiaPaCa-2 tumors were moderately responsive [384] and SU.86.86 tumors were resistant to TH-302 monotherapy [385]. The differential response of PDAC cells *in vitro* and *in vivo* emphasizes the importance of the hypoxic fraction within a tumor for maximal TH-302 efficacy *in vivo* as SU.86.86 tumors are highly vascularized and well oxygenated, while Hs766t tumors have large hypoxic fractions [363].

### *pH electrode results indicate that MiaPaCa-2 tumors exhibit “Steal” effect in response to hydralazine*

Since hydralazine treatment has previously been shown to reduce tumor blood flow *in vivo* [370], we hypothesized that hydralazine could be used to transiently increase the hypoxic fraction in tumors and increase TH-302 efficacy. Hydralazine has also been shown to increase

tumor acidosis [144], which may be an effective method to identify tumors exhibiting a “Steal” effect that would be more responsive to combination therapy. To test our hypothesis, mice bearing subcutaneous SU.86.86, MiaPaCa-2 or Hs766t tumors were anesthetized and tumor pH was measured using a pH microelectrode (performed by Heather H. Cornnell). To measure pH changes resulting from blood flow changes, mice were administered 10 mg/kg hydralazine via intraperitoneal (ip) injection. Tumor pH measurements were obtained every 30 minutes following hydralazine treatment for three hours. We hypothesized that tumors exhibiting the “Steal” effect will experience tumor acidification following hydralazine treatment. The TH-302 sensitive Hs766t tumors (n = 3) exhibited no change in average pH following treatment with hydralazine (**Figure 4.2**). TH-302 resistant SU.86.86 tumors (n = 7), however, experience a paradoxical small increase in pH (+ 0.05 pH units) following treatment with hydralazine (**Figure 4.2**). MiaPaCa-2 tumors (n = 4), which are moderately responsive to TH-302, consistently exhibited a “Steal” effect following hydralazine treatment, experiencing a significant reduction in pH (- 0.12 pH units) relative to SU.86.86 ( $p < 0.007$ ) and Hs766t ( $p < 0.05$ ) (**Figure 4.2**). Though heterogeneity existed between tumor samples, each sample tested responded similarly to the other tumors within their cohorts, as evidenced by observing the single animal maximum change, the average of the maximal response from each animal during the experiment and the average change in pH for each animal for each time point measured (**Figure 4.2**). These results indicate that administration of hydralazine led to decreased perfusion in MiaPaCa-2 tumors, but did not affect perfusion in either Hs766t or SU.86.86 tumors.

*Hydralazine treatment results in a reduction in tumor blood flow within 15 minutes*

To further explore the effects of hydralazine on tumors that exhibited the “Steal” effect, used Doppler ultrasound was used to measure the tumor blood flow following hydralazine treatment

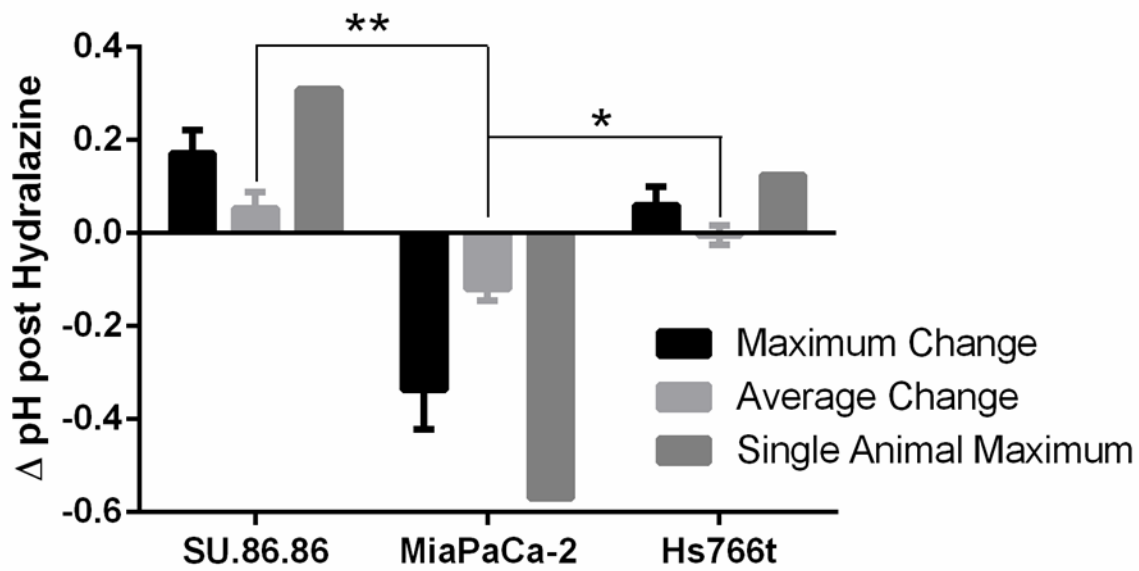


**Figure 4.2** pH electrode results indicate that MiaPaCa-2 tumors exhibit “Steal” Effect in response to hydralazine. Mice bearing subcutaneous SU.86.86 ( $n = 7$ ), Hs766t ( $n = 3$ ) or MiaPaCa-2 ( $n = 4$ ) flank tumors were anesthetized and tumor pH measurements were obtained. A reference electrode was inserted under the skin of the mouse in a non-tumor site while the pH electrode was inserted up to 1.3 cm into the center of each tumor. Two measurements were taken at each time point and averaged. Following initial pH measurements, mice were administered 10 mg/kg hydralazine via ip injection. Tumor pH was measured for 3 hours following treatment. Data reported represents the average maximum change in each cohort, the average pH change for each cohort and the single animal maximum pH change for each cohort. Data is reported as mean change in pH  $\pm$  SEM. \* $p < 0.05$ ; \*\* $p < 0.007$ .

in MiaPaCa-2 tumors. Prior to hydralazine treatment, color Doppler images were obtained across MiaPaCa-2 tumors ( $n = 4$ ) to identify major tumor vasculature (**Figure 4.3, left panel**). Using a pulsed wave (PW) Doppler, blood flow through tumor vasculature was measured over 30 minutes following hydralazine ip administration (**Figure 4.3, right panel**). A reduction in blood flow was observed within 15 minutes of hydralazine injection (**Figure 4.3, right panel**). Quantification of these data confirmed a reduction in tumor blood flow beginning 15 minutes after hydralazine injection with a continued decline through 30 minutes (**Figure 4.4**).

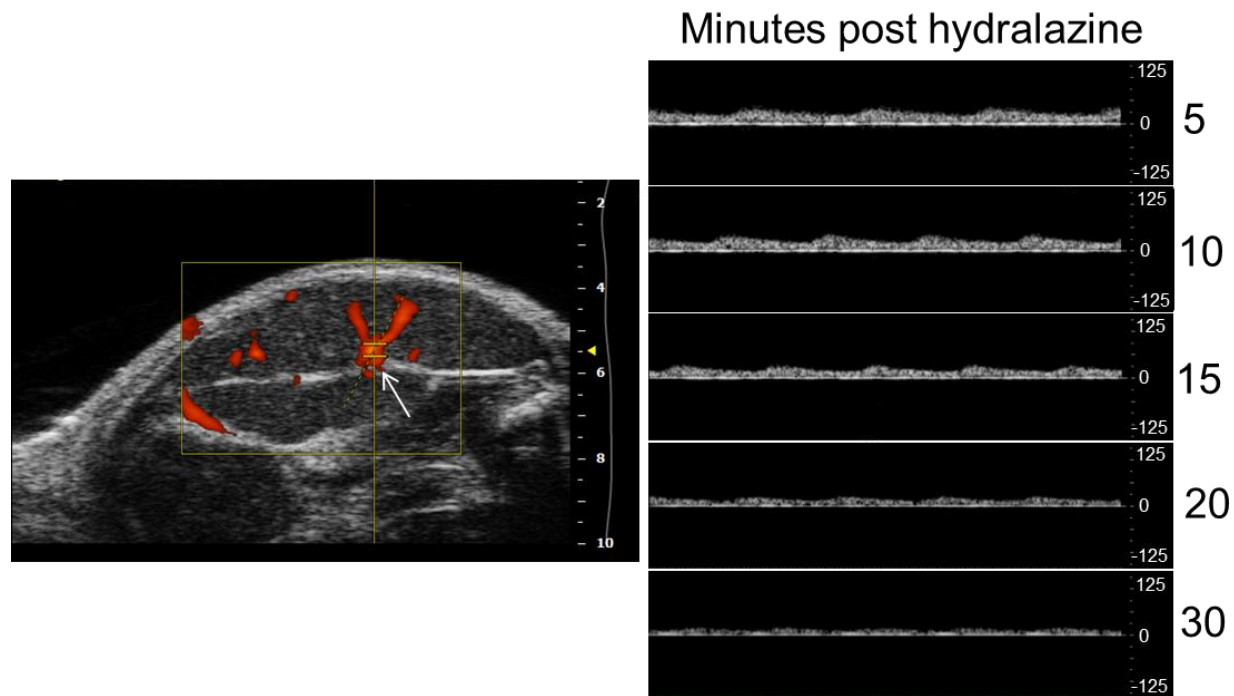


**Figure 4.3** Hydralazine treatment results in reduction in tumor blood flow. Mice bearing MiaPaCa-2 tumors were analyzed by Doppler ultrasound to quantify tumor blood flow. (Left Panel) Tumors were scanned using color Doppler imaging to identify major tumor vasculature prior to treatment. Red represents blood flow through tumor vasculature. White arrow marks vasculature chosen for analysis. (Right Panel) Following hydralazine administration, pulsed wave (PW) Doppler was used every 5 minutes for 30 minutes to quantify blood flow following hydralazine treatment.

*MiaPaCa-2 tumors lack tonal mature vasculature*

Tumor samples from each cell line were analyzed histologically to characterize the vasculature. CD31 and smooth muscle actin (SMA) are two common tumor vasculature immunohistochemistry (IHC) markers that identify the presence (CD31), and the maturity and tone (SMA) of vasculature. Tumors with significant vasculature that are tonal would not be expected to exhibit the “Steal” phenomenon, as the tumor vasculature would dilate in coordination with the systemic effects of hydralazine treatment. Using positive pixel analysis, we quantified the percentage of Hs766t, SU.86.86 and MiaPaCa-2 tumors that contained CD31 and SMA staining. Consistent with the prior results, SU.86.86 tumors had significantly more

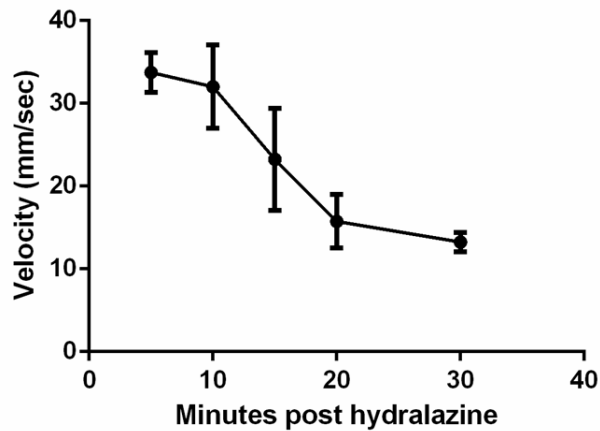


**Figure 4.4** Hydralazine treatment results in a reduction in tumor blood flow within 15 minutes. Mice bearing MiaPaCa-2 tumors were analyzed by Doppler ultrasound to quantify tumor blood flow. Quantification of tumor blood flow changes in MiaPaCa-2 tumors ( $n = 4$ ) following hydralazine treatment. Data is reported as mean velocity (mm/sec)  $\pm$  SEM.

CD31 ( $p < 0.05$ ) staining than either Hs766t or MiaPaCa-2 (**Figure 4.5A-B**), and significantly more SMA ( $p < 0.005$ ) than MiaPaCa-2 tumor samples (**Figure 4.5A, C**). These data indicate that SU.86.86 tumors are well vascularized with mature vessels that would be expected to dilate in response to hydralazine treatment. MiaPaCa-2 and Hs766t tumors had similar amounts of CD31 staining (**Figure 4.5A-B**). MiaPaCa-2 tumors had the least amount of SMA staining among the three tumors tested (**Figure 4.5A, C**). These data indicate that MiaPaCa-2 vasculature is immature and atonal. As MiaPaCa-2 tumors displayed decreased tumor blood flow (**Figure 4.3 and 4.4**) and a subsequent decrease in tumor pH (**Figure 4.2**), we conclude that MiaPaCa-2 tumors exhibit the “Steal” effect due to immature tumor vasculature.

*Vasculature markers identify “Steal” responsive melanoma tumors*

Two melanoma tumor xenograft models were also studied for their response to the “Steal” phenomenon following treatment with hydralazine. pH electrode measurements show that 1205Lu xenografts experience a reduction in pH following hydralazine treatment, which is



consistent with “Steal” responsive tumors (**Figure 4.6A**). MDAMB435 tumors, however, do not exhibit the “Steal” effect in response to hydralazine treatment, maintaining their pH throughout the course of the experiment (**Figure 4.6A**). Tumor samples were analyzed for vasculature markers, CD31 and SMA, using immunohistochemistry to confirm the biomarker patterns observed in pancreatic tumors (**Figure 4.5**). Consistent with vasculature staining in pancreatic tumors, positive pixel analysis of CD31 staining shows that “Steal” responsive tumors, 1205Lu, have significantly less tumor vasculature ( $p < 0.01$ ) than “Steal” resistant tumors, MDAMB435 (**Figure 4.6B**). SMA staining analysis shows a similar trend, that “Steal” responsive tumors have less mature vasculature than “Steal” resistant tumors (**Figure 4.6C**). These data indicate that tumor vasculature markers are an effective biomarker to identify tumors that exhibit the “Steal” effect in response to vasodilator treatment.

*MiaPaCa-2 tumors are moderately sensitive to TH-302, and the effect is slightly enhanced with hydralazine*

To test TH-302 monotherapy and combination therapy with hydralazine for each cell line xenograft, mice were implanted with subcutaneous Hs766t, SU.86.86 or MiaPaCa-2 flank tumors, and pair-matched into four cohorts: untreated (saline), TH-302 alone (50 mg/kg ip), hydralazine alone (10 mg/kg ip) and TH-302/hydralazine combination therapy. In combination therapy, TH-302 was administered 30 minutes following hydralazine administration as this appeared to be the time of maximal effect on perfusion post-hydralazine. All cohorts were treated for two cycles of 5 consecutive treatments followed by 2 days off, and tumor volumes were monitored with electronic calipers during the course of the study. As anticipated, Hs766t tumor growth was completely inhibited with TH-302 monotherapy (**Figure 4.7**), SU.86.86 tumor growth was unaffected by TH-302 monotherapy (**Figure 4.8**) and MiaPaCa-2 tumors responded

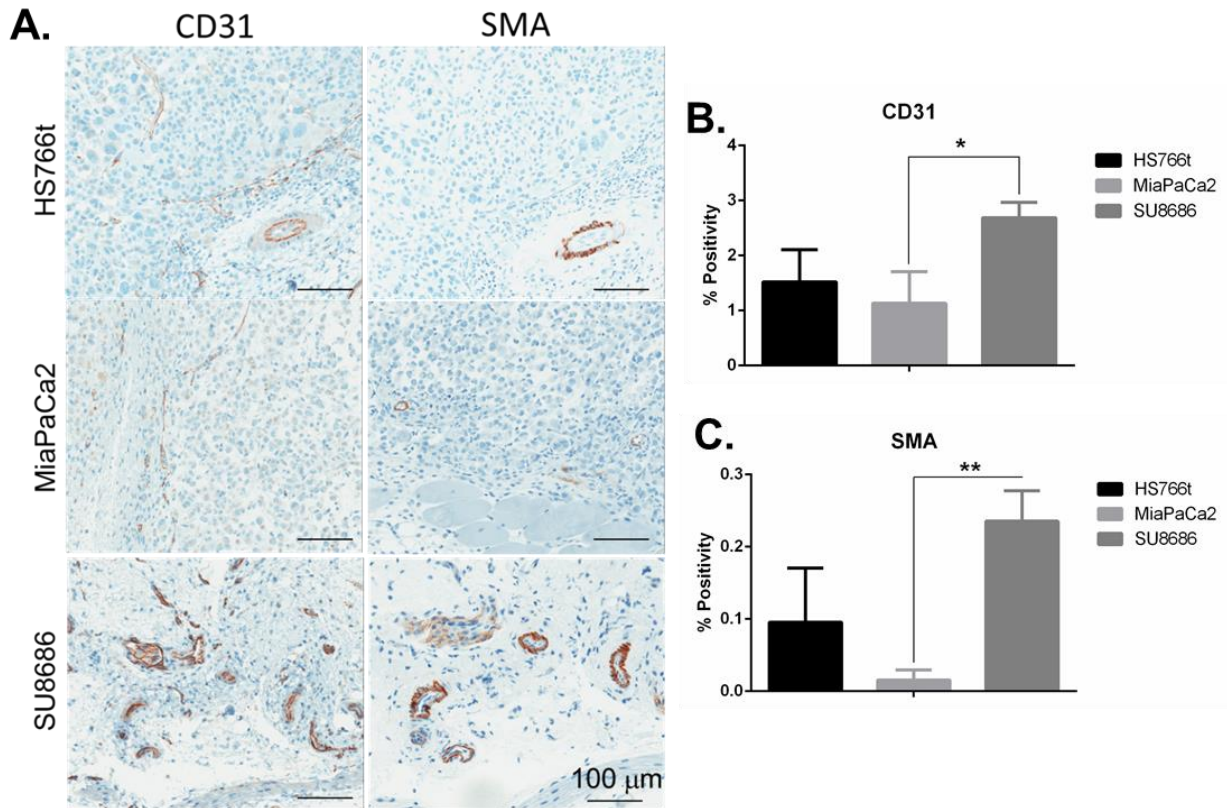


**Figure 4.5** MiaPaCa-2 tumors lack tonal mature vasculature. Hs766t, MiaPaCa-2 and SU.86.86 tumors were fixed and embedded in paraffin in preparation for IHC staining for tumor vasculature markers, CD31 and SMA. (A) Representative images of tumors stained with CD31 and SMA. Scale bars represent 100  $\mu$ m. Positive pixel analysis of (B) CD31 and (C) SMA staining across the whole area of a tumor. Data is presented as % Positivity [(positive pixels/total pixels) x 100]  $\pm$  SEM. \* $p$  < 0.05; \*\* $p$  < 0.005.

moderately to treatment (**Figure 4.9**). Combination therapy of hydralazine followed by administration of TH-302 had no beneficial effect on tumor volume control in mice bearing Hs766t or SU.86.86 tumors relative to cohorts treated with TH-302 monotherapy (**Figures 4.7 and 4.8**). Importantly, neither of these tumor models exhibited the “Steal” effect following hydralazine administration (**Figure 4.2**). MiaPaCa-2 tumors respond moderately to TH-302 monotherapy (**Figure 4.9**) and experienced an increase in tumor acidosis due to reduced tumor blood flow following hydralazine treatment (**Figure 4.2**). Mice bearing MiaPaCa-2 tumors

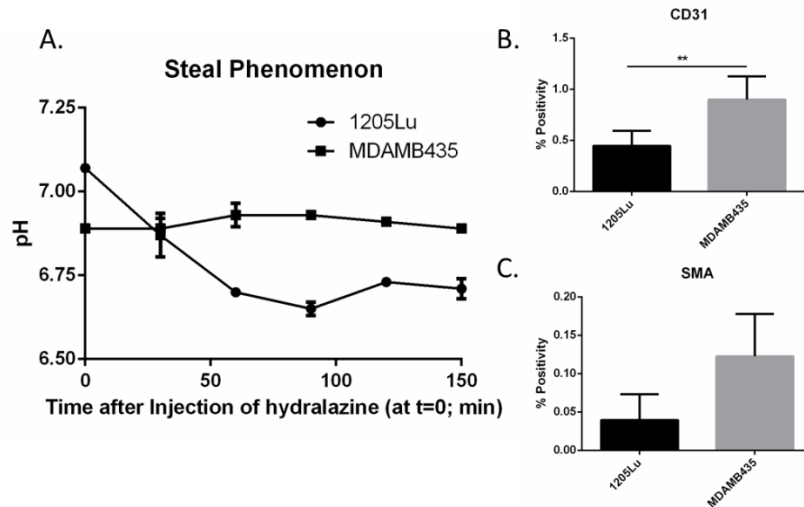


**Figure 4.6** Vasculature markers identify “Steal” responsive melanoma tumors. (A) Mice bearing subcutaneous 1205Lu ( $n = 2$ ) and MDAMB435 ( $n = 2$ ) melanoma tumors were anesthetized and tumor pH measurements were obtained following 10 mg/kg hydralazine treatment. Data is presented as the average  $\pm$  SEM. 1205Lu and MDAMB435 tumors were fixed and embedded in paraffin in preparation for IHC staining for vasculature markers, CD31 and SMA. Positive pixel analysis of (B) CD31 and (C) SMA staining across the whole area of the tumor. Data is presented as % Positivity [(positive pixels/total pixels)  $\times$  100]  $\pm$  SD.  $**p < 0.01$

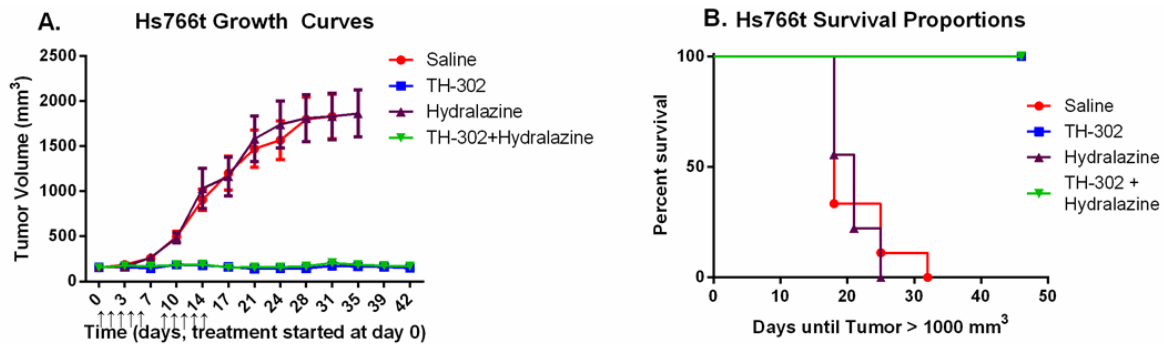


**Figure 4.7** Hs766t tumors are sensitive to TH-302, and the effect is not enhanced with hydralazine. Mice bearing subcutaneous Hs766t tumors ( $n = 9$  per cohort) were pair-matched into 4 cohorts: saline control, TH-302 alone, hydralazine alone, and TH-302 + hydralazine. TH-302 (50mg/kg ip) was administered 30 minutes after hydralazine (10 mg/kg ip) in the combination therapy cohort. (A) Hs766t tumor volumes and (B) Kaplan-Meier curve showing time until tumor volumes reach 1000 mm<sup>3</sup>. Tumor volumes are presented as mean tumor volume  $\pm$  SEM.  $\uparrow$  = dose administered.

experienced a modest further reduction in tumor volume growth when treated with TH-302/hydralazine combination therapy compared to TH-302 monotherapy (**Figure 4.9**). Despite a trending reduction in tumor growth between TH-302/hydralazine combination therapy and TH-302 monotherapy, statistical analyses of the growth curves indicate that the differences did not achieve statistical significance ( $p < 0.08$ ). This experiment was repeated a total of three times, once by myself, with similar results (data not shown). In all cases, MiaPaCa-2 tumors treated with combination therapy had reduced growth, but it was not significantly lower ( $p = 0.07$ ) than that of the TH-302 monotherapy group.

*Combination therapy dosing regimen optimization increases TH-302 efficacy in MiaPaCa-2 tumors*

The regimen for combination therapy above included hydralazine treatment 30 minutes prior to TH-302 administration. However, it is possible that the reduced blood flow at 30 minutes also prevented delivery of TH-302 to the tumor, thus reducing prodrug penetration and activation. Hence, we investigated if an alternate combination dosing regimen would enhance TH-302 efficacy. In a subsequent set of experiments, TH-302 and hydralazine was administered simultaneously to maximize the amount of time TH-302 was exposed to hypoxia due to reduced tumor blood flow. Mice bearing MiaPaCa-2 tumors were pair-matched into three cohorts: TH-302 monotherapy, administration of TH-302 30 minutes after hydralazine, and simultaneous administration of TH-302 and hydralazine. Drug treatments were administered in the same doses as previously described, and were given for two cycles of 5 consecutive days followed by 2 days off. As before, TH-302 treatment 30 minutes post hydralazine trended towards reducing tumor volume growth compared to TH-302 monotherapy, though again the results did not reach statistical significance ( $p = 0.08$ ) (**Figure 4.10**). Interestingly, administration of TH-302 and

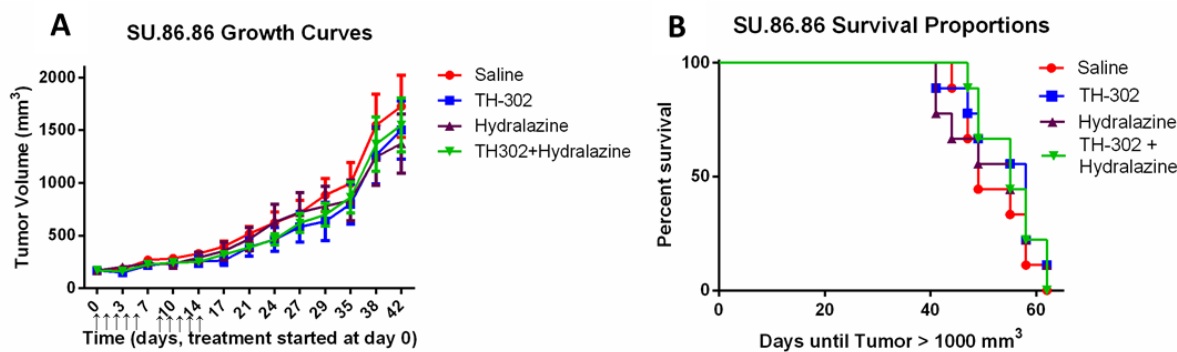


**Figure 4.8** SU.86.86 tumors are resistant to TH-302, and the effect is not enhanced with hydralazine. Mice bearing subcutaneous SU.86.86 tumors ( $n = 9$  per cohort) were pair-matched into 4 cohorts: saline control, TH-302 alone, hydralazine alone, and TH-302 + hydralazine. TH-302 (50mg/kg ip) was administered 30 minutes after hydralazine (10 mg/kg ip) in the combination therapy cohort. (A) SU.86.86 tumor volumes and (B) Kaplan-Meier curve showing time until tumor volumes reach  $1000 \text{ mm}^3$ . Tumor volumes are presented as mean tumor volume  $\pm$  SEM.  $\uparrow$  = dose administered.

hydrilazine simultaneously resulted in better tumor volume control and was significantly better than TH-302 monotherapy ( $p < 0.05$ ) immediately following the completion of the treatment regimen (day 18) (**Figure 4.10**). While simultaneous combination therapy did increase TH-302 efficacy, long term tumor volume control was not achieved after therapy was completed.

## Discussion

Drugs targeting or activated by the physiological tumor microenvironment have the potential to increase antitumor efficacy while reducing side effects from non-specific toxicities. One such class of drug, hypoxia activated prodrugs (HAP), are relatively inert under physiological  $pO_2$  levels in normal tissues, but are activated in areas of hypoxia, which is a common characteristic of solid tumors [28,29]. TH-302, a HAP that is built upon a 2-nitroimidazole scaffold, has been successful in the treatment of pre-clinical models [121,124] and is currently being investigated in clinical trials. Though in phase III trials to treat pancreatic patients in combination with gemcitabine (NCT01746979), long-term control of pancreatic

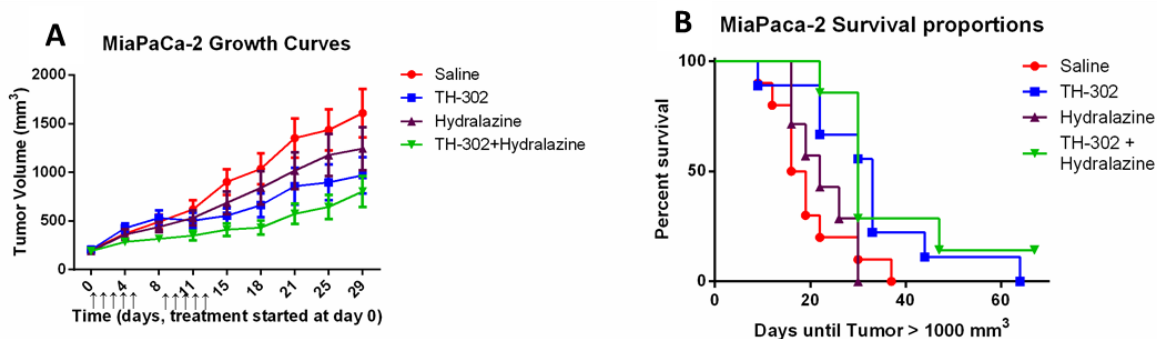


**Figure 4.9** MiaPaCa-2 tumors are moderately sensitive to TH-302, and the effect is slightly enhanced with hydralazine. Mice bearing subcutaneous MiaPaCa-2 tumors were pair-matched into 4 cohorts: saline control ( $n = 10$ ), TH-302 alone ( $n = 9$ ), hydralazine alone ( $n = 7$ ), and TH-302 + hydralazine ( $n = 7$ ). TH-302 (50mg/kg ip) was administered 30 minutes after hydralazine (10 mg/kg ip) in the combination therapy cohort. (A) MiaPaCa-2 tumor volumes and (B) Kaplan-Meier curve showing time until tumor volumes reach 1000 mm<sup>3</sup>. Tumor volumes are presented as mean tumor volume  $\pm$  SEM.  $\uparrow$  = dose administered.

patients in combination with gemcitabine (NCT01746979), long-term control of pancreatic cancer progression has yet to be achieved. We hypothesize that TH-302 activity can be increased *in vivo* by transiently increasing hypoxia within tumors. The use of anti-angiogenic agents, such as vascular endothelial growth factor receptor (VEGFR) inhibitor sunitinib, have been investigated, but the effect on tumor hypoxia varies depending upon the model and regimen employed [386]. We have previously demonstrated that TH-302 efficacy can be exacerbated in pre-clinical pancreatic tumor models by transiently increasing tumor hypoxic fraction metabolically with bolus pyruvate administration (unpublished observations).

In this study, we aimed to determine if the hypoxic fraction of pancreatic tumors could be increased with vasodilators to improve TH-302 efficacy. Hydralazine, a vasodilator used clinically to treat hypertension, has been shown previously to reduce tumor blood flow through the “Steal” phenomenon [370]. By measuring the change in pH in pancreatic tumor models following hydralazine treatment, we were able to identify tumors that exhibit the “Steal” effect *in vivo*. MiaPaCa-2 tumors experienced a significant drop in pH following treatment with

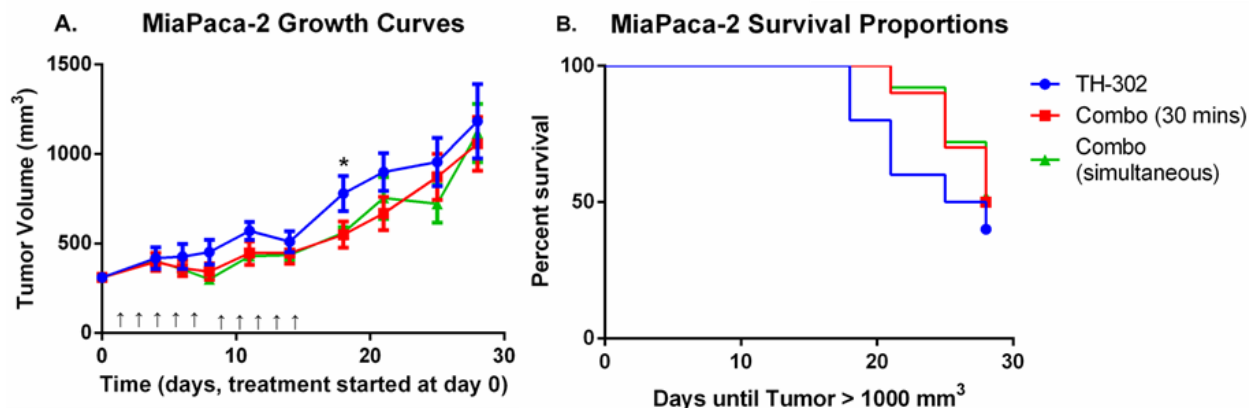


**Figure 4.10** Combination therapy dosing regimen optimization increases TH-302 efficacy in MiaPaCa-2 tumors. Mice bearing MiaPaCa-2 tumors were pair-matched into 3 cohorts ( $n = 10$  per cohort): TH-302 monotherapy, TH-302 30 minutes after hydralazine, and simultaneous administration of TH-302 and hydralazine. TH-302 (50 mg/kg) and hydralazine (10 mg/kg) were administered ip, and treatment consisted of 2 cycles of 5 continuous treatments with 2 days off. (A) Tumor volume measurements of MiaPaCa-2 tumors. (B) Kaplan-Meier curve showing time until MiaPaCa-2 tumors reached 1000 mm<sup>3</sup>. Tumor volumes are presented as mean tumor volume  $\pm$  SEM. \* $p < 0.05$ ;  $\uparrow$  = dose administered.

hydralazine, which is associated with reduced blood flow through the tumor, and these effects were consistent with reduced blood flow, measured by Doppler ultrasound. Neither SU.86.86 nor Hs766t tumors exhibited the “Steal” effect *in vivo* following hydralazine treatment. There was no change in pH in Hs766t or SU.86.86 tumors, possibly due to the presence of mature patent vasculature. Staining of histology sections for smooth muscle actin, SMA, and CD31 was a negative predictor of response to hydralazine in both pancreatic and melanoma tumor models.

As the maximal reduction in blood flow following hydralazine treatment was 30 minutes, we designed the treatment regimen to dose TH-302 30 minutes after hydralazine to maximize the exposure to increased hypoxia. Mice bearing Hs766t and SU.86.86 tumors saw no benefit to combination therapy of hydralazine and TH-302 compared to TH-302 monotherapy, in accordance with the lack of a “Steal” effect observed above. In three separate experiments, mice bearing MiaPaCa-2 tumors, experienced a consistent and modest ( $p = 0.07$ ) reduction in tumor

growth with combination hydralazine and TH-302 therapy compared to TH-302 monotherapy. Further, the therapeutic effect was identical whether hydralazine and TH-302 were given sequentially or simultaneously. Interestingly, studies have been performed to study the effectiveness of topical vasodilators to initiate the “Steal” response over repeated treatments. Abramovic et al. demonstrated that the magnitude of hypoxia and the duration of response following vasodilator treatment decreased with each subsequent dose, leading to a reduction in efficacy over time [387]. The treatment schedule used in this study required 5 consecutive days of treatment, which may have resulted in a reduction in the “Steal” response of MiaPaCa-2 tumors by the end of each treatment cycle. The lack of significant long-term control of MiaPaCa-2 pancreatic tumors with combination therapy and the possibility that hydralazine therapy may become ineffective after multiple treatment cycles indicate that vasodilators will likely not be used clinically to enhance HAP efficacy. However, the study served as a proof of concept that tumor hypoxia can be modulated to improve the efficacy of HAPs.

## **Materials and Methods**

### *Cell Culture*

SU.86.86 and Hs766t cells were obtained from Threshold Pharmaceuticals (South San Francisco, CA) and MiaPaCa-2 cells were obtained from American Type Cell Collection (ATCC, Manassas, VA). Cells were maintained in accordance with ATCC guidelines. Cells were incubated in RPMI 1640 supplemented with 10% FBS (Hs766t and SU.86.86) or DMEM supplemented with 10% FBS (MiaPaCa-2), and were maintained at 37° C in 5% CO<sub>2</sub>. Mycoplasma and cell line authenticity (karyotype) tests were performed.



### *Animal Studies*

All animals were cared for in compliance with Institutional Animal Care and Use Committee (IACUC) approved protocols, and housed at either the USF Vivarium within Moffitt Cancer Center or within the Arizona Cancer Center facility. SCID-beige female mice (Harlan Laboratories, Indianapolis, IN) were inoculated with  $5 - 10 \times 10^6$  cells in 1:1 Matrigel (BD Biosciences, Franklin Lakes, NJ): PBS solution subcutaneously on the right flank. Tumor growth was monitored biweekly with electronic calipers throughout the duration of the experiments.

### *pH Electrode*

pH measurements were obtained using an FE20 Five Easy pH meter (Mettler-Toledo, Columbus, OH). All animals were sedated with isoflurane (3.5%), and remained under anesthesia (1.5 – 3.5% isoflurane) for the duration of the experiment. A reference and pH electrode (MI-401F and MI-408B, respectively, Microelectrodes Inc., Bedford, NH) were used to measure the pH by first inserting the reference electrode (OD 1mm) under the skin of the mouse near the tumor (flank). The pH electrode (OD 0.8mm) was then inserted up to 1.3 cm into the center of each subcutaneous tumor. Electrodes were calibrated prior to and following each set of measurements. Two measurements were taken at each time point and averaged. After the initial pH measurements, the animals were administered 100  $\mu$ L intraperitoneal (ip) injection of 10 mg/kg hydralazine (Sigma Aldrich, St. Louis, MO). The pH was measured every 30 minutes up to three hours after ip injection, and care was taken to measure the pH in approximately the same place in the tumor at each time point. After the final pH measurement, animals were sacrificed and tumors were harvested for histology. Data were processed by taking the average of the two pH values measured at each time point. The change in pH, or delta ( $\Delta(t)$ , where  $t$  is the time

after injection of hydralazine or saline, in minutes) was measured as the difference between the first time point pH and each subsequent time point pH. For each tumor type, the average delta ( $Avg\Delta$ ) is the average delta for all animals of that tumor type:

$$Avg\Delta = \frac{\sum_A \sum_{30 \rightarrow 180}^t \Delta(t)}{n_A}$$

Where  $t$  is time, which ranges from 30 to 180 minutes after injection,  $A$  is the animal,  $n_t$  is the number time points measured, and  $n_A$  is the number of animals with that tumor type. The maximum change in pH at any time after injection was identified for each individual animal. The average maximum across each tumor type was calculated, and the largest change for any one animal in each group was also identified. The number of animals measured varied per tumor type: Hs 766T,  $n=3$ ; MIA PaCa-2  $n=4$ ; and SU.86.86,  $n=7$ .

### *Ultrasound Imaging*

Ultrasound imaging was performed on the Vevo2100 with the 22-55 MHz transducer MS550D (Visual Sonics, Toronto, Ontario, Canada). Mice bearing MiaPaCa-2 tumors ( $n = 4$ ) were sedated (as described above) through the duration of imaging. Color Doppler images were taken to establish the location of a major blood vessel within the tumor. Once a sufficiently large blood vessel was located, a pulsed wave (PW) Doppler was taken for quantification of flow. The animal received a 100  $\mu$ L injection of 10 mg/kg hydralazine, and the flow in the same blood vessel was remeasured every 5 minutes for 30 minutes.

### *Drug Regimens and Tumor Growth Kinetics Monitoring*

Animals were pair matched by tumor volume (as calculated by electronic calipers) when tumors reached  $\sim 200 \text{ mm}^3$ . Animals were separated into four drug treatment groups ( $n = 9$

animals per treatment group for Hs 766T and SU.86.86, numbers listed for MiaPaCa-2): i) TH-302 (n = 9), ii) Hydralazine (n = 7), iii) TH-302 + Hydralazine (n = 7) and iv) Saline (control, n = 10). The treatments were administered as ip injections to un-anesthetized animals. The doses were 50 mg/kg TH-302 in 200  $\mu$ L saline for each animal in groups i and iii, 10 mg/kg hydralazine in 100  $\mu$ L saline per animal [144] in groups ii and iii, and 200  $\mu$ L saline for group iv. Group iii received hydralazine 30 minutes before the administration of TH-302. During simultaneous dosing of hydralazine and TH-302, hydralazine was injected ip immediately before TH-302. All treatment plans were administered Q5D for two concurrent weeks. The tumor volumes were measured twice a week using electronic calipers for the duration of the experiment.

#### *Tissue Processing and Immunohistochemistry*

At the completion of the *in vivo* studies, animals were euthanized and tumors were excised. Tumors were fixed in formalin and embedded in paraffin for further processing. Staining for hematoxylin and eosin (H&E) was performed on 4  $\mu$ m slices. Immunohistochemical (IHC) staining was completed at the Moffitt Tissue Core using Res IHC Omni0UltraMap HRP XT Discovery XT Staining Module (Ventana Medical Systems Inc.). IHC analysis was completed for CD31 (Abcam ab28364) and Smooth Muscle Actin [SMA (Abcam ab32575)]. Slides were scanned with the Aperio™ ScanScope XT (Vista, CA), and positive pixel analysis was performed using Aperio Genie® v1 software. Briefly, the algorithm measured staining intensity across the entire area of the tumor and classified the number of pixels containing stained tissue. The results are presented as percent positivity, which was calculated as the number of positive pixels divided by the total number of pixels multiplied by 100.

### *Data Analysis*

Data were analyzed using GraphPad Prism v6.02 (GraphPad Software Inc.). Statistics were performed using an unpaired 2-tailed Student's t test with Welch's correction. Data are reported as mean  $\pm$  SEM.

## **CHAPTER 5**

### **CONCLUSION**

Cancer prevalence is increasing annually in the United States, and is the second most common disease behind heart disease. Approximately 14 million Americans are living with the disease, and unfortunately over half a million people will die from cancer this year [388]. Ninety percent of these cancer related deaths are attributed to metastatic disease [294]. The field of cancer research is exploding with valuable novel understanding of such a complex disease. Improved techniques with incredible sensitivity have allowed us to form new fields to understand cancer from every angle: genomics, proteomics, metabolomics, radiomics, etc. Despite the influx of knowledge, we are still struggling to control the disease. Cancer prevention and early detection methods have revolutionized the field [389], but for most patients, cancer is not detected until a sizable tumor is found or the patient develops side effects.

Molecular biology in particular has transformed cancer research and clinical practices. Mutated oncogenes and tumor suppressors have been identified and key oncogenic signaling pathways have been described. Drug discovery efforts have yielded many therapies that are specifically targeted to inhibit mutated proteins, halting oncogenic cell signaling pathways and killing cancer cells. Despite developing excellent drugs, these targeted therapies are only efficacious temporarily with tumors ultimately becoming resistant to therapy [12]. Due to inherent heterogeneity within a tumor, resistant populations (whether innate or acquired) will

emerge upon selection with a targeted therapy [9,10,336]. The inevitable emergence of resistance indicates an urgent need to develop novel methods to treat cancer in patients.

Targeting the tumor microenvironment, however, focuses on targeting phenotypic characteristics of tumors rather than genotypic, reducing the likelihood for the development of resistance. Two phenotypic characteristics of the tumor microenvironment are hypoxia and acidosis and occur in nearly every solid tumor. Hypoxia occurs due to chaotic and immature tumor vasculature, and can be transiently and spatially heterogeneous within a tumor [20]. Lack of oxygen promotes metabolism of glucose through glycolysis, which eventually becomes a fixed trait of solid tumors regardless of the oxygenation status [23,283]. Aerobic glycolysis, or the Warburg Effect, generates significant lactic acid waste product, which is then shuttled into the tumor microenvironment to maintain proper intracellular pH. Lactic acid waste builds up in the tumor microenvironment, unable to be removed by inadequate tumor vasculature, resulting in acidosis [15,16]. Both hypoxia and acidosis contribute significantly to tumor progression, malignancy and chemoresistance [26,216,217].

Efforts to target the tumor microenvironment have been made in earnest, some of which have been more successful than others. Inhibitors have been generated for many enzymatic steps of glycolysis, from glucose transporters to lactate dehydrogenase inhibitors. Interestingly, one 2-hexokinase inhibitor, 2-DG, has had a transformative effect on cancer imaging, much more so than its effectiveness to kill tumor cells.  $^{18}\text{F}$ -2DG is used to diagnose and stage up to 90% of tumors and identify sites of metastatic dissemination [338], illustrating the universal importance of the glycolytic pathway in cancer. Targeting acidosis with systemic buffers has been proven to be an effective method to prevent cancer progression and metastatic dissemination in murine models. Ingestion of buffers, such as sodium bicarbonate, imidazoles, TRIS and lysine, increase

the buffering capacity of blood through the alkaline tide phenomenon [259,261,334]. Tumor acidosis is selectively targeted and buffered following treatment with orally available buffers, increasing the pH of the tumor microenvironment. When buffer therapy treatment is initiated prior to tumor development, cancer progression is successfully inhibited in a transgenic prostate cancer model [262]. Once a tumor has formed, however, buffer therapy is ineffective in controlling tumor growth, but importantly is effective in preventing progression to metastatic disease, which is the lethal stage in cancer.

Unfortunately, buffer therapy is not universally effective. Chapter 3 focuses on identifying mechanisms of buffer therapy resistance, where we effectively showed that cell lines that are sensitive to buffer therapy treatment use a pH-dependent mechanism for metastatic dissemination [279]. Buffer therapy sensitive tumors are more acidic than buffer therapy resistant tumors, which is supported by a significantly higher glycolytic flux. Acidic culture conditions alter cellular morphology and migration patterns of buffer therapy sensitive cells, which ultimately contributed to increased invasion. Treatment with buffer therapy effectively increases the pH in sensitive tumors, preventing acid-mediated changes in cellular morphology and migration and preventing invasion. Buffer therapy resistant cells, however, use a pH-independent mechanism for metastatic dissemination, rendering them unresponsive to buffer therapy treatment. Buffer therapy resistant cells constitutively express proteases and maintained protease activity, even during treatment with buffers. By identifying mechanisms of buffer resistance, we can focus on identifying biomarkers that will predict sensitivity to buffer therapy treatment. As  $^{18}\text{F}$ -2DG is commonly used clinically, we will study its effectiveness to differentiate tumors that will be responsive to buffer therapy versus tumors that will be unresponsive to buffer therapy.

Chapter 4 focused on another method of manipulating the tumor microenvironment for therapeutic benefit. Hypoxia is a major contributor to tumor development, malignancy and resistance to therapy [22]. Cellular response pathways to hypoxia have long been a target of drug discover and many drugs have been clinically investigated and approved by the FDA (**Table 2.1**). Hypoxia activated prodrugs (HAPs) target cells residing in hypoxic niches by selective activation by hypoxia. One such compound, TH-302, is activated in regions of extreme hypoxia (< 0.05% O<sub>2</sub>) and is being investigated clinically in many cancers, including pancreatic cancer (**Table 4.1**) [120,121,124,363]. In Chapter 4, a method to increase hypoxia transiently in pancreatic tumors using a vasodilator, hydralazine, to increase TH-302 efficacy was investigated. Treatment with hydralazine causes a systemic reduction in blood pressure that cannot be matched by the tumor vasculature, which is unresponsive to vasodilators. Pressure differences between systemic vasculature and tumor vasculature creates a sink, pulling or “stealing” blood from a tumor, ultimately resulting in a transient increase in hypoxia [370]. Hydralazine treatment reduces blood flow in a pancreatic tumor model, exacerbating acidosis in tumors that exhibited the “steal” effect. Measuring tumor pH and using vasculature markers CD31 and smooth muscle actin (SMA) were predictive of tumors that exhibit the “steal” effect and were responsive to hydralazine and TH-302 combination therapy. While hydralazine marginally increased TH-302 efficacy in our pancreatic model and did not achieve long term control, this study served as proof-of-concept that the tumor microenvironment can effectively manipulated to enhance therapeutic efficacy.

While targeting the tumor microenvironment lessens the likelihood for the development of resistance, the emergence of resistant populations following therapy is still a potential clinical issue. The presence of inherently resistant populations for both methods of targeting the tumor



microenvironment in this dissertation suggests that tumoral heterogeneity may limit the efficacy of therapies targeting the tumor microenvironment. Identification of biomarkers that can effectively predict response to either buffer therapy or treatment with hypoxia activated prodrugs will be essential to maximize clinical efficacy. Additionally, more research is needed to understand the potential for the development of resistance to therapies that target the tumor microenvironment. There is evidence for the development of resistance to buffer therapy, as metastases begin to form after several weeks of therapy (**Figures 3.3 and 3.6**). Efforts to study the metastasis that form in mice that are receiving buffer therapy are being conducted to identify additional mechanisms of resistance that can arise during the course of therapy. As our understanding of resistance to microenvironmental therapies increases, we can better tailor therapeutic regimens and use combinations of targeted therapies and therapies targeting the tumor microenvironment to achieve better clinical outcomes.

As we become more knowledgeable about the development and progression of cancer, it is ever more imperative to take a step back and consider the “big picture” of cancer evolution. Bombarding patients with high dose targeted therapy has shown time and time again to lead directly to drug resistance. Understanding the evolutionary selection forces that result from drug treatment and learning how to harness the drugs we currently have available by using adaptive therapy will help to alleviate drug resistance. Finally, identifying novel therapies and optimize existing therapies that target the tumor microenvironment will ultimately lead to better cancer prevention and tumor control practices clinically.

## CHAPTER 6

### REFERENCES

1. Breasted JH (1980) *The Edwin Smith surgical papyrus*. Chicago: Univ. Chicago Press.
2. DeVita VT, Jr., Chu E (2008) A history of cancer chemotherapy. *Cancer Res* 68: 8643-8653.
3. Sequist LV, Martins RG, Spigel D, Grunberg SM, Spira A, et al. (2008) First-line gefitinib in patients with advanced non-small-cell lung cancer harboring somatic EGFR mutations. *J Clin Oncol* 26: 2442-2449.
4. Vogel CL, Cobleigh MA, Tripathy D, Gutheil JC, Harris LN, et al. (2002) Efficacy and safety of trastuzumab as a single agent in first-line treatment of HER2-overexpressing metastatic breast cancer. *J Clin Oncol* 20: 719-726.
5. Chapman PB, Hauschild A, Robert C, Haanen JB, Ascierto P, et al. (2011) Improved survival with vemurafenib in melanoma with BRAF V600E mutation. *N Engl J Med* 364: 2507-2516.
6. Vogelstein B, Fearon ER, Hamilton SR, Kern SE, Preisinger AC, et al. (1988) Genetic alterations during colorectal-tumor development. *N Engl J Med* 319: 525-532.
7. Fearon ER, Vogelstein B (1990) A genetic model for colorectal tumorigenesis. *Cell* 61: 759-767.
8. Fearon ER, Hamilton SR, Vogelstein B (1987) Clonal analysis of human colorectal tumors. *Science* 238: 193-197.
9. Wood LD, Parsons DW, Jones S, Lin J, Sjoblom T, et al. (2007) The genomic landscapes of human breast and colorectal cancers. *Science* 318: 1108-1113.

10. Gerlinger M, Rowan AJ, Horswell S, Larkin J, Endesfelder D, et al. (2012) Intratumor heterogeneity and branched evolution revealed by multiregion sequencing. *N Engl J Med* 366: 883-892.
11. Loeb LA (1991) Mutator phenotype may be required for multistage carcinogenesis. *Cancer Res* 51: 3075-3079.
12. Shaw AT, Engelman JA (2013) ALK in lung cancer: past, present, and future. *J Clin Oncol* 31: 1105-1111.
13. Orlando PA, Gatenby RA, Brown JS (2012) Cancer treatment as a game: integrating evolutionary game theory into the optimal control of chemotherapy. *Phys Biol* 9: 065007.
14. Silva AS, Kam Y, Khin ZP, Minton SE, Gillies RJ, et al. (2012) Evolutionary approaches to prolong progression-free survival in breast cancer. *Cancer Res* 72: 6362-6370.
15. Griffiths JR (1991) Are cancer cells acidic? *Br J Cancer* 64: 425-427.
16. Wike-Hooley JL, Haveman J, Reinhold HS (1984) The relevance of tumour pH to the treatment of malignant disease. *Radiother Oncol* 2: 343-366.
17. Chitneni SK, Palmer GM, Zalutsky MR, Dewhirst MW (2011) Molecular imaging of hypoxia. *J Nucl Med* 52: 165-168.
18. Wykoff CC, Beasley N, Watson PH, Campo L, Chia SK, et al. (2001) Expression of the hypoxia-inducible and tumor-associated carbonic anhydrases in ductal carcinoma in situ of the breast. *Am J Pathol* 158: 1011-1019.
19. Gillies RJ, Gatenby RA (2007) Adaptive landscapes and emergent phenotypes: why do cancers have high glycolysis? *J Bioenerg Biomembr* 39: 251-257.
20. Dewhirst MW, Cao Y, Moeller B (2008) Cycling hypoxia and free radicals regulate angiogenesis and radiotherapy response. *Nat Rev Cancer* 8: 425-437.
21. Klein TJ, Glazer PM (2010) The tumor microenvironment and DNA repair. *Semin Radiat Oncol* 20: 282-287.

22. Bristow RG, Hill RP (2008) Hypoxia and metabolism. Hypoxia, DNA repair and genetic instability. *Nat Rev Cancer* 8: 180-192.
23. Warburg O, Wind F, Negelein E (1927) The Metabolism of Tumors in the Body. *J Gen Physiol* 8: 519-530.
24. Morita T, Nagaki T, Fukuda I, Okumura K (1992) Clastogenicity of low pH to various cultured mammalian cells. *Mutat Res* 268: 297-305.
25. Wojtkowiak JW, Verduzco D, Schramm KJ, Gillies RJ (2011) Drug resistance and cellular adaptation to tumor acidic pH microenvironment. *Mol Pharm* 8: 2032-2038.
26. Rofstad EK (2000) Microenvironment-induced cancer metastasis. *Int J Radiat Biol* 76: 589-605.
27. Gatenby RA, Gillies RJ (2008) A microenvironmental model of carcinogenesis. *Nat Rev Cancer* 8: 56-61.
28. Hanahan D, Weinberg RA (2000) The hallmarks of cancer. *Cell* 100: 57-70.
29. Hanahan D, Weinberg RA (2011) Hallmarks of cancer: the next generation. *Cell* 144: 646-674.
30. Gillies RJ, Verduzco D, Gatenby RA (2012) Evolutionary dynamics of carcinogenesis and why targeted therapy does not work. *Nat Rev Cancer* 12: 487-493.
31. Gillies RJ, Flowers CI, Drukteinis JS, Gatenby RA (2012) A unifying theory of carcinogenesis, and why targeted therapy doesn't work. *Eur J Radiol* 81 Suppl 1: S48-50.
32. Gatenby RA, Gillies RJ, Brown JS (2011) Of cancer and cave fish. *Nat Rev Cancer* 11: 237-238.
33. Hrustanovic G, Lee BJ, Bivona TG (2013) Mechanisms of resistance to EGFR targeted therapies. *Cancer Biol Ther* 14: 304-314.
34. Bailey KM, Wojtkowiak JW, Hashim AI, Gillies RJ (2012) Targeting the metabolic microenvironment of tumors. *Adv Pharmacol* 65: 63-107.

35. Gillies RJ, Robey I, Gatenby RA (2008) Causes and consequences of increased glucose metabolism of cancers. *J Nucl Med* 49 Suppl 2: 24S-42S.
36. Gillies RJ, Schornack PA, Secomb TW, Raghunand N (1999) Causes and effects of heterogeneous perfusion in tumors. *Neoplasia* 1: 197-207.
37. Hockel M, Vaupel P (2001) Tumor hypoxia: definitions and current clinical, biologic, and molecular aspects. *J Natl Cancer Inst* 93: 266-276.
38. Jaakkola P, Mole DR, Tian YM, Wilson MI, Gielbert J, et al. (2001) Targeting of HIF- $\alpha$  to the von Hippel-Lindau ubiquitylation complex by O<sub>2</sub>-regulated prolyl hydroxylation. *Science* 292: 468-472.
39. Ohh M, Park CW, Ivan M, Hoffman MA, Kim TY, et al. (2000) Ubiquitination of hypoxia-inducible factor requires direct binding to the beta-domain of the von Hippel-Lindau protein. *Nat Cell Biol* 2: 423-427.
40. Semenza GL (2003) Targeting HIF-1 for cancer therapy. *Nat Rev Cancer* 3: 721-732.
41. Birner P, Schindl M, Obermair A, Plank C, Breitenecker G, et al. (2000) Overexpression of hypoxia-inducible factor 1 $\alpha$  is a marker for an unfavorable prognosis in early-stage invasive cervical cancer. *Cancer Res* 60: 4693-4696.
42. Bos R, van der Groep P, Greijer AE, Shvarts A, Meijer S, et al. (2003) Levels of hypoxia-inducible factor-1 $\alpha$  independently predict prognosis in patients with lymph node negative breast carcinoma. *Cancer* 97: 1573-1581.
43. Giatromanolaki A, Koukourakis MI, Sivridis E, Turley H, Talks K, et al. (2001) Relation of hypoxia inducible factor 1  $\alpha$  and 2  $\alpha$  in operable non-small cell lung cancer to angiogenic/molecular profile of tumours and survival. *Br J Cancer* 85: 881-890.
44. Osada R, Horiuchi A, Kikuchi N, Yoshida J, Hayashi A, et al. (2007) Expression of hypoxia-inducible factor 1 $\alpha$ , hypoxia-inducible factor 2 $\alpha$ , and von Hippel-Lindau protein in epithelial ovarian neoplasms and allelic loss of von Hippel-Lindau gene: nuclear expression of hypoxia-inducible factor 1 $\alpha$  is an independent prognostic factor in ovarian carcinoma. *Hum Pathol* 38: 1310-1320.
45. Vaupel P (2004) The role of hypoxia-induced factors in tumor progression. *Oncologist* 9 Suppl 5: 10-17.

46. Hsiang YH, Hertzberg R, Hecht S, Liu LF (1985) Camptothecin induces protein-linked DNA breaks via mammalian DNA topoisomerase I. *J Biol Chem* 260: 14873-14878.
47. Rapisarda A, Uranchimeg B, Scudiero DA, Selby M, Sausville EA, et al. (2002) Identification of small molecule inhibitors of hypoxia-inducible factor 1 transcriptional activation pathway. *Cancer Res* 62: 4316-4324.
48. Rapisarda A, Uranchimeg B, Sordet O, Pommier Y, Shoemaker RH, et al. (2004) Topoisomerase I-mediated inhibition of hypoxia-inducible factor 1: mechanism and therapeutic implications. *Cancer Res* 64: 1475-1482.
49. Rapisarda A, Zalek J, Hollingshead M, Braunschweig T, Uranchimeg B, et al. (2004) Schedule-dependent inhibition of hypoxia-inducible factor-1alpha protein accumulation, angiogenesis, and tumor growth by topotecan in U251-HRE glioblastoma xenografts. *Cancer Res* 64: 6845-6848.
50. Kummar S, Raffeld M, Juwara L, Horneffer Y, Strassberger A, et al. (2011) Multihistology, target-driven pilot trial of oral topotecan as an inhibitor of hypoxia-inducible factor-1alpha in advanced solid tumors. *Clin Cancer Res* 17: 5123-5131.
51. Li L, Lin X, Staver M, Shoemaker A, Semizarov D, et al. (2005) Evaluating hypoxia-inducible factor-1alpha as a cancer therapeutic target via inducible RNA interference in vivo. *Cancer Res* 65: 7249-7258.
52. Greenberger LM, Horak ID, Filpula D, Sapra P, Westergaard M, et al. (2008) A RNA antagonist of hypoxia-inducible factor-1alpha, EZN-2968, inhibits tumor cell growth. *Mol Cancer Ther* 7: 3598-3608.
53. Vester B, Wengel J (2004) LNA (locked nucleic acid): high-affinity targeting of complementary RNA and DNA. *Biochemistry* 43: 13233-13241.
54. Welsh S, Williams R, Kirkpatrick L, Paine-Murrieta G, Powis G (2004) Antitumor activity and pharmacodynamic properties of PX-478, an inhibitor of hypoxia-inducible factor-1alpha. *Mol Cancer Ther* 3: 233-244.
55. Jordan BF, Runquist M, Raghunand N, Baker A, Williams R, et al. (2005) Dynamic contrast-enhanced and diffusion MRI show rapid and dramatic changes in tumor microenvironment in response to inhibition of HIF-1alpha using PX-478. *Neoplasia* 7: 475-485.

56. Koh MY, Spivak-Kroizman T, Venturini S, Welsh S, Williams RR, et al. (2008) Molecular mechanisms for the activity of PX-478, an antitumor inhibitor of the hypoxia-inducible factor-1alpha. *Mol Cancer Ther* 7: 90-100.
57. Palayoor ST, Mitchell JB, Cerna D, Degraff W, John-Aryankalayil M, et al. (2008) PX-478, an inhibitor of hypoxia-inducible factor-1alpha, enhances radiosensitivity of prostate carcinoma cells. *Int J Cancer* 123: 2430-2437.
58. Schwartz DL, Powis G, Thitai-Kumar A, He Y, Bankson J, et al. (2009) The selective hypoxia inducible factor-1 inhibitor PX-478 provides in vivo radiosensitization through tumor stromal effects. *Mol Cancer Ther* 8: 947-958.
59. Tibes RFGS, Von Hoff, D.D., Weiss, G.J., Iyengar, T., Kurzrock, R., Pestano, L., et al. (2010) Results from a phase I, dose-escalation study of PX-478, an orally available inhibitor of HIF-1a. *Journal of Clinical Oncology* 28.
60. Dazert E, Hall MN (2011) mTOR signaling in disease. *Curr Opin Cell Biol* 23: 744-755.
61. Jung CH, Ro SH, Cao J, Otto NM, Kim DH (2010) mTOR regulation of autophagy. *FEBS Lett* 584: 1287-1295.
62. Skeen JE, Bhaskar PT, Chen CC, Chen WS, Peng XD, et al. (2006) Akt deficiency impairs normal cell proliferation and suppresses oncogenesis in a p53-independent and mTORC1-dependent manner. *Cancer Cell* 10: 269-280.
63. Liu L, Cash TP, Jones RG, Keith B, Thompson CB, et al. (2006) Hypoxia-induced energy stress regulates mRNA translation and cell growth. *Mol Cell* 21: 521-531.
64. Li Y, Wang Y, Kim E, Beemiller P, Wang CY, et al. (2007) Bnip3 mediates the hypoxia-induced inhibition on mammalian target of rapamycin by interacting with Rheb. *J Biol Chem* 282: 35803-35813.
65. Bernardi R, Guernah I, Jin D, Grisendi S, Alimonti A, et al. (2006) PML inhibits HIF-1alpha translation and neoangiogenesis through repression of mTOR. *Nature* 442: 779-785.
66. Graeber TG, Osmanian C, Jacks T, Housman DE, Koch CJ, et al. (1996) Hypoxia-mediated selection of cells with diminished apoptotic potential in solid tumours. *Nature* 379: 88-91.

67. Connolly E, Braunstein S, Formenti S, Schneider RJ (2006) Hypoxia inhibits protein synthesis through a 4E-BP1 and elongation factor 2 kinase pathway controlled by mTOR and uncoupled in breast cancer cells. *Mol Cell Biol* 26: 3955-3965.
68. Kaper F, Dornhoefer N, Giaccia AJ (2006) Mutations in the PI3K/PTEN/TSC2 pathway contribute to mammalian target of rapamycin activity and increased translation under hypoxic conditions. *Cancer Res* 66: 1561-1569.
69. Vezina C, Kudelski A, Sehgal SN (1975) Rapamycin (AY-22,989), a new antifungal antibiotic. I. Taxonomy of the producing streptomycete and isolation of the active principle. *J Antibiot (Tokyo)* 28: 721-726.
70. Heitman J, Movva NR, Hall MN (1991) Targets for cell cycle arrest by the immunosuppressant rapamycin in yeast. *Science* 253: 905-909.
71. Houchens DP, Ovejera AA, Riblet SM, Slagel DE (1983) Human brain tumor xenografts in nude mice as a chemotherapy model. *Eur J Cancer Clin Oncol* 19: 799-805.
72. Hess G, Herbrecht R, Romaguera J, Verhoef G, Crump M, et al. (2009) Phase III study to evaluate temsirolimus compared with investigator's choice therapy for the treatment of relapsed or refractory mantle cell lymphoma. *J Clin Oncol* 27: 3822-3829.
73. Hudes G, Carducci M, Tomczak P, Dutcher J, Figlin R, et al. (2007) Temsirolimus, interferon alfa, or both for advanced renal-cell carcinoma. *N Engl J Med* 356: 2271-2281.
74. Rini BI (2008) Temsirolimus, an inhibitor of mammalian target of rapamycin. *Clin Cancer Res* 14: 1286-1290.
75. Gabardi S, Baroletti SA (2010) Everolimus: a proliferation signal inhibitor with clinical applications in organ transplantation, oncology, and cardiology. *Pharmacotherapy* 30: 1044-1056.
76. Motzer RJ, Escudier B, Oudard S, Hutson TE, Porta C, et al. (2008) Efficacy of everolimus in advanced renal cell carcinoma: a double-blind, randomised, placebo-controlled phase III trial. *Lancet* 372: 449-456.
77. Ayral-Kaloustian S, Gu J, Lucas J, Cinque M, Gaydos C, et al. (2010) Hybrid inhibitors of phosphatidylinositol 3-kinase (PI3K) and the mammalian target of rapamycin (mTOR):



design, synthesis, and superior antitumor activity of novel wortmannin-rapamycin conjugates. *J Med Chem* 53: 452-459.

78. Cirstea D, Hideshima T, Rodig S, Santo L, Pozzi S, et al. (2010) Dual inhibition of akt/mammalian target of rapamycin pathway by nanoparticle albumin-bound-rapamycin and perifosine induces antitumor activity in multiple myeloma. *Mol Cancer Ther* 9: 963-975.
79. Ikezoe T, Nishioka C, Bandobashi K, Yang Y, Kuwayama Y, et al. (2007) Longitudinal inhibition of PI3K/Akt/mTOR signaling by LY294002 and rapamycin induces growth arrest of adult T-cell leukemia cells. *Leuk Res* 31: 673-682.
80. Hundal RS, Krssak M, Dufour S, Laurent D, Lebon V, et al. (2000) Mechanism by which metformin reduces glucose production in type 2 diabetes. *Diabetes* 49: 2063-2069.
81. Stumvoll M, Nurjhan N, Perriello G, Dailey G, Gerich JE (1995) Metabolic effects of metformin in non-insulin-dependent diabetes mellitus. *N Engl J Med* 333: 550-554.
82. Zhou G, Myers R, Li Y, Chen Y, Shen X, et al. (2001) Role of AMP-activated protein kinase in mechanism of metformin action. *J Clin Invest* 108: 1167-1174.
83. Inoki K, Zhu T, Guan KL (2003) TSC2 mediates cellular energy response to control cell growth and survival. *Cell* 115: 577-590.
84. Bowker SL, Majumdar SR, Veugelers P, Johnson JA (2006) Increased cancer-related mortality for patients with type 2 diabetes who use sulfonylureas or insulin. *Diabetes Care* 29: 254-258.
85. Evans JM, Donnelly LA, Emslie-Smith AM, Alessi DR, Morris AD (2005) Metformin and reduced risk of cancer in diabetic patients. *BMJ* 330: 1304-1305.
86. Dowling RJ, Zakikhani M, Fantus IG, Pollak M, Sonenberg N (2007) Metformin inhibits mammalian target of rapamycin-dependent translation initiation in breast cancer cells. *Cancer Res* 67: 10804-10812.
87. Zakikhani M, Dowling R, Fantus IG, Sonenberg N, Pollak M (2006) Metformin is an AMP kinase-dependent growth inhibitor for breast cancer cells. *Cancer Res* 66: 10269-10273.

88. Ben Sahra I, Laurent K, Loubat A, Giorgetti-Peraldi S, Colosetti P, et al. (2008) The antidiabetic drug metformin exerts an antitumoral effect in vitro and in vivo through a decrease of cyclin D1 level. *Oncogene* 27: 3576-3586.
89. Saito S, Furuno A, Sakurai J, Sakamoto A, Park HR, et al. (2009) Chemical genomics identifies the unfolded protein response as a target for selective cancer cell killing during glucose deprivation. *Cancer Res* 69: 4225-4234.
90. Koumenis C, Naczki C, Koritzinsky M, Rastani S, Diehl A, et al. (2002) Regulation of protein synthesis by hypoxia via activation of the endoplasmic reticulum kinase PERK and phosphorylation of the translation initiation factor eIF2alpha. *Mol Cell Biol* 22: 7405-7416.
91. Bi M, Naczki C, Koritzinsky M, Fels D, Blais J, et al. (2005) ER stress-regulated translation increases tolerance to extreme hypoxia and promotes tumor growth. *EMBO J* 24: 3470-3481.
92. Romero-Ramirez L, Cao H, Nelson D, Hammond E, Lee AH, et al. (2004) XBP1 is essential for survival under hypoxic conditions and is required for tumor growth. *Cancer Res* 64: 5943-5947.
93. Rouschop KM, van den Beucken T, Dubois L, Niessen H, Bussink J, et al. (2010) The unfolded protein response protects human tumor cells during hypoxia through regulation of the autophagy genes MAP1LC3B and ATG5. *J Clin Invest* 120: 127-141.
94. Travers KJ, Patil CK, Wodicka L, Lockhart DJ, Weissman JS, et al. (2000) Functional and genomic analyses reveal an essential coordination between the unfolded protein response and ER-associated degradation. *Cell* 101: 249-258.
95. Lee AH, Iwakoshi NN, Anderson KC, Glimcher LH (2003) Proteasome inhibitors disrupt the unfolded protein response in myeloma cells. *Proc Natl Acad Sci U S A* 100: 9946-9951.
96. Nawrocki ST, Carew JS, Dunner K, Jr., Boise LH, Chiao PJ, et al. (2005) Bortezomib inhibits PKR-like endoplasmic reticulum (ER) kinase and induces apoptosis via ER stress in human pancreatic cancer cells. *Cancer Res* 65: 11510-11519.
97. Fels DR, Ye J, Segan AT, Kridel SJ, Spiotto M, et al. (2008) Preferential cytotoxicity of bortezomib toward hypoxic tumor cells via overactivation of endoplasmic reticulum stress pathways. *Cancer Res* 68: 9323-9330.

98. Santo L, Hideshima T, Kung AL, Tseng JC, Tamang D, et al. (2012) Preclinical activity, pharmacodynamic, and pharmacokinetic properties of a selective HDAC6 inhibitor, ACY-1215, in combination with bortezomib in multiple myeloma. *Blood* 119: 2579-2589.
99. Dong B, Niwa M, Walter P, Silverman RH (2001) Basis for regulated RNA cleavage by functional analysis of RNase L and Ire1p. *RNA* 7: 361-373.
100. Nock S, Gonzalez TN, Sidrauski C, Niwa M, Walter P (2001) Purification and activity assays of the catalytic domains of the kinase/endoribonuclease Ire1p from *Saccharomyces cerevisiae*. *Methods Enzymol* 342: 3-10.
101. Han D, Lerner AG, Vande Walle L, Upton JP, Xu W, et al. (2009) IRE1alpha kinase activation modes control alternate endoribonuclease outputs to determine divergent cell fates. *Cell* 138: 562-575.
102. Korennykh AV, Egea PF, Korostelev AA, Finer-Moore J, Zhang C, et al. (2009) The unfolded protein response signals through high-order assembly of Ire1. *Nature* 457: 687-693.
103. Papandreou I, Denko NC, Olson M, Van Melckebeke H, Lust S, et al. (2011) Identification of an Ire1alpha endonuclease specific inhibitor with cytotoxic activity against human multiple myeloma. *Blood* 117: 1311-1314.
104. Back SH, Lee K, Vink E, Kaufman RJ (2006) Cytoplasmic IRE1alpha-mediated XBP1 mRNA splicing in the absence of nuclear processing and endoplasmic reticulum stress. *J Biol Chem* 281: 18691-18706.
105. Volkmann K, Lucas JL, Vuga D, Wang X, Brumm D, et al. (2011) Potent and selective inhibitors of the inositol-requiring enzyme 1 endoribonuclease. *J Biol Chem* 286: 12743-12755.
106. Schwartz HS, Sodergren JE, Philips FS (1963) Mitomycin C: Chemical and Biological Studies on Alkylation. *Science* 142: 1181-1183.
107. Iyer VN, Szybalski W (1964) Mitomycins and Porfiromycin: Chemical Mechanism of Activation and Cross-Linking of DNA. *Science* 145: 55-58.

108. Zeman EM, Brown JM, Lemmon MJ, Hirst VK, Lee WW (1986) SR-4233: a new bioreductive agent with high selective toxicity for hypoxic mammalian cells. *Int J Radiat Oncol Biol Phys* 12: 1239-1242.
109. Anderson RF, Shinde SS, Hay MP, Gamage SA, Denny WA (2003) Activation of 3-amino-1,2,4-benzotriazine 1,4-dioxide antitumor agents to oxidizing species following their one-electron reduction. *J Am Chem Soc* 125: 748-756.
110. Baker MA, Zeman EM, Hirst VK, Brown JM (1988) Metabolism of SR 4233 by Chinese hamster ovary cells: basis of selective hypoxic cytotoxicity. *Cancer Res* 48: 5947-5952.
111. Zagorevskii D, Song M, Breneman C, Yuan Y, Fuchs T, et al. (2003) A mass spectrometry study of tirapazamine and its metabolites. insights into the mechanism of metabolic transformations and the characterization of reaction intermediates. *J Am Soc Mass Spectrom* 14: 881-892.
112. Evans JW, Chernikova SB, Kachnic LA, Banath JP, Sordet O, et al. (2008) Homologous recombination is the principal pathway for the repair of DNA damage induced by tirapazamine in mammalian cells. *Cancer Res* 68: 257-265.
113. Le QT, McCoy J, Williamson S, Ryu J, Gaspar LE, et al. (2004) Phase I study of tirapazamine plus cisplatin/etoposide and concurrent thoracic radiotherapy in limited-stage small cell lung cancer (S0004): a Southwest Oncology Group study. *Clin Cancer Res* 10: 5418-5424.
114. Rischin D, Peters L, Fisher R, Macann A, Denham J, et al. (2005) Tirapazamine, Cisplatin, and Radiation versus Fluorouracil, Cisplatin, and Radiation in patients with locally advanced head and neck cancer: a randomized phase II trial of the Trans-Tasman Radiation Oncology Group (TROG 98.02). *J Clin Oncol* 23: 79-87.
115. Rischin D, Peters LJ, O'Sullivan B, Giralt J, Fisher R, et al. (2010) Tirapazamine, cisplatin, and radiation versus cisplatin and radiation for advanced squamous cell carcinoma of the head and neck (TROG 02.02, HeadSTART): a phase III trial of the Trans-Tasman Radiation Oncology Group. *J Clin Oncol* 28: 2989-2995.
116. von Pawel J, von Roemeling R, Gatzemeier U, Boyer M, Elisson LO, et al. (2000) Tirapazamine plus cisplatin versus cisplatin in advanced non-small-cell lung cancer: A report of the international CATAPULT I study group. Cisplatin and Tirapazamine in Subjects with Advanced Previously Untreated Non-Small-Cell Lung Tumors. *J Clin Oncol* 18: 1351-1359.

117. Hicks KO, Fleming Y, Siim BG, Koch CJ, Wilson WR (1998) Extravascular diffusion of tirapazamine: effect of metabolic consumption assessed using the multicellular layer model. *Int J Radiat Oncol Biol Phys* 42: 641-649.
118. Kyle AH, Minchinton AI (1999) Measurement of delivery and metabolism of tirapazamine to tumour tissue using the multilayered cell culture model. *Cancer Chemother Pharmacol* 43: 213-220.
119. Hicks KO, Siim BG, Jaiswal JK, Pruijn FB, Fraser AM, et al. (2010) Pharmacokinetic/pharmacodynamic modeling identifies SN30000 and SN29751 as tirapazamine analogues with improved tissue penetration and hypoxic cell killing in tumors. *Clin Cancer Res* 16: 4946-4957.
120. Duan JX, Jiao H, Kaizerman J, Stanton T, Evans JW, et al. (2008) Potent and highly selective hypoxia-activated achiral phosphoramidate mustards as anticancer drugs. *J Med Chem* 51: 2412-2420.
121. Sun JD, Liu Q, Wang J, Ahluwalia D, Ferraro D, et al. (2012) Selective tumor hypoxia targeting by hypoxia-activated prodrug TH-302 inhibits tumor growth in preclinical models of cancer. *Clin Cancer Res* 18: 758-770.
122. Zhang J, Tian Q, Yung Chan S, Chuen Li S, Zhou S, et al. (2005) Metabolism and transport of oxazaphosphorines and the clinical implications. *Drug Metab Rev* 37: 611-703.
123. Hu J, Handisides DR, Van Valckenborgh E, De Raeve H, Menu E, et al. (2010) Targeting the multiple myeloma hypoxic niche with TH-302, a hypoxia-activated prodrug. *Blood* 116: 1524-1527.
124. Meng F, Evans JW, Bhupathi D, Banica M, Lan L, et al. (2012) Molecular and cellular pharmacology of the hypoxia-activated prodrug TH-302. *Mol Cancer Ther* 11: 740-751.
125. Ganjoo KN, Cranmer LD, Butrynski JE, Rushing D, Adkins D, et al. (2011) A phase I study of the safety and pharmacokinetics of the hypoxia-activated prodrug TH-302 in combination with doxorubicin in patients with advanced soft tissue sarcoma. *Oncology* 80: 50-56.
126. Weiss GJ, Infante JR, Chiorean EG, Borad MJ, Bendell JC, et al. (2011) Phase 1 study of the safety, tolerability, and pharmacokinetics of TH-302, a hypoxia-activated prodrug, in patients with advanced solid malignancies. *Clin Cancer Res* 17: 2997-3004.

127. Smith PJ, Blunt NJ, Desnoyers R, Giles Y, Patterson LH (1997) DNA topoisomerase II-dependent cytotoxicity of alkylaminoanthraquinones and their N-oxides. *Cancer Chemother Pharmacol* 39: 455-461.
128. Gallagher R, Hughes CM, Murray MM, Friery OP, Patterson LH, et al. (2001) The chemopotential of cisplatin by the novel bioreductive drug AQ4N. *Br J Cancer* 85: 625-629.
129. Patterson LH, McKeown SR, Ruparella K, Double JA, Bibby MC, et al. (2000) Enhancement of chemotherapy and radiotherapy of murine tumours by AQ4N, a bioreductively activated anti-tumour agent. *Br J Cancer* 82: 1984-1990.
130. Williams KJ, Albertella MR, Fitzpatrick B, Loadman PM, Shnyder SD, et al. (2009) In vivo activation of the hypoxia-targeted cytotoxin AQ4N in human tumor xenografts. *Mol Cancer Ther* 8: 3266-3275.
131. Papadopoulos KP, Goel S, Beeram M, Wong A, Desai K, et al. (2008) A phase 1 open-label, accelerated dose-escalation study of the hypoxia-activated prodrug AQ4N in patients with advanced malignancies. *Clin Cancer Res* 14: 7110-7115.
132. Steward WP, Middleton M, Benghiat A, Loadman PM, Hayward C, et al. (2007) The use of pharmacokinetic and pharmacodynamic end points to determine the dose of AQ4N, a novel hypoxic cell cytotoxin, given with fractionated radiotherapy in a phase I study. *Ann Oncol* 18: 1098-1103.
133. Hendricksen K, van der Heijden AG, Cornel EB, Vergunst H, de Reijke TM, et al. (2009) Two-year follow-up of the phase II marker lesion study of intravesical apaziquone for patients with non-muscle invasive bladder cancer. *World J Urol* 27: 337-342.
134. McKeage MJ, Gu Y, Wilson WR, Hill A, Amies K, et al. (2011) A phase I trial of PR-104, a pre-prodrug of the bioreductive prodrug PR-104A, given weekly to solid tumour patients. *BMC Cancer* 11: 432.
135. Parveen I, Naughton DP, Whish WJ, Threadgill MD (1999) 2-nitroimidazol-5-ylmethyl as a potential bioreductively activated prodrug system: reductively triggered release of the PARP inhibitor 5-bromoisoquinolinone. *Bioorg Med Chem Lett* 9: 2031-2036.
136. Saito K, Matsumoto S, Devasahayam N, Subramanian S, Munasinghe JP, et al. (2012) Transient decrease in tumor oxygenation after intravenous administration of pyruvate. *Magn Reson Med* 67: 801-807.

137. Kauppinen RA, Nicholls DG (1986) Synaptosomal bioenergetics. The role of glycolysis, pyruvate oxidation and responses to hypoglycaemia. *Eur J Biochem* 158: 159-165.
138. Xie J, Wang BS, Yu DH, Lu Q, Ma J, et al. (2011) Dichloroacetate shifts the metabolism from glycolysis to glucose oxidation and exhibits synergistic growth inhibition with cisplatin in HeLa cells. *Int J Oncol* 38: 409-417.
139. Chung AS, Lee J, Ferrara N (2010) Targeting the tumour vasculature: insights from physiological angiogenesis. *Nat Rev Cancer* 10: 505-514.
140. Mitchell DC, Bryan BA (2010) Anti-angiogenic therapy: adapting strategies to overcome resistant tumors. *J Cell Biochem* 111: 543-553.
141. Dachs GU, Steele AJ, Coralli C, Kanthou C, Brooks AC, et al. (2006) Anti-vascular agent Combretastatin A-4-P modulates hypoxia inducible factor-1 and gene expression. *BMC Cancer* 6: 280.
142. Sonveaux P (2008) Provascular strategy: targeting functional adaptations of mature blood vessels in tumors to selectively influence the tumor vascular reactivity and improve cancer treatment. *Radiother Oncol* 86: 300-313.
143. Horsman MR, Christensen KL, Overgaard J (1992) Relationship between the hydralazine-induced changes in murine tumor blood supply and mouse blood pressure. *Int J Radiat Oncol Biol Phys* 22: 455-458.
144. Adachi E, Tannock IF (1999) The effects of vasodilating drugs on pH in tumors. *Oncol Res* 11: 179-185.
145. Belfi CA, Paul CR, Shan S, Ngo FQ (1994) Comparison of the effects of hydralazine on tumor and normal tissue blood perfusion by MRI. *Int J Radiat Oncol Biol Phys* 29: 473-479.
146. Nordsmark M, Maxwell RJ, Wood PJ, Stratford IJ, Adams GE, et al. (1996) Effect of hydralazine in spontaneous tumours assessed by oxygen electrodes and <sup>31</sup>P-magnetic resonance spectroscopy. *Br J Cancer Suppl* 27: S232-235.
147. Okunieff P, Kallinowski F, Vaupel P, Neuringer LJ (1988) Effects of hydralazine-induced vasodilation on the energy metabolism of murine tumors studied by in vivo <sup>31</sup>P-nuclear magnetic resonance spectroscopy. *J Natl Cancer Inst* 80: 745-750.

148. Kroemer G, Pouyssegur J (2008) Tumor cell metabolism: cancer's Achilles' heel. *Cancer Cell* 13: 472-482.
149. Kasahara M, Hinkle PC (1977) Reconstitution and purification of the D-glucose transporter from human erythrocytes. *J Biol Chem* 252: 7384-7390.
150. Ayala FR, Rocha RM, Carvalho KC, Carvalho AL, da Cunha IW, et al. (2010) GLUT1 and GLUT3 as potential prognostic markers for Oral Squamous Cell Carcinoma. *Molecules* 15: 2374-2387.
151. Cantuaria G, Fagotti A, Ferrandina G, Magalhaes A, Nadji M, et al. (2001) GLUT-1 expression in ovarian carcinoma: association with survival and response to chemotherapy. *Cancer* 92: 1144-1150.
152. Pinheiro C, Sousa B, Albergaria A, Paredes J, Dufloth R, et al. (2011) GLUT1 and CAIX expression profiles in breast cancer correlate with adverse prognostic factors and MCT1 overexpression. *Histol Histopathol* 26: 1279-1286.
153. Burant CF, Bell GI (1992) Mammalian facilitative glucose transporters: evidence for similar substrate recognition sites in functionally monomeric proteins. *Biochemistry* 31: 10414-10420.
154. Gould GW, Thomas HM, Jess TJ, Bell GI (1991) Expression of human glucose transporters in *Xenopus* oocytes: kinetic characterization and substrate specificities of the erythrocyte, liver, and brain isoforms. *Biochemistry* 30: 5139-5145.
155. Shepherd PR, Kahn BB (1999) Glucose transporters and insulin action--implications for insulin resistance and diabetes mellitus. *N Engl J Med* 341: 248-257.
156. Birnbaum MJ, Haspel HC, Rosen OM (1987) Transformation of rat fibroblasts by FSV rapidly increases glucose transporter gene transcription. *Science* 235: 1495-1498.
157. Bos R, van Der Hoeven JJ, van Der Wall E, van Der Groep P, van Diest PJ, et al. (2002) Biologic correlates of (18)fluorodeoxyglucose uptake in human breast cancer measured by positron emission tomography. *J Clin Oncol* 20: 379-387.
158. Flier JS, Mueckler MM, Usher P, Lodish HF (1987) Elevated levels of glucose transport and transporter messenger RNA are induced by ras or src oncogenes. *Science* 235: 1492-1495.



159. Hatanaka M (1974) Transport of sugars in tumor cell membranes. *Biochim Biophys Acta* 355: 77-104.
160. Rastogi S, Banerjee S, Chellappan S, Simon GR (2007) Glut-1 antibodies induce growth arrest and apoptosis in human cancer cell lines. *Cancer Lett* 257: 244-251.
161. Taverna RD, Langdon RG (1973) Reversible association of cytochalasin B with the human erythrocyte membrane. Inhibition of glucose transport and the stoichiometry of cytochalasin binding. *Biochim Biophys Acta* 323: 207-219.
162. Vera JC, Reyes AM, Velasquez FV, Rivas CI, Zhang RH, et al. (2001) Direct inhibition of the hexose transporter GLUT1 by tyrosine kinase inhibitors. *Biochemistry* 40: 777-790.
163. Schimmer AD, Thomas MP, Hurren R, Gronda M, Pellicchia M, et al. (2006) Identification of small molecules that sensitize resistant tumor cells to tumor necrosis factor-family death receptors. *Cancer Res* 66: 2367-2375.
164. Wood TE, Dalili S, Simpson CD, Hurren R, Mao X, et al. (2008) A novel inhibitor of glucose uptake sensitizes cells to FAS-induced cell death. *Mol Cancer Ther* 7: 3546-3555.
165. Chan DA, Sutphin PD, Nguyen P, Turcotte S, Lai EW, et al. (2011) Targeting GLUT1 and the Warburg effect in renal cell carcinoma by chemical synthetic lethality. *Sci Transl Med* 3: 94ra70.
166. Goel S, Duda DG, Xu L, Munn LL, Boucher Y, et al. (2011) Normalization of the vasculature for treatment of cancer and other diseases. *Physiol Rev* 91: 1071-1121.
167. Mathupala SP, Heese C, Pedersen PL (1997) Glucose catabolism in cancer cells. The type II hexokinase promoter contains functionally active response elements for the tumor suppressor p53. *J Biol Chem* 272: 22776-22780.
168. Kurtoglu M, Maher JC, Lampidis TJ (2007) Differential toxic mechanisms of 2-deoxy-D-glucose versus 2-fluorodeoxy-D-glucose in hypoxic and normoxic tumor cells. *Antioxid Redox Signal* 9: 1383-1390.
169. Lampidis TJ, Kurtoglu M, Maher JC, Liu H, Krishan A, et al. (2006) Efficacy of 2-halogen substituted D-glucose analogs in blocking glycolysis and killing "hypoxic tumor cells". *Cancer Chemother Pharmacol* 58: 725-734.

170. Ramirez-Peinado S, Alcazar-Limones F, Lagares-Tena L, El Mjiyad N, Caro-Maldonado A, et al. (2011) 2-deoxyglucose induces Noxa-dependent apoptosis in alveolar rhabdomyosarcoma. *Cancer Res* 71: 6796-6806.
171. Song CW, Clement JJ, Levitt SH (1976) Preferential cytotoxicity of 5-thio-D-glucose against hypoxic tumor cells. *J Natl Cancer Inst* 57: 603-605.
172. Ko YH, Pedersen PL, Geschwind JF (2001) Glucose catabolism in the rabbit VX2 tumor model for liver cancer: characterization and targeting hexokinase. *Cancer Lett* 173: 83-91.
173. Meloche HP, Luczak MA, Wurster JM (1972) The substrate analog, bromopyruvate, as both a substrate and alkylating agent for 2-keto-3-deoxy-6-phosphogluconic aldolase. Kinetic and stereochemical studies. *J Biol Chem* 247: 4186-4191.
174. Thangaraju M, Karunakaran SK, Itagaki S, Gopal E, Elangovan S, et al. (2009) Transport by SLC5A8 with subsequent inhibition of histone deacetylase 1 (HDAC1) and HDAC3 underlies the antitumor activity of 3-bromopyruvate. *Cancer* 115: 4655-4666.
175. Nakano A, Tsuji D, Miki H, Cui Q, El Sayed SM, et al. (2011) Glycolysis inhibition inactivates ABC transporters to restore drug sensitivity in malignant cells. *PLoS One* 6: e27222.
176. Zhou Y, Tozzi F, Chen J, Fan F, Xia L, et al. (2012) Intracellular ATP levels are a pivotal determinant of chemoresistance in colon cancer cells. *Cancer Res* 72: 304-314.
177. Floridi A, Lehninger AL (1983) Action of the antitumor and antispermatogenic agent lonidamine on electron transport in Ehrlich ascites tumor mitochondria. *Arch Biochem Biophys* 226: 73-83.
178. Floridi A, Paggi MG, Marcante ML, Silvestrini B, Caputo A, et al. (1981) Lonidamine, a selective inhibitor of aerobic glycolysis of murine tumor cells. *J Natl Cancer Inst* 66: 497-499.
179. Brawer MK (2005) Lonidamine: basic science and rationale for treatment of prostatic proliferative disorders. *Rev Urol* 7 Suppl 7: S21-26.

180. Li YC, Fung KP, Kwok TT, Lee CY, Suen YK, et al. (2002) Mitochondrial targeting drug lonidamine triggered apoptosis in doxorubicin-resistant HepG2 cells. *Life Sci* 71: 2729-2740.
181. Ravagnan L, Marzo I, Costantini P, Susin SA, Zamzami N, et al. (1999) Lonidamine triggers apoptosis via a direct, Bcl-2-inhibited effect on the mitochondrial permeability transition pore. *Oncogene* 18: 2537-2546.
182. Ditonno P, Battaglia M, Selvaggio O, Garofalo L, Lorusso V, et al. (2005) Clinical Evidence Supporting the Role of Lonidamine for the Treatment of BPH. *Rev Urol* 7 Suppl 7: S27-33.
183. Milane L, Duan Z, Amiji M (2011) Therapeutic efficacy and safety of paclitaxel/lonidamine loaded EGFR-targeted nanoparticles for the treatment of multi-drug resistant cancer. *PLoS One* 6: e24075.
184. Milane L, Duan Z, Amiji M (2011) Development of EGFR-targeted polymer blend nanocarriers for combination paclitaxel/lonidamine delivery to treat multi-drug resistance in human breast and ovarian tumor cells. *Mol Pharm* 8: 185-203.
185. Bosca L, Mojena M, Ghysdael J, Rousseau GG, Hue L (1986) Expression of the v-src or v-fps oncogene increases fructose 2,6-bisphosphate in chick-embryo fibroblasts. Novel mechanism for the stimulation of glycolysis by retroviruses. *Biochem J* 236: 595-599.
186. Kole HK, Resnick RJ, Van Doren M, Racker E (1991) Regulation of 6-phosphofructo-1-kinase activity in ras-transformed rat-1 fibroblasts. *Arch Biochem Biophys* 286: 586-590.
187. Atsumi T, Chesney J, Metz C, Leng L, Donnelly S, et al. (2002) High expression of inducible 6-phosphofructo-2-kinase/fructose-2,6-bisphosphatase (iPFK-2; PFKFB3) in human cancers. *Cancer Res* 62: 5881-5887.
188. Bensaad K, Tsuruta A, Selak MA, Vidal MN, Nakano K, et al. (2006) TIGAR, a p53-inducible regulator of glycolysis and apoptosis. *Cell* 126: 107-120.
189. Clem B, Telang S, Clem A, Yalcin A, Meier J, et al. (2008) Small-molecule inhibition of 6-phosphofructo-2-kinase activity suppresses glycolytic flux and tumor growth. *Mol Cancer Ther* 7: 110-120.

190. Akter S, Clem BF, Lee HJ, Chesney J, Bae Y (2012) Block copolymer micelles for controlled delivery of glycolytic enzyme inhibitors. *Pharm Res* 29: 847-855.
191. Seo M, Kim JD, Neau D, Sehgal I, Lee YH (2011) Structure-based development of small molecule PFKFB3 inhibitors: a framework for potential cancer therapeutic agents targeting the Warburg effect. *PLoS One* 6: e24179.
192. Christofk HR, Vander Heiden MG, Harris MH, Ramanathan A, Gerszten RE, et al. (2008) The M2 splice isoform of pyruvate kinase is important for cancer metabolism and tumour growth. *Nature* 452: 230-233.
193. Elekes K, Helyes Z, Kereskai L, Sandor K, Pinter E, et al. (2008) Inhibitory effects of synthetic somatostatin receptor subtype 4 agonists on acute and chronic airway inflammation and hyperreactivity in the mouse. *Eur J Pharmacol* 578: 313-322.
194. Stetak A, Veress R, Ovadi J, Csermely P, Keri G, et al. (2007) Nuclear translocation of the tumor marker pyruvate kinase M2 induces programmed cell death. *Cancer Res* 67: 1602-1608.
195. Greenberg R, Haddad R, Kashtan H, Kaplan O (2000) The effects of somatostatin and octreotide on experimental and human acute pancreatitis. *J Lab Clin Med* 135: 112-121.
196. Stetak A, Lankenau A, Vantus T, Csermely P, Ullrich A, et al. (2001) The antitumor somatostatin analogue TT-232 induces cell cycle arrest through PKCdelta and c-Src. *Biochem Biophys Res Commun* 285: 483-488.
197. Vantus T, Keri G, Krivickiene Z, Valius M, Stetak A, et al. (2001) The somatostatin analogue TT-232 induces apoptosis in A431 cells: sustained activation of stress-activated kinases and inhibition of signalling to extracellular signal-regulated kinases. *Cell Signal* 13: 717-725.
198. Holness MJ, Sugden MC (2003) Regulation of pyruvate dehydrogenase complex activity by reversible phosphorylation. *Biochem Soc Trans* 31: 1143-1151.
199. Stacpoole PW, Lorenz AC, Thomas RG, Harman EM (1988) Dichloroacetate in the treatment of lactic acidosis. *Ann Intern Med* 108: 58-63.

200. Bowker-Kinley MM, Davis WI, Wu P, Harris RA, Popov KM (1998) Evidence for existence of tissue-specific regulation of the mammalian pyruvate dehydrogenase complex. *Biochem J* 329 ( Pt 1): 191-196.
201. Knoechel TR, Tucker AD, Robinson CM, Phillips C, Taylor W, et al. (2006) Regulatory roles of the N-terminal domain based on crystal structures of human pyruvate dehydrogenase kinase 2 containing physiological and synthetic ligands. *Biochemistry* 45: 402-415.
202. Stacpoole PW (1989) The pharmacology of dichloroacetate. *Metabolism* 38: 1124-1144.
203. Wong JY, Huggins GS, Debidda M, Munshi NC, De Vivo I (2008) Dichloroacetate induces apoptosis in endometrial cancer cells. *Gynecol Oncol* 109: 394-402.
204. Bonnet S, Archer SL, Allalunis-Turner J, Haromy A, Beaulieu C, et al. (2007) A mitochondria-K<sup>+</sup> channel axis is suppressed in cancer and its normalization promotes apoptosis and inhibits cancer growth. *Cancer Cell* 11: 37-51.
205. Cao W, Yacoub S, Shiverick KT, Namiki K, Sakai Y, et al. (2008) Dichloroacetate (DCA) sensitizes both wild-type and over expressing Bcl-2 prostate cancer cells in vitro to radiation. *Prostate* 68: 1223-1231.
206. Michelakis ED, Sutendra G, Dromparis P, Webster L, Haromy A, et al. (2010) Metabolic modulation of glioblastoma with dichloroacetate. *Sci Transl Med* 2: 31ra34.
207. Firth JD, Ebert BL, Ratcliffe PJ (1995) Hypoxic regulation of lactate dehydrogenase A. Interaction between hypoxia-inducible factor 1 and cAMP response elements. *J Biol Chem* 270: 21021-21027.
208. Semenza GL, Jiang BH, Leung SW, Passantino R, Concordet JP, et al. (1996) Hypoxia response elements in the aldolase A, enolase 1, and lactate dehydrogenase A gene promoters contain essential binding sites for hypoxia-inducible factor 1. *J Biol Chem* 271: 32529-32537.
209. Fantin VR, St-Pierre J, Leder P (2006) Attenuation of LDH-A expression uncovers a link between glycolysis, mitochondrial physiology, and tumor maintenance. *Cancer Cell* 9: 425-434.

210. Goldman RD, Kaplan NO, Hall TC (1964) Lactic Dehydrogenase in Human Neoplastic Tissues. *Cancer Res* 24: 389-399.
211. Xie H, Valera VA, Merino MJ, Amato AM, Signoretti S, et al. (2009) LDH-A inhibition, a therapeutic strategy for treatment of hereditary leiomyomatosis and renal cell cancer. *Mol Cancer Ther* 8: 626-635.
212. Kim Y, Lin Q, Glazer PM, Yun Z (2009) Hypoxic tumor microenvironment and cancer cell differentiation. *Curr Mol Med* 9: 425-434.
213. Yu Y, Deck JA, Hunsaker LA, Deck LM, Royer RE, et al. (2001) Selective active site inhibitors of human lactate dehydrogenases A4, B4, and C4. *Biochem Pharmacol* 62: 81-89.
214. Le A, Cooper CR, Gouw AM, Dinavahi R, Maitra A, et al. (2010) Inhibition of lactate dehydrogenase A induces oxidative stress and inhibits tumor progression. *Proc Natl Acad Sci U S A* 107: 2037-2042.
215. Granchi C, Roy S, Giacomelli C, Macchia M, Tuccinardi T, et al. (2011) Discovery of N-hydroxyindole-based inhibitors of human lactate dehydrogenase isoform A (LDH-A) as starvation agents against cancer cells. *J Med Chem* 54: 1599-1612.
216. Moellering RE, Black KC, Krishnamurty C, Baggett BK, Stafford P, et al. (2008) Acid treatment of melanoma cells selects for invasive phenotypes. *Clin Exp Metastasis* 25: 411-425.
217. Rofstad EK, Mathiesen B, Kindem K, Galappathi K (2006) Acidic extracellular pH promotes experimental metastasis of human melanoma cells in athymic nude mice. *Cancer Res* 66: 6699-6707.
218. Neri D, Supuran CT (2011) Interfering with pH regulation in tumours as a therapeutic strategy. *Nat Rev Drug Discov* 10: 767-777.
219. Grinstein S, Rotin D, Mason MJ (1989) Na<sup>+</sup>/H<sup>+</sup> exchange and growth factor-induced cytosolic pH changes. Role in cellular proliferation. *Biochim Biophys Acta* 988: 73-97.
220. Matsuyama S, Llopis J, Deveraux QL, Tsien RY, Reed JC (2000) Changes in intramitochondrial and cytosolic pH: early events that modulate caspase activation during apoptosis. *Nat Cell Biol* 2: 318-325.

221. Harguindey S, Orive G, Luis Pedraz J, Paradiso A, Reshkin SJ (2005) The role of pH dynamics and the Na<sup>+</sup>/H<sup>+</sup> antiporter in the etiopathogenesis and treatment of cancer. Two faces of the same coin--one single nature. *Biochim Biophys Acta* 1756: 1-24.
222. Opavsky R, Pastorekova S, Zelnik V, Gibadulinova A, Stanbridge EJ, et al. (1996) Human MN/CA9 gene, a novel member of the carbonic anhydrase family: structure and exon to protein domain relationships. *Genomics* 33: 480-487.
223. Tureci O, Sahin U, Vollmar E, Siemer S, Gottert E, et al. (1998) Human carbonic anhydrase XII: cDNA cloning, expression, and chromosomal localization of a carbonic anhydrase gene that is overexpressed in some renal cell cancers. *Proc Natl Acad Sci U S A* 95: 7608-7613.
224. Potter CP, Harris AL (2003) Diagnostic, prognostic and therapeutic implications of carbonic anhydrases in cancer. *Br J Cancer* 89: 2-7.
225. Lou Y, McDonald PC, Oloumi A, Chia S, Ostlund C, et al. (2011) Targeting tumor hypoxia: suppression of breast tumor growth and metastasis by novel carbonic anhydrase IX inhibitors. *Cancer Res* 71: 3364-3376.
226. Supuran CT (2008) Carbonic anhydrases: novel therapeutic applications for inhibitors and activators. *Nat Rev Drug Discov* 7: 168-181.
227. Chiche J, Ilc K, Laferriere J, Trottier E, Dayan F, et al. (2009) Hypoxia-inducible carbonic anhydrase IX and XII promote tumor cell growth by counteracting acidosis through the regulation of the intracellular pH. *Cancer Res* 69: 358-368.
228. Parks SK, Chiche J, Pouyssegur J (2011) pH control mechanisms of tumor survival and growth. *J Cell Physiol* 226: 299-308.
229. Vullo D, Franchi M, Gallori E, Pastorek J, Scozzafava A, et al. (2003) Carbonic anhydrase inhibitors: inhibition of the tumor-associated isozyme IX with aromatic and heterocyclic sulfonamides. *Bioorg Med Chem Lett* 13: 1005-1009.
230. Vullo D, Innocenti A, Nishimori I, Pastorek J, Scozzafava A, et al. (2005) Carbonic anhydrase inhibitors. Inhibition of the transmembrane isozyme XII with sulfonamides--a new target for the design of antitumor and antiglaucoma drugs? *Bioorg Med Chem Lett* 15: 963-969.

231. Owa T, Yoshino H, Okauchi T, Yoshimatsu K, Ozawa Y, et al. (1999) Discovery of novel antitumor sulfonamides targeting G1 phase of the cell cycle. *J Med Chem* 42: 3789-3799.
232. Abbate F, Casini A, Owa T, Scozzafava A, Supuran CT (2004) Carbonic anhydrase inhibitors: E7070, a sulfonamide anticancer agent, potently inhibits cytosolic isozymes I and II, and transmembrane, tumor-associated isozyme IX. *Bioorg Med Chem Lett* 14: 217-223.
233. Owa T, Yokoi A, Yamazaki K, Yoshimatsu K, Yamori T, et al. (2002) Array-based structure and gene expression relationship study of antitumor sulfonamides including N-[2-[(4-hydroxyphenyl)amino]-3-pyridinyl]-4-methoxybenzenesulfonamide and N-(3-chloro-7-indolyl)-1,4-benzenedisulfonamide. *J Med Chem* 45: 4913-4922.
234. Dittrich C, Dumez H, Calvert H, Hanauske A, Faber M, et al. (2003) Phase I and pharmacokinetic study of E7070, a chloroindolyl-sulfonamide anticancer agent, administered on a weekly schedule to patients with solid tumors. *Clin Cancer Res* 9: 5195-5204.
235. Punt CJ, Fumoleau P, van de Walle B, Faber MN, Ravic M, et al. (2001) Phase I and pharmacokinetic study of E7070, a novel sulfonamide, given at a daily times five schedule in patients with solid tumors. A study by the EORTC-early clinical studies group (ECSG). *Ann Oncol* 12: 1289-1293.
236. Raymond E, ten Bokkel Huinink WW, Taieb J, Beijnen JH, Faivre S, et al. (2002) Phase I and pharmacokinetic study of E7070, a novel chloroindolyl sulfonamide cell-cycle inhibitor, administered as a one-hour infusion every three weeks in patients with advanced cancer. *J Clin Oncol* 20: 3508-3521.
237. Rigas JR, Tong WP, Kris MG, Orazem JP, Young CW, et al. (1992) Phase I clinical and pharmacological study of chloroquinoline sulfonamide. *Cancer Res* 52: 6619-6623.
238. Terret C, Zanetta S, Roche H, Schellens JH, Faber MN, et al. (2003) Phase I clinical and pharmacokinetic study of E7070, a novel sulfonamide given as a 5-day continuous infusion repeated every 3 weeks in patients with solid tumours. A study by the EORTC Early Clinical Study Group (ECSG). *Eur J Cancer* 39: 1097-1104.
239. Talbot DC, von Pawel J, Cattell E, Yule SM, Johnston C, et al. (2007) A randomized phase II pharmacokinetic and pharmacodynamic study of indisulam as second-line therapy in patients with advanced non-small cell lung cancer. *Clin Cancer Res* 13: 1816-1822.



240. Shepherd FA, Rodrigues Pereira J, Ciuleanu T, Tan EH, Hirsh V, et al. (2005) Erlotinib in previously treated non-small-cell lung cancer. *N Engl J Med* 353: 123-132.
241. Martinez-Zaguilan R, Lynch RM, Martinez GM, Gillies RJ (1993) Vacuolar-type H(+)-ATPases are functionally expressed in plasma membranes of human tumor cells. *Am J Physiol* 265: C1015-1029.
242. Nishi T, Forgac M (2002) The vacuolar (H+)-ATPases--nature's most versatile proton pumps. *Nat Rev Mol Cell Biol* 3: 94-103.
243. Hinton A, Bond S, Forgac M (2009) V-ATPase functions in normal and disease processes. *Pflugers Arch* 457: 589-598.
244. Murakami T, Shibuya I, Ise T, Chen ZS, Akiyama S, et al. (2001) Elevated expression of vacuolar proton pump genes and cellular PH in cisplatin resistance. *Int J Cancer* 93: 869-874.
245. Torigoe T, Izumi H, Ishiguchi H, Uramoto H, Murakami T, et al. (2002) Enhanced expression of the human vacuolar H+-ATPase c subunit gene (ATP6L) in response to anticancer agents. *J Biol Chem* 277: 36534-36543.
246. Bowman EJ, Siebers A, Altendorf K (1988) Bafilomycins: a class of inhibitors of membrane ATPases from microorganisms, animal cells, and plant cells. *Proc Natl Acad Sci U S A* 85: 7972-7976.
247. Perez-Sayans M, Somoza-Martin JM, Barros-Angueira F, Rey JM, Garcia-Garcia A (2009) V-ATPase inhibitors and implication in cancer treatment. *Cancer Treat Rev* 35: 707-713.
248. Luciani F, Spada M, De Milito A, Molinari A, Rivoltini L, et al. (2004) Effect of proton pump inhibitor pretreatment on resistance of solid tumors to cytotoxic drugs. *J Natl Cancer Inst* 96: 1702-1713.
249. Bowman BJ, McCall ME, Baertsch R, Bowman EJ (2006) A model for the proteolipid ring and bafilomycin/concanamycin-binding site in the vacuolar ATPase of *Neurospora crassa*. *J Biol Chem* 281: 31885-31893.
250. De Milito A, Fais S (2005) Tumor acidity, chemoresistance and proton pump inhibitors. *Future Oncol* 1: 779-786.

251. Finbow ME, Harrison MA (1997) The vacuolar H<sup>+</sup>-ATPase: a universal proton pump of eukaryotes. *Biochem J* 324 ( Pt 3): 697-712.
252. Asada K, Miyamoto K, Fukutomi T, Tsuda H, Yagi Y, et al. (2003) Reduced expression of GNA11 and silencing of MCT1 in human breast cancers. *Oncology* 64: 380-388.
253. Pinheiro C, Longatto-Filho A, Ferreira L, Pereira SM, Etlinger D, et al. (2008) Increasing expression of monocarboxylate transporters 1 and 4 along progression to invasive cervical carcinoma. *Int J Gynecol Pathol* 27: 568-574.
254. Pinheiro C, Longatto-Filho A, Scapulatempo C, Ferreira L, Martins S, et al. (2008) Increased expression of monocarboxylate transporters 1, 2, and 4 in colorectal carcinomas. *Virchows Arch* 452: 139-146.
255. Sonveaux P, Vegran F, Schroeder T, Wergin MC, Verrax J, et al. (2008) Targeting lactate-fueled respiration selectively kills hypoxic tumor cells in mice. *J Clin Invest* 118: 3930-3942.
256. Bueno V, Binet I, Steger U, Bundick R, Ferguson D, et al. (2007) The specific monocarboxylate transporter (MCT1) inhibitor, AR-C117977, a novel immunosuppressant, prolongs allograft survival in the mouse. *Transplantation* 84: 1204-1207.
257. Silva AS, Yunes JA, Gillies RJ, Gatenby RA (2009) The potential role of systemic buffers in reducing intratumoral extracellular pH and acid-mediated invasion. *Cancer Res* 69: 2677-2684.
258. Jahde E, Glusenkamp KH, Rajewsky MF (1990) Protection of cultured malignant cells from mitoxantrone cytotoxicity by low extracellular pH: a possible mechanism for chemoresistance in vivo. *Eur J Cancer* 26: 101-106.
259. Robey IF, Baggett BK, Kirkpatrick ND, Roe DJ, Dosesco J, et al. (2009) Bicarbonate increases tumor pH and inhibits spontaneous metastases. *Cancer Res* 69: 2260-2268.
260. Raghunand N, Mahoney B, van Sluis R, Baggett B, Gillies RJ (2001) Acute metabolic alkalosis enhances response of C3H mouse mammary tumors to the weak base mitoxantrone. *Neoplasia* 3: 227-235.

261. Ibrahim Hashim A, Cornnell HH, Coelho Ribeiro Mde L, Abrahams D, Cunningham J, et al. (2011) Reduction of metastasis using a non-volatile buffer. *Clin Exp Metastasis* 28: 841-849.
262. Ibrahim-Hashim A, Cornnell HH, Abrahams D, Lloyd M, Bui M, et al. (2012) Systemic buffers inhibit carcinogenesis in TRAMP mice. *J Urol* 188: 624-631.
263. Coleman MC, Asbury CR, Daniels D, Du J, Aykin-Burns N, et al. (2008) 2-deoxy-D-glucose causes cytotoxicity, oxidative stress, and radiosensitization in pancreatic cancer. *Free Radic Biol Med* 44: 322-331.
264. Lin X, Zhang F, Bradbury CM, Kaushal A, Li L, et al. (2003) 2-Deoxy-D-glucose-induced cytotoxicity and radiosensitization in tumor cells is mediated via disruptions in thiol metabolism. *Cancer Res* 63: 3413-3417.
265. Simons AL, Ahmad IM, Mattson DM, Dornfeld KJ, Spitz DR (2007) 2-Deoxy-D-glucose combined with cisplatin enhances cytotoxicity via metabolic oxidative stress in human head and neck cancer cells. *Cancer Res* 67: 3364-3370.
266. Zhang F, Aft RL (2009) Chemosensitizing and cytotoxic effects of 2-deoxy-D-glucose on breast cancer cells. *J Cancer Res Ther* 5 Suppl 1: S41-43.
267. Ben Sahra I, Laurent K, Giuliano S, Larbret F, Ponzio G, et al. (2010) Targeting cancer cell metabolism: the combination of metformin and 2-deoxyglucose induces p53-dependent apoptosis in prostate cancer cells. *Cancer Res* 70: 2465-2475.
268. Cheong JH, Park ES, Liang J, Dennison JB, Tsavachidou D, et al. (2011) Dual inhibition of tumor energy pathway by 2-deoxyglucose and metformin is effective against a broad spectrum of preclinical cancer models. *Mol Cancer Ther* 10: 2350-2362.
269. Mohanti BK, Rath GK, Anantha N, Kannan V, Das BS, et al. (1996) Improving cancer radiotherapy with 2-deoxy-D-glucose: phase I/II clinical trials on human cerebral gliomas. *Int J Radiat Oncol Biol Phys* 35: 103-111.
270. Singh D, Banerji AK, Dwarakanath BS, Tripathi RP, Gupta JP, et al. (2005) Optimizing cancer radiotherapy with 2-deoxy-d-glucose dose escalation studies in patients with glioblastoma multiforme. *Strahlenther Onkol* 181: 507-514.

271. Jain RK (2001) Normalizing tumor vasculature with anti-angiogenic therapy: a new paradigm for combination therapy. *Nat Med* 7: 987-989.
272. Jain RK (2005) Normalization of tumor vasculature: an emerging concept in antiangiogenic therapy. *Science* 307: 58-62.
273. Tong RT, Boucher Y, Kozin SV, Winkler F, Hicklin DJ, et al. (2004) Vascular normalization by vascular endothelial growth factor receptor 2 blockade induces a pressure gradient across the vasculature and improves drug penetration in tumors. *Cancer Res* 64: 3731-3736.
274. Matsumoto S, Batra S, Saito K, Yasui H, Choudhuri R, et al. (2011) Antiangiogenic agent sunitinib transiently increases tumor oxygenation and suppresses cycling hypoxia. *Cancer Res* 71: 6350-6359.
275. Winkler F, Kozin SV, Tong RT, Chae SS, Booth MF, et al. (2004) Kinetics of vascular normalization by VEGFR2 blockade governs brain tumor response to radiation: role of oxygenation, angiopoietin-1, and matrix metalloproteinases. *Cancer Cell* 6: 553-563.
276. Willett CG, Boucher Y, di Tomaso E, Duda DG, Munn LL, et al. (2004) Direct evidence that the VEGF-specific antibody bevacizumab has antivascular effects in human rectal cancer. *Nat Med* 10: 145-147.
277. Willett CG, Duda DG, di Tomaso E, Boucher Y, Ancukiewicz M, et al. (2009) Efficacy, safety, and biomarkers of neoadjuvant bevacizumab, radiation therapy, and fluorouracil in rectal cancer: a multidisciplinary phase II study. *J Clin Oncol* 27: 3020-3026.
278. Willett CG, Duda DG, Ancukiewicz M, Shah M, Czito BG, et al. (2010) A safety and survival analysis of neoadjuvant bevacizumab with standard chemoradiation in a phase I/II study compared with standard chemoradiation in locally advanced rectal cancer. *Oncologist* 15: 845-851.
279. Bailey KM, Wojtkowiak JW, Cornell HH, Ribeiro MC, Balagurunathan Y, et al. (2014) Mechanisms of buffer therapy resistance. *Neoplasia* 16: 354-364 e353.
280. Rothberg JM, Bailey KM, Wojtkowiak JW, Ben-Nun Y, Bogyo M, et al. (2013) Acid-mediated tumor proteolysis: contribution of cysteine cathepsins. *Neoplasia* 15: 1125-1137.

281. Ribeiro MdLC SA, Bailey KM, Kumar NB, Sellers TA, Gatenby RA, Ibrahim-Hashim A, Gillies RJ (2012) Buffer Therapy for Cancer. *J Nutr Food Sci* S2.
282. Altenberg B, Greulich KO (2004) Genes of glycolysis are ubiquitously overexpressed in 24 cancer classes. *Genomics* 84: 1014-1020.
283. Warburg O (1956) On the origin of cancer cells. *Science* 123: 309-314.
284. Weinhouse S (1976) The Warburg hypothesis fifty years later. *Z Krebsforsch Klin Onkol Cancer Res Clin Oncol* 87: 115-126.
285. Kelloff GJ, Hoffman JM, Johnson B, Scher HI, Siegel BA, et al. (2005) Progress and promise of FDG-PET imaging for cancer patient management and oncologic drug development. *Clin Cancer Res* 11: 2785-2808.
286. Christofk HR, Vander Heiden MG, Wu N, Asara JM, Cantley LC (2008) Pyruvate kinase M2 is a phosphotyrosine-binding protein. *Nature* 452: 181-186.
287. Epstein T, Xu, L., Gillies, R.J., Gatenby, R.A. (2014) Separation of metabolic supply and demand: Aerobic glycolysis as a normal physiological response to fluctuating energetic demands in the membrane. *Cancer and Metabolism* 2014.
288. DeBerardinis RJ, Lum JJ, Hatzivassiliou G, Thompson CB (2008) The biology of cancer: metabolic reprogramming fuels cell growth and proliferation. *Cell Metab* 7: 11-20.
289. Nathan C, Ding A (2010) SnapShot: Reactive Oxygen Intermediates (ROI). *Cell* 140: 951-951 e952.
290. DeBerardinis RJ, Mancuso A, Daikhin E, Nissim I, Yudkoff M, et al. (2007) Beyond aerobic glycolysis: transformed cells can engage in glutamine metabolism that exceeds the requirement for protein and nucleotide synthesis. *Proc Natl Acad Sci U S A* 104: 19345-19350.
291. Estrella V, Chen T, Lloyd M, Wojtkowiak J, Cornnell HH, et al. (2013) Acidity generated by the tumor microenvironment drives local invasion. *Cancer Res* 73: 1524-1535.

292. Ord JJ, Agrawal S, Thamboo TP, Roberts I, Campo L, et al. (2007) An investigation into the prognostic significance of necrosis and hypoxia in high grade and invasive bladder cancer. *J Urol* 178: 677-682.
293. Hussain SA, Ganesan R, Reynolds G, Gross L, Stevens A, et al. (2007) Hypoxia-regulated carbonic anhydrase IX expression is associated with poor survival in patients with invasive breast cancer. *Br J Cancer* 96: 104-109.
294. Chambers AF, Groom AC, MacDonald IC (2002) Dissemination and growth of cancer cells in metastatic sites. *Nat Rev Cancer* 2: 563-572.
295. Bartelink H, Horiot J., Poortmans, P., et al. Impact of radiation dose on local control, fibrosis and survival after breast conserving treatment: 10-year results of the EORTC trial 22881-10882; 2006. pp. Oral Presentation.
296. Goodgame B, Viswanathan A, Zoole J, Gao F, Miller CR, et al. (2009) Risk of recurrence of resected stage I non-small cell lung cancer in elderly patients as compared with younger patients. *J Thorac Oncol* 4: 1370-1374.
297. Francken AB, Accortt NA, Shaw HM, Wiener M, Soong SJ, et al. (2008) Prognosis and determinants of outcome following locoregional or distant recurrence in patients with cutaneous melanoma. *Ann Surg Oncol* 15: 1476-1484.
298. Stucky CC, Gray RJ, Dueck AC, Wasif N, Laman SD, et al. (2010) Risk factors associated with local and in-transit recurrence of cutaneous melanoma. *Am J Surg* 200: 770-774; discussion 774-775.
299. Patanaphan V, Salazar OM, Risco R (1988) Breast cancer: metastatic patterns and their prognosis. *South Med J* 81: 1109-1112.
300. Kang Y, Siegel PM, Shu W, Drobnjak M, Kakonen SM, et al. (2003) A multigenic program mediating breast cancer metastasis to bone. *Cancer Cell* 3: 537-549.
301. Minn AJ, Gupta GP, Siegel PM, Bos PD, Shu W, et al. (2005) Genes that mediate breast cancer metastasis to lung. *Nature* 436: 518-524.
302. Bos PD, Zhang XH, Nadal C, Shu W, Gomis RR, et al. (2009) Genes that mediate breast cancer metastasis to the brain. *Nature* 459: 1005-1009.

303. Tabaries S, Dong Z, Annis MG, Omeroglu A, Pepin F, et al. (2011) Claudin-2 is selectively enriched in and promotes the formation of breast cancer liver metastases through engagement of integrin complexes. *Oncogene* 30: 1318-1328.
304. Edlund M, Sung SY, Chung LW (2004) Modulation of prostate cancer growth in bone microenvironments. *J Cell Biochem* 91: 686-705.
305. Hess KR, Varadhachary GR, Taylor SH, Wei W, Raber MN, et al. (2006) Metastatic patterns in adenocarcinoma. *Cancer* 106: 1624-1633.
306. Patanaphan V, Salazar OM (1993) Colorectal cancer: metastatic patterns and prognosis. *South Med J* 86: 38-41.
307. Hart IR, Fidler IJ (1980) Role of organ selectivity in the determination of metastatic patterns of B16 melanoma. *Cancer Res* 40: 2281-2287.
308. Kessenbrock K, Plaks V, Werb Z (2010) Matrix metalloproteinases: regulators of the tumor microenvironment. *Cell* 141: 52-67.
309. Deryugina EI, Quigley JP (2006) Matrix metalloproteinases and tumor metastasis. *Cancer Metastasis Rev* 25: 9-34.
310. McCawley LJ, Matrisian LM (2000) Matrix metalloproteinases: multifunctional contributors to tumor progression. *Mol Med Today* 6: 149-156.
311. Sternlicht MD, Werb Z (2001) How matrix metalloproteinases regulate cell behavior. *Annu Rev Cell Dev Biol* 17: 463-516.
312. Whittaker M, Floyd CD, Brown P, Gearing AJ (1999) Design and therapeutic application of matrix metalloproteinase inhibitors. *Chem Rev* 99: 2735-2776.
313. Overall CM, Kleinfeld O (2006) Tumour microenvironment - opinion: validating matrix metalloproteinases as drug targets and anti-targets for cancer therapy. *Nat Rev Cancer* 6: 227-239.
314. Coussens LM, Fingleton B, Matrisian LM (2002) Matrix metalloproteinase inhibitors and cancer: trials and tribulations. *Science* 295: 2387-2392.

315. Reich R, Thompson EW, Iwamoto Y, Martin GR, Deason JR, et al. (1988) Effects of inhibitors of plasminogen activator, serine proteinases, and collagenase IV on the invasion of basement membranes by metastatic cells. *Cancer Res* 48: 3307-3312.
316. Brown PD (2000) Ongoing trials with matrix metalloproteinase inhibitors. *Expert Opin Investig Drugs* 9: 2167-2177.
317. Sledge GW, Jr., Qulali M, Goulet R, Bone EA, Fife R (1995) Effect of matrix metalloproteinase inhibitor batimastat on breast cancer regrowth and metastasis in athymic mice. *J Natl Cancer Inst* 87: 1546-1550.
318. Turk V, Stoka V, Vasiljeva O, Renko M, Sun T, et al. (2012) Cysteine cathepsins: from structure, function and regulation to new frontiers. *Biochim Biophys Acta* 1824: 68-88.
319. Mohamed MM, Cavallo-Medved D, Rudy D, Anbalagan A, Moin K, et al. (2010) Interleukin-6 increases expression and secretion of cathepsin B by breast tumor-associated monocytes. *Cell Physiol Biochem* 25: 315-324.
320. Cavallo-Medved D, Dosesescu J, Linebaugh BE, Sameni M, Rudy D, et al. (2003) Mutant K-ras regulates cathepsin B localization on the surface of human colorectal carcinoma cells. *Neoplasia* 5: 507-519.
321. Mason SD, Joyce JA (2011) Proteolytic networks in cancer. *Trends Cell Biol* 21: 228-237.
322. Mohamed MM, Sloane BF (2006) Cysteine cathepsins: multifunctional enzymes in cancer. *Nat Rev Cancer* 6: 764-775.
323. Yan S, Sloane BF (2003) Molecular regulation of human cathepsin B: implication in pathologies. *Biol Chem* 384: 845-854.
324. Rozhin J, Sameni M, Ziegler G, Sloane BF (1994) Pericellular pH affects distribution and secretion of cathepsin B in malignant cells. *Cancer Res* 54: 6517-6525.
325. Gatenby RA, Gawlinski ET, Gmitro AF, Kaylor B, Gillies RJ (2006) Acid-mediated tumor invasion: a multidisciplinary study. *Cancer Res* 66: 5216-5223.



326. Jedeszko C, Sameni M, Olive MB, Moin K, Sloane BF (2008) Visualizing protease activity in living cells: from two dimensions to four dimensions. *Curr Protoc Cell Biol* Chapter 4: Unit 4 20.
327. Blum G, Mullins SR, Keren K, Fonovic M, Jedeszko C, et al. (2005) Dynamic imaging of protease activity with fluorescently quenched activity-based probes. *Nat Chem Biol* 1: 203-209.
328. Friedl P, Locker J, Sahai E, Segall JE (2012) Classifying collective cancer cell invasion. *Nat Cell Biol* 14: 777-783.
329. Friedl P, Alexander S (2011) Cancer invasion and the microenvironment: plasticity and reciprocity. *Cell* 147: 992-1009.
330. Sahai E, Marshall CJ (2003) Differing modes of tumour cell invasion have distinct requirements for Rho/ROCK signalling and extracellular proteolysis. *Nat Cell Biol* 5: 711-719.
331. Reshkin SJ, Bellizzi A, Albarani V, Guerra L, Tommasino M, et al. (2000) Phosphoinositide 3-kinase is involved in the tumor-specific activation of human breast cancer cell Na<sup>(+)</sup>/H<sup>(+)</sup> exchange, motility, and invasion induced by serum deprivation. *J Biol Chem* 275: 5361-5369.
332. Stock C, Gassner B, Hauck CR, Arnold H, Mally S, et al. (2005) Migration of human melanoma cells depends on extracellular pH and Na<sup>+</sup>/H<sup>+</sup> exchange. *J Physiol* 567: 225-238.
333. Denker SP, Barber DL (2002) Cell migration requires both ion translocation and cytoskeletal anchoring by the Na-H exchanger NHE1. *J Cell Biol* 159: 1087-1096.
334. Ibrahim Hashim A, Wojtkowiak, J. W., de Lourdes Coelho Ribeiro, M., Estrella, V., Bailey, K. M., Cornnell, H.H., et al. (2011) Free Base Lysine Increases Survival and Reduces Metastasis in Prostate Cancer Model. *Journal of Cancer Science and Therapy* S1.
335. Rothberg JM, Bailey K.M., Wojtkowiak J.W., Bennun Y., Boygo M.S., Weber E., Moin K., Blum G., Mattingly R.R., Gillies R.J., Sloane B.F. (In Press 2013) Acidic Extracellular pH Increases Contribution of Cysteine Cathepsins, Including Cathepsin B, to Breast Carcinoma-Associated Proteolysis. *Neoplasia*.

336. Yachida S, Jones S, Bozic I, Antal T, Leary R, et al. (2010) Distant metastasis occurs late during the genetic evolution of pancreatic cancer. *Nature* 467: 1114-1117.
337. Gatenby RA, Gillies RJ (2004) Why do cancers have high aerobic glycolysis? *Nat Rev Cancer* 4: 891-899.
338. Gambhir SS (2002) Molecular imaging of cancer with positron emission tomography. *Nat Rev Cancer* 2: 683-693.
339. Laird AK (1964) Dynamics of Tumor Growth. *Br J Cancer* 13: 490-502.
340. Mehrara E, Forssell-Aronsson E, Johanson V, Kolby L, Hultborn R, et al. (2013) A new method to estimate parameters of the growth model for metastatic tumours. *Theor Biol Med Model* 10: 31.
341. Pries AR, Cornelissen AJ, Sloot AA, Hinkeldey M, Dreher MR, et al. (2009) Structural adaptation and heterogeneity of normal and tumor microvascular networks. *PLoS Comput Biol* 5: e1000394.
342. Erler JT, Cawthorne CJ, Williams KJ, Koritzinsky M, Wouters BG, et al. (2004) Hypoxia-mediated down-regulation of Bid and Bax in tumors occurs via hypoxia-inducible factor 1-dependent and -independent mechanisms and contributes to drug resistance. *Mol Cell Biol* 24: 2875-2889.
343. Cairns RA, Harris IS, Mak TW (2011) Regulation of cancer cell metabolism. *Nat Rev Cancer* 11: 85-95.
344. Guzy RD, Hoyos B, Robin E, Chen H, Liu L, et al. (2005) Mitochondrial complex III is required for hypoxia-induced ROS production and cellular oxygen sensing. *Cell Metab* 1: 401-408.
345. Huang LE, Bindra RS, Glazer PM, Harris AL (2007) Hypoxia-induced genetic instability--a calculated mechanism underlying tumor progression. *J Mol Med (Berl)* 85: 139-148.
346. Brizel DM, Scully SP, Harrelson JM, Layfield LJ, Bean JM, et al. (1996) Tumor oxygenation predicts for the likelihood of distant metastases in human soft tissue sarcoma. *Cancer Res* 56: 941-943.

347. Chaudary N, Hill RP (2007) Hypoxia and metastasis. *Clin Cancer Res* 13: 1947-1949.
348. Vaupel P, Mayer A (2007) Hypoxia in cancer: significance and impact on clinical outcome. *Cancer Metastasis Rev* 26: 225-239.
349. Wilson WR, Hay MP (2011) Targeting hypoxia in cancer therapy. *Nat Rev Cancer* 11: 393-410.
350. Teicher BA (1994) Hypoxia and drug resistance. *Cancer Metastasis Rev* 13: 139-168.
351. Gatenby RA, Kessler HB, Rosenblum JS, Coia LR, Moldofsky PJ, et al. (1988) Oxygen distribution in squamous cell carcinoma metastases and its relationship to outcome of radiation therapy. *Int J Radiat Oncol Biol Phys* 14: 831-838.
352. Frankenberg-Schwager M, Frankenberg D, Harbich R (1991) Different oxygen enhancement ratios for induced and unrejoined DNA double-strand breaks in eukaryotic cells. *Radiat Res* 128: 243-250.
353. Durand RE (1994) The influence of microenvironmental factors during cancer therapy. *In Vivo* 8: 691-702.
354. Shannon AM, Bouchier-Hayes DJ, Condron CM, Toomey D (2003) Tumour hypoxia, chemotherapeutic resistance and hypoxia-related therapies. *Cancer Treat Rev* 29: 297-307.
355. Minchinton AI, Tannock IF (2006) Drug penetration in solid tumours. *Nat Rev Cancer* 6: 583-592.
356. Olive PL, Banath JP (2004) Phosphorylation of histone H2AX as a measure of radiosensitivity. *Int J Radiat Oncol Biol Phys* 58: 331-335.
357. Brown JM, Evans J, Kovacs MS (1992) The prediction of human tumor radiosensitivity in situ: an approach using chromosome aberrations detected by fluorescence in situ hybridization. *Int J Radiat Oncol Biol Phys* 24: 279-286.
358. Moeller BJ, Richardson RA, Dewhirst MW (2007) Hypoxia and radiotherapy: opportunities for improved outcomes in cancer treatment. *Cancer Metastasis Rev* 26: 241-248.

359. Moeller BJ, Dreher MR, Rabbani ZN, Schroeder T, Cao Y, et al. (2005) Pleiotropic effects of HIF-1 blockade on tumor radiosensitivity. *Cancer Cell* 8: 99-110.
360. Unruh A, Ressel A, Mohamed HG, Johnson RS, Nadrowitz R, et al. (2003) The hypoxia-inducible factor-1 alpha is a negative factor for tumor therapy. *Oncogene* 22: 3213-3220.
361. Bennewith KL, Raleigh JA, Durand RE (2002) Orally administered pimonidazole to label hypoxic tumor cells. *Cancer Res* 62: 6827-6830.
362. Evans SM, Judy KD, Dunphy I, Jenkins WT, Nelson PT, et al. (2004) Comparative measurements of hypoxia in human brain tumors using needle electrodes and EF5 binding. *Cancer Res* 64: 1886-1892.
363. Liu Q, Sun JD, Wang J, Ahluwalia D, Baker AF, et al. (2012) TH-302, a hypoxia-activated prodrug with broad in vivo preclinical combination therapy efficacy: optimization of dosing regimens and schedules. *Cancer Chemother Pharmacol* 69: 1487-1498.
364. Borad MJ, Reddy, S., Uronis, H., Sigal, D.S., Cohn, A.L., Schelman, W.R., Stephenson, J., Chiorean, E.G., Rosen, P.J., Ulrich, B., Dragovich, T., Del Prete, S., Rarick, M., Eng, C., Kroll, S., Ryan, D. (2012) Randomized phase II study of the efficacy and safety of gemcitabine + TH-302 (G+T) vs gemcitabine (G) alone in previously untreated patients with advanced pancreatic cancer. . Proceedings of the 103rd Annual Meeting of the American Association for Cancer Research: LB-121.
365. Secomb TW, Hsu R, Ong ET, Gross JF, Dewhirst MW (1995) Analysis of the effects of oxygen supply and demand on hypoxic fraction in tumors. *Acta Oncol* 34: 313-316.
366. Cairns RA, Papandreou I, Sutphin PD, Denko NC (2007) Metabolic targeting of hypoxia and HIF1 in solid tumors can enhance cytotoxic chemotherapy. *Proc Natl Acad Sci U S A* 104: 9445-9450.
367. Takakusagi Y, Matsumoto S., Saito, K., Matsuo, M., DeGraff, W., Choudhuri, R., Devasahayam, N., Subramanian, S., Munasinghe, J.P., Mitchell, J.B., Hart, C.P., Krishna, M.C. (2013) Imaging-guided determination of the treatment regimens of the hypoxia-activated prodrug TH-302. *Global Biotechnology Congress 2013 Poster Presentation*.
368. Kruuv JA, Inch WR, McCredie JA (1967) Blood flow and oxygenation of tumors in mice. II. Effects of vasodilator drugs. *Cancer* 20: 60-65.

369. Chaplin DJ (1988) Postirradiation modification of tumor blood flow: a method to increase the effectiveness of chemical radiosensitizers. *Radiat Res* 115: 292-302.
370. Trotter MJ, Acker BD, Chaplin DJ (1989) Histological evidence for nonperfused vasculature in a murine tumor following hydralazine administration. *Int J Radiat Oncol Biol Phys* 17: 785-789.
371. Jirtle RL (1988) Chemical modification of tumour blood flow. *Int J Hyperthermia* 4: 355-371.
372. Stratford IJ, Adams GE, Godden J, Nolan J, Howells N, et al. (1988) Potentiation of the anti-tumour effect of melphalan by the vasoactive agent, hydralazine. *Br J Cancer* 58: 122-127.
373. Bhujwala ZM, Tozer GM, Field SB, Maxwell RJ, Griffiths JR (1990) The energy metabolism of RIF-1 tumours following hydralazine. *Radiother Oncol* 19: 281-291.
374. Bhujwala ZM, Tozer GM, Field SB, Proctor E, Busza A, et al. (1990) The combined measurement of blood flow and metabolism in RIF-1 tumours in vivo. A study using H<sub>2</sub> flow and <sup>31</sup>P NMR spectroscopy. *NMR Biomed* 3: 178-183.
375. Bhujwala ZM, Shungu DC, Glickson JD (1996) Effects of blood flow modifiers on tumor metabolism observed in vivo by proton magnetic resonance spectroscopic imaging. *Magn Reson Med* 36: 204-211.
376. Stone HB, Minchinton AI, Lemmon M, Menke D, Brown JM (1992) Pharmacological modification of tumor blood flow: lack of correlation between alteration of mean arterial blood pressure and changes in tumor perfusion. *Int J Radiat Oncol Biol Phys* 22: 79-86.
377. Chaplin DJ (1989) Hydralazine-induced tumor hypoxia: a potential target for cancer chemotherapy. *J Natl Cancer Inst* 81: 618-622.
378. Chaplin DJ, Acker B (1987) The effect of hydralazine on the tumor cytotoxicity of the hypoxic cell cytotoxin RSU-1069: evidence for therapeutic gain. *Int J Radiat Oncol Biol Phys* 13: 579-585.
379. Horsman MR, Christensen KL, Overgaard J (1989) Hydralazine-induced enhancement of hyperthermic damage in a C3H mammary carcinoma in vivo. *Int J Hyperthermia* 5: 123-136.

380. Kalmus J, Okunieff P, Vaupel P (1990) Dose-dependent effects of hydralazine on microcirculatory function and hyperthermic response of murine FSall tumors. *Cancer Res* 50: 15-19.
381. Chu GC, Kimmelman AC, Hezel AF, DePinho RA (2007) Stromal biology of pancreatic cancer. *J Cell Biochem* 101: 887-907.
382. Mahadevan D, Von Hoff DD (2007) Tumor-stroma interactions in pancreatic ductal adenocarcinoma. *Mol Cancer Ther* 6: 1186-1197.
383. Erkan M, Reiser-Erkan C, Michalski CW, Deucker S, Sauliunaite D, et al. (2009) Cancer-stellate cell interactions perpetuate the hypoxia-fibrosis cycle in pancreatic ductal adenocarcinoma. *Neoplasia* 11: 497-508.
384. Cardenas-Rodriguez J, Li Y, Galons JP, Cornell H, Gillies RJ, et al. (2012) Imaging biomarkers to monitor response to the hypoxia-activated prodrug TH-302 in the MiaPaCa2 flank xenograft model. *Magn Reson Imaging* 30: 1002-1009.
385. Horsman MR, Nordmark M, Hoyer M, Overgaard J (1995) Direct evidence that hydralazine can induce hypoxia in both transplanted and spontaneous murine tumours. *Br J Cancer* 72: 1474-1478.
386. Matsumoto S, Saito K, Takakusagi Y, Matsuo M, Munasinghe JP, et al. (2014) In Vivo Imaging of Tumor Physiological, Metabolic, and Redox Changes in Response to the Anti-Angiogenic Agent Sunitinib: Longitudinal Assessment to Identify Transient Vascular Renormalization. *Antioxid Redox Signal*.
387. Abramovic Z, Hou H, Julijana K, Sentjurc M, Lariviere JP, et al. (2011) Modulation of tumor hypoxia by topical formulations with vasodilators for enhancing therapy. *Adv Exp Med Biol* 701: 75-82.
388. Society AC (2013) *Cancer Facts & Figures 2013*. Atlanta: American Cancer Society.
389. Society AC (2013) *Cancer Prevention & Early Detection Facts & Figures 2013*. Atlanta: American Cancer Society.

## **APPENDICES**

## Appendix A: Copyright Permission from *Advances in Pharmacology*

Elsevier's copyright policy allows for the use of final published article materials for inclusion in a thesis or dissertation.

### How authors can use their own journal articles

Authors can use their articles for a wide range of scholarly, non-commercial purposes as outlined below. These rights apply for all Elsevier authors who publish their article as either a subscription article or an open access article.

We require that all Elsevier authors always include a full acknowledgement and, if appropriate, a link to the final published version hosted on Science Direct.

For open access articles these rights are separate from how readers can reuse your article as defined by the author's choice of Creative Commons user license options.

Authors can use either their <a href="#">accepted author manuscript</a> or <a href="#">final published article</a> for:	
	Use at a conference, meeting or for teaching purposes
	Internal training by their company
	Sharing individual articles with colleagues for their research use* (also known as 'scholarly sharing')
	Use in a subsequent compilation of the author's works
	Inclusion in a thesis or dissertation
	Reuse of portions or extracts from the article in other works
	Preparation of derivative works (other than for commercial purposes)



## Appendix B: Copyright Permission from *Neoplasia*


Elsevier's copyright policy allows for the use of final published article materials for inclusion in a thesis or dissertation.

### How authors can use their own journal articles

Authors can use their articles for a wide range of scholarly, non-commercial purposes as outlined below. These rights apply for all Elsevier authors who publish their article as either a subscription article or an open access article.

We require that all Elsevier authors always include a full acknowledgement and, if appropriate, a link to the final published version hosted on Science Direct.

For open access articles these rights are separate from how readers can reuse your article as defined by the author's choice of Creative Commons user license options.

Authors can use either their <a href="#">accepted author manuscript</a> or <a href="#">final published article</a> for:	
	Use at a conference, meeting or for teaching purposes
	Internal training by their company
	Sharing individual articles with colleagues for their research use* (also known as 'scholarly sharing')
	Use in a subsequent compilation of the author's works
	Inclusion in a thesis or dissertation
	Reuse of portions or extracts from the article in other works
	Preparation of derivative works (other than for commercial purposes)

## **Appendix C: Copyright Permission from *Journal of Nutrition & Food Sciences***

All works published by OMICS Group are under the terms of the Creative Commons Attribution License. This permits anyone to copy, distribute, transmit and adapt the work provided the original work and source is appropriately cited.

### **Copyright:**

Submission of a manuscript implies that the work described has not been published before (except in the form of an abstract or as part of a published lecture, or thesis) and that it is not under consideration for publication elsewhere.

All works published by OMICS Group are under the terms of the Creative Commons Attribution License. This permits anyone to copy, distribute, transmit and adapt the work provided the original work and source is appropriately cited.

## **Appendix D: Copyright Permission from *Journal of Cancer Science & Therapy***

All works published by OMICS Group are under the terms of the Creative Commons Attribution License. This permits anyone to copy, distribute, transmit and adapt the work provided the original work and source is appropriately cited.

### **Copyright:**

Submission of a manuscript implies that the work described has not been published before (except in the form of an abstract or as part of a published lecture, or thesis) and that it is not under consideration for publication elsewhere.

All works published by OMICS Group are under the terms of the Creative Commons Attribution License. This permits anyone to copy, distribute, transmit and adapt the work provided the original work and source is appropriately cited.

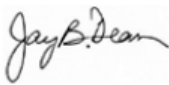
## Appendix E: Institutional Animal Care and Use Committee Approval – Protocol R4029



DIVISION OF RESEARCH INTEGRITY AND COMPLIANCE  
INSTITUTIONAL ANIMAL CARE USE COMMITTEE

### MEMORANDUM

TO: Robert Gillies, Ph.D.  
Dept. of Radiology  
SRB-2

FROM: Jay B. Dean, Ph.D, Chairperson  
Institutional Animal Care & Use Committee  
Division of Research Integrity and Compliance 

DATE: 7/14/2011

PROJECT TITLE: Causes and Consequences of Acid Tumor pH

AGENCY/SOURCE OF SUPPORT: NIH/NCI R01CA077575

IACUC PROTOCOL#: **R 4029**

PROTOCOL STATUS: **APPROVED**

The Institutional Animal Care and Use Committee (IACUC) reviewed your application requesting the use of animals in research for the above-entitled study. The IACUC requested modifications/further information in response to that review and has received the required information. The IACUC **APPROVED** your request to use the following animals in your protocol for a one-year period beginning **7/14/2011**:

- 612 Mice

Please reference the above IACUC protocol number in all correspondence regarding this project with the IACUC, Comparative Medicine, or the Division of Research Integrity and Compliance. In addition, please take note of the following:

- **IACUC approval is granted for a one-year period at the end of which, an annual renewal form must be submitted for years two (2) and three (3) of the protocol.** After three years all continuing studies must be completely re-described in a new application and submitted to IACUC for review.
- **All Comparative Medicine pre-performance safety and logistic meetings must occur prior to implementation of this protocol** [IACUC policy V.10]. Please contact the program coordinator at [compmed@research.usf.edu](mailto:compmed@research.usf.edu) to schedule a pre-performance meeting.
- **All changes to the IACUC-Approved Protocol must be pre-approved by the IACUC [IACUC policy III.11].** Minor changes can be submitted to the IACUC for review and approval as an amendment or procedural change, whereas major changes to the protocol require submission of a new IACUC application. Minor changes are changes considered to be within the scope of the original research hypothesis or involve the original species and are submitted to the IACUC as an Amendment or Procedural change. Any change in the IACUC-approved protocol that does not meet the latter definition is considered a major protocol change and requires the submission of a new application. More information on what constitutes a minor versus major protocol change and procedural steps necessary for IACUC review and approval are available on the Comparative Medicine web site at <http://www.research.usf.edu/cm/amendments.htm>
- **All costs invoiced to a grant account must be allocable to the purpose of the grant [IACUC policies IV.5 and V.10].** Costs allocable to one protocol may not be shifted to another in order to meet deficiencies caused by overruns, or for other reasons of convenience. Rotation of charges among protocols by month without establishing that the rotation schedule credibly reflects the relative benefit to each protocol is unacceptable.

For more information on IACUC policies and procedures, please visit the Comparative Medicine web site at <http://www.research.usf.edu/cm/default.htm>.

cc: Comparative Medicine  
Division of Research Grants

OFFICE OF RESEARCH · DIVISION OF RESEARCH INTEGRITY AND COMPLIANCE  
INSTITUTIONAL ANIMAL CARE AND USE COMMITTEE  
PHS No. A4100-01, AAALAC No.58-15, USDA No. 58-15  
University of South Florida · 12901 Bruce B. Downs Blvd., MDC35 · Tampa, FL 33612-4799  
(813) 974-7106 · FAX (813) 974-7091

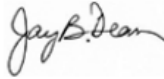
## Appendix F: Institutional Animal Care and Use Committee Approval – Protocol R4033



DIVISION OF RESEARCH INTEGRITY AND COMPLIANCE  
INSTITUTIONAL ANIMAL CARE USE COMMITTEE

### MEMORANDUM

TO: Robert Gillies, Ph.D.  
Dept. of Radiology  
SRB-2

FROM: Jay B. Dean, Ph.D, Chairperson  
Institutional Animal Care & Use Committee  
Division of Research Integrity and Compliance 

DATE: 8/8/2011

PROJECT TITLE: Imaging Biomarkers of Cancer Therapy

AGENCY/SOURCE OF SUPPORT: NIH/NCI CA125627-01A2

IACUC PROTOCOL#: **R 4033**

PROTOCOL STATUS: **APPROVED**

The Institutional Animal Care and Use Committee (IACUC) reviewed your application requesting the use of animals in research for the above-entitled study. The IACUC requested modifications/further information in response to that review and has received the required information. The IACUC **APPROVED** your request to use the following animals in your protocol for a one-year period

**beginning 8/1/2011 :**

- 1620 Mice

Please reference the above IACUC protocol number in all correspondence regarding this project with the IACUC, Comparative Medicine, or the Division of Research Integrity and Compliance. In addition, please take note of the following:

- **IACUC approval is granted for a one-year period at the end of which, an annual renewal form must be submitted for years two (2) and three (3) of the protocol.** After three years all continuing studies must be completely re-described in a new application and submitted to IACUC for review.
- **All Comparative Medicine pre-performance safety and logistic meetings must occur prior to implementation of this protocol** [IACUC policy V.10]. Please contact the program coordinator at [compmed@research.usf.edu](mailto:compmed@research.usf.edu) to schedule a pre-performance meeting.
- **All changes to the IACUC-Approved Protocol must be pre-approved by the IACUC [IACUC policy III.11].** Minor changes can be submitted to the IACUC for review and approval as an amendment or procedural change, whereas major changes to the protocol require submission of a new IACUC application. Minor changes are changes considered to be within the scope of the original research hypothesis or involve the original species and are submitted to the IACUC as an Amendment or Procedural change. Any change in the IACUC-approved protocol that does not meet the latter definition is considered a major protocol change and requires the submission of a new application. More information on what constitutes a minor versus major protocol change and procedural steps necessary for IACUC review and approval are available on the Comparative Medicine web site at <http://www.research.usf.edu/cm/amendments.htm>
- **All costs invoiced to a grant account must be allocable to the purpose of the grant [IACUC policies IV.5 and V.10].** Costs allocable to one protocol may not be shifted to another in order to meet deficiencies caused by overruns, or for other reasons of convenience. Rotation of charges among protocols by month without establishing that the rotation schedule credibly reflects the relative benefit to each protocol is unacceptable.

For more information on IACUC policies and procedures, please visit the Comparative Medicine web site at <http://www.research.usf.edu/cm/default.htm>.

cc: Comparative Medicine  
Division of Research Grants

OFFICE OF RESEARCH · DIVISION OF RESEARCH INTEGRITY AND COMPLIANCE  
INSTITUTIONAL ANIMAL CARE AND USE COMMITTEE  
PHS No. A4100-01, AAALAC No.58-15, USDA No. 58-15  
University of South Florida · 12901 Bruce B. Downs Blvd., MDC35 · Tampa, FL 33612-4799  
(813) 974-7106 · FAX (813) 974-7091

## Appendix G: Individual Contributions in Authored Publications

**Bailey KM**, Wojtkowiak JW, Cornell HH, Ribeiro MC, Balagurunathan Y, Hashim AI, Gillies RJ. Mechanisms of buffer therapy resistance. *Neoplasia* 2014; 16:354-64.

-KMB contributed to the experimental design, acquisition of data, and analysis and interpretation of the data presented in Figures 1B-F, 2, 3A-F, and 4-6

-KMB contributed significantly to writing and editing the manuscript

**Bailey KM\***, Cornell HH\*, Hashim AI, Wojtkowiak JW, Hart CP, Zhang X, Martinez GV, Baker AF, Gillies RJ. Evaluation of the “Steal” Phenomenon on the efficacy of hypoxia activated prodrug TH-302 in pancreatic cancer. Submitted for publication—contents in Chapter 4.

-KMB contributed to the experimental design, acquisition of data, and analysis and interpretation of the data presented in Figures 4.3, 4.4, 4.6, 4.9 and 4.10

-KMB contributed significantly to writing and editing the manuscript

**Bailey KM**, Wojtkowiak JW, Hashim AI, Gillies RJ. Targeting the metabolic microenvironment of tumors. *Adv Pharmacology*. 2012; 65:63-107. Book Chapter.

-KMB contributed significantly to the research, writing, editing and figure design of the manuscript

Wojtkowiak JW, Cornell HH, Matsumoto S, Saito K, Takakusagi Y, Dutta P, Kim Munju, Zhang X, Leo R, **Bailey KM**, Martinez G, Lloyd MC, Weber C, Mitchell JB, Lynch RM, Baker AF, Gatenby RA, Rejniak KA, Hart C, Krishna MC, Gillies RJ. Pyruvate sensitizes tumors to a hypoxia activated pro-drug. Submitted for publication.

-KMB contributed to the acquisition of data of an *in vivo* experiment

-KMB contributed to editing the manuscript

Rothberg JM, **Bailey KM**, Wojtkowiak JW, Ben-Nun Y, Bogyo M, Weber E, Moin K, Blum G, Mattingly RR, Gillies RJ, Sloane BF. Acid-mediated tumor proteolysis: contribution of cysteine cathepsins. *Neoplasia*. 2013; 15:1125-1137.

-KMB contributed to the experimental design, acquisition of data and analysis and interpretation of the data presented in Figure 7

-KMB contributed to writing and editing the manuscript

Estrella V, Chen T, Lloyd M, Wojtkowiak J, Cornell HH, Ibrahim-Hashim A, **Bailey K**, Balagurunathan Y, Rothberg JM, Sloane BF, Johnson J, Gatenby RA, Gillies RJ. Acidity generated by the tumor microenvironment drives local invasion. *Cancer Research*. 2013; 73:1524-1535.

-KMB contributed to the experimental design and acquisition of data presented in Supplementary Figure 9

Ribeiro MD, Silva AS, **Bailey KM**, Kumar NB, Sellers TA, Gatenby RA, Ibrahim-Hashim A, Gillies RJ. Buffer Therapy for Cancer. J Nutr Food Sci. 2012; 2:6.

-KMB contributed to the experimental design, acquisition of data and analysis and interpretation of the data presented in Figure 3

-KMB contributed to writing and editing the manuscript

Ibrahim-Hashim A, Wojtkowiak JW, de Lourdes Coelho Ribeiro M, Estrella V, **Bailey KM**, Cornell HH, Gatenby RA, Gillies RJ. Free Base Lysine Increases Survival and Reduces Metastasis in Prostate Cancer Model. J Cancer Sci Ther. 2011.

-KMB contributed to the acquisition of data and analysis and interpretation of the data presented in Figure 3

-KMB contributed to editing the manuscript